A rat assay for CNS repair

Thesis

A Rat Assay for CNS Repair

Berend Rah, MD

Research thesis submitted for the
degree of Doctor of Philosophy
at the Open University

Supervisor: Prof Geoffrey Raisman, FRS

Division of Neurobiology
National Institute for Medical Research
Mill Hill, London

2007

DATE OF SUBMISSION: 14 AUGUST 2006
DATE OF AWARD: 23 MAY 2007

ProQuest LLC.
789 East Eisenhower Parkway
P.O. Box 1346
Ann Arbor, MI 48106 – 1346

Table of abbreviations **1**

Table of figures **2**

Abstract **6**

Introduction **13**

CNS injury 13

Schwann cells 14

Neural stem cells 15

Olfactory ensheathing cells 18

The astrocytic response to injury 26

Myelin-associated inhibitory molecules 31

Requirements for an assay system 34

Creation of cell columns in the thalamus 36

Transplanting human cells into the rat CNS 37

Translating animal studies into therapeutic approaches 37

Mechanisms of rejection in syngeneic, allo- and xenografts 38

Markers of rejection 44

Reducing graft rejection/ immunosuppression 45

The fornix system as a potential assay system 47

Material and Methods **49**

Culturing and preparation of candidate repair cells 49

Adult Schwann cells 49

Olfactory ensheathing cells 50

Neonatal Schwann cells 51

Human and rat ensheathing cells from the olfactory mucosa 52

Neural crest stem cells 53

Foetal brain cells 54
Labelling with green fluorescent protein 55
Preparation of cell suspensions 56
Immunosuppression of xenograft recipients 57
Oral cyclosporine 57
Intraperitoneal cyclosporine 57
Liposomal tacrolimus 57
Surgery 59
Preparation and anaesthesia 59
Extrusion of columns in the thalamus 59
Generating a lesion and microinjection of cells into the fornix .. 63
Skin closure and recovery 65
Tissue fixation 68
Intracardial perfusion 68
Simple PBS perfusion 69
Perfusion with 4% paraformaldehyde 69
Perfusion with 4% paraformaldehyde suitable for cryostat sections 70
Tissue sectioning 70
Cryostat sections 70
Vibratome sections 71
Staining procedures 71
Staining for light microscopy 71
Staining for confocal microscopy 73
Staining for markers of immunorejection 74

Quantitative analysis 76

Results **77**

Columns extruded into the thalamus 77

General observations 77

Olfactory ensheathing cells 82

Olfactory ensheathing cells from the rat olfactory mucosa 111

Olfactory ensheathing cells from the human olfactory mucosa 116

Neural crest stem cells 127

The fornix system 136

Pure lesions 136

General appearance of fornix grafts 140

Neonatal Schwann cells 141

Olfactory ensheathing cells 145

Delayed transplantation 145

Foetal brain cells 148

Statistical results 151

Kruskal-Wallis Test 153

Discussion **159**

The thalamus as a model 159

General considerations 159

Neural crest stem cells 171

Human olfactory ensheathing cells 172

The fornix as a model 175

Failure of axon regeneration 175

Improved experimental design for future studies **178**

Donor cell purification 178

Schwann cells derived from neonatal tissue 178

Schwann cells derived from adult tissue 179

Olfactory ensheathing cells 180

Labelling of donor cells 180

Transplantation sites and improved lesioning techniques 183

Control of host immune response 184

Immunohistochemistry 186

Light microscopy 186

Confocal microscopy 187

Antibodies 187

Data collection and analysis 191

Conclusions **192**

Acknowledgements **196**

Reference List **197**

Table of abbreviations

ASC	Adult Schwann cells
CNS	Central nervous system
DMEM	Dulbecco's Modified Eagle Medium
ECM	Extracellular matrix
GDNF	Glial derived neurotrophic factor
GFAP	Glial fibrillary acidic protein
GFP	Green fluorescent protein
L15	Leibovitz medium
mRNA	Messenger ribonucleic acid
MIT	Anti human mitochondrial antibody
NCSS	Neural crest stem cells
NF	Neurofilament
NSC	Neonatal Schwann cells
OEC	Olfactory ensheathing cells
p75	Low affinity nerve growth factor receptor
PNS	Peripheral nervous system
PBS	Phosphate buffered saline
post OP	Post operatively
RPM	Revolutions per minute
RT	Reticular thalamic nucleus
S-100	Small set of calcium-binding proteins
vWF	von Willebrand factor

Table of figures

Figure 1 Schematic representation of the olfactory system. 20

Figure 2 Schematic representation of the steps involved in cell transplantation into the thalamus. 61

Figure 3 Surgery on the post-commissural fornix 66

Figure 4 Quantitative analysis of axon recruitment in the control group. 80

Figure 5 Comparison of cell-type characteristics in mucosal OECs, NSC and bulbar OECs 84

Figure 6 Axon recruitment by OEC grafts transplanted into the thalamus. 86

Figure 7 Comparison of axon recruitment by mucosal OECs, NSCs and bulbar OECs. 88

Figure 8 Comparison of axon recruitment by mucosal OECs, NSCs and bulbar OECs 14 days post operatively 90

Figure 9 Comparison of axon recruitment by mucosal OECs, NSCs and bulbar OECs 21 days post operatively 92

Figure 10 Comparison of astrocytic behaviour and axon recruitment in mucosal OECs, NSCs and bulbar OECs at 21 days post operatively. 94

Figure 11 Quantitative analysis of axon recruitment by olfactory ensheathing cells from the bulb. 96

Figure 12 Axon recruitment by ASC grafts in the thalamus. 99

Figure 13 Quantitative analysis of axon recruitment by adult Schwann cells. 101

Figure 14 Axon recruitment by NSC grafts in the thalamus. 105

Figure 15 Neovascularisation of the graft. 107

Figure 16 Quantitative analysis of axon recruitment by neonatal Schwann cells. 109

Figure 17 Mucosal-derived OECs 14 days post-OP in the thalamus. 112

Figure 18 Quantitative analysis of axon recruitment by olfactory ensheathing cells from the mucosa. 114

Figure 19 Immunorejection of human olfactory ensheathing cells in rats receiving oral or intraperitoneal cyclosporine. 119

Figure 20 Human OECs from the mucosa transplanted into rat thalamus. 121

Figure 21 Quantitative analysis of axon recruitment by human mucosal olfactory ensheathing cells. 123

Figure 22 Immune response to human OECs in rats receiving intraperitoneal cyclosporine. 125

Figure 23 Migration of neural crest stem cells.....130

Figure 24 Cell fate of neural crest stem cells grafted into the thalamus. 132

Figure 25 Axon recruitment by neural crest stem cells. 134

Figure 26 Histological appearance of the intact and lesioned fornix. 138

Figure 27 NSCs grafted into the lesioned postcommissural fornix. 143

Figure 28 OECs transplanted into the lesioned fornix. 146

Figure 29 14 day old embryonic brain cells transplanted into the lesioned fornix.....149

Table 1 Overview of measurements 152

Abstract

Olfactory ensheathing cells from the adult olfactory bulb (OECs) have been shown at our laboratory to facilitate axon regeneration in the spinal cord. They share similarities with Schwann cells at the histological level but appear to be more efficient at promoting axon regeneration. In particular, they enable axons to leave the transplant and re-enter the host CNS and establish lost connections with the target area. OECs and Schwann cells have been used at different stages of maturity and at varying purities. Besides these two cell types there are other candidate repair cells, most notably neural stem cells and OECs from the olfactory mucosa which may also be of use in reconstruction of severed fibre tracts. For screening the reparative abilities of these different cell types experiments in the spinal cord are time-consuming and technically challenging. The following experiments were therefore designed to address the need for an assay system to allow comparison of various candidate repair cells and deliver reliable, time-efficient and reproducible results.

Based on previous work from this laboratory, stereotaxically guided microinjection of cell suspensions into the lateral ventroposterior thalamic nucleus (VPL) was used to compare the behaviour of different cell types in terms of cell survival, cell migration, interaction with the host tissue and axon recruitment. OECs, adult Schwann cells (ASCs), neonatal Schwann cells (NSCs), neural crest stem cells

(NCSSs) and OECs derived from either the rat or human olfactory mucosa were investigated. The sham group only received injections of medium into the thalamus.

Approximately 3-5 μl of cell suspension at a concentration of $100x10^6$ cells/ml was injected into the thalamus via a micropipette that was slowly withdrawn so as to lay an artificial tract of the grafted cells. Animals were culled after survival times of one, two and three weeks and their brains processed for immunohistochemistry. Donor cells were identified by expression of the low affinity nerve growth factor receptor (p75), fibronectin and nestin. OECs from surgical biopsy samples of the human olfactory mucosa were detected by an antibody directed against human mitochondria (MIT) or by a human-specific p75 antibody. Axons were identified by immunoreactivity for neurofilament (NF). Host astrocytes and their processes were identified by glial fibrillary acidic protein (GFAP). An antibody against peripherin was used to identify NCSSs.

Samples were processed for immunohistochemistry based on the avidin-biotin complex method or for immunofluorescence studies using confocal microscopy. Immunohistochemistry was primarily employed to obtain tissue slides for quantitative assessment and to examine the immune response to human OECs transplanted into the thalamus.

Histological sections were then subjected to both qualitative and quantitative analysis. For qualitative analysis cell alignment and survival, interactions between host and donor tissue, and the recruitment of axons were examined.

The qualitative analysis showed all cell types survived. The cells formed a vertically orientated column aligned in parallel strands along the line of the pipette penetration of the thalamus. Differences in the shape and alignment of cells were noted. Neonatal Schwann cells and OECs from the rat mucosa displayed the highest degree of alignment and cells had long and slender cell nuclei in contrast to OECs from the bulb that had nuclei of plump and more oval morphology. NSC, ASC and OECs from bulb and mucosa could all be identified by p75. Fibronectin staining identified fibroblasts in OECs and Schwann cell transplants. Columns derived from all cell types were capable of recruiting axons. The astrocytic processes appeared to provide a guidance structure for axons. Astrocytes in close vicinity of the graft were hypertrophied but no significant differences were observed in their response to the different transplanted cell types employed.

NCSSs behaved in much the same way *in vivo* as they did *in vitro*. They differentiated into either neurons of immunohistochemically peripheral type or Schwann cell-like glial cells. They also appeared

to recruit axons but it was impossible to ascertain the origin or destination of delicate axons seen inside the graft.

Human xenografts were investigated for immune rejection using antibodies directed against CD4, CD8, MHC I and MHC II. OECs derived from the human olfactory mucosa were invariably rejected by the rat immune system if only oral immunosuppression with cyclosporine was employed. The immune response was significantly reduced in animals receiving systemic cyclosporine with few lymphocytes infiltrating the graft and better cell survival. However, the immune response was not completely abolished. The grafts were surrounded by MHC II-positive cells of microglial origin, but some grafted OECs could clearly be identified and survived well. The immune response measured by the degree of perivascular lymphocyte cuffing was notably stronger in animals that had only received oral cyclosporine. Perivascular cuffing of lymphocytes, a hallmark or intense rejection, was clearly visible in the vicinity of human grafts in orally treated animals. These cells also often displayed a honey-comb like arrangement and focal areas of necrosis.

Quantitative analysis was carried out for all cell types except NCSSs. It revealed that all cell types could recruit axons at a higher density than the sham group. NSC recruited the longest axons and at the highest density. There were unexpected differences between OECs

obtained from the rat olfactory bulb and those from the olfactory mucosa, with the latter cell type being almost as successful at axon recruitment as the NSC in terms of mean axon density and mean axon length. OECs from the bulb recruited axons at far lesser density and axons of slightly shorter length than their counterparts from the olfactory mucosa. Axon density and mean axon length for adult Schwann cells fell between that for OECs from the bulb and NSCs. OECs from the human olfactory mucosa attracted the least number of axons which did not differ much from the sham group, although they achieved a slightly higher axon density than the sham group after 2 weeks. The mean axon length was comparable to the sham group. These measurements probably reflect persistent immunorejection of the graft despite the fact that these animals had received systemic immunosuppression with cyclosporine.

The thalamus as a model did not lend itself to the study of axon re-entry into the host parenchyma given the lack of a suitable labelling method and a well-defined pathway. Hence, the postcommissural fornix was chosen to investigate host re-entry of fibres. The fornix is a very accessible white matter tract with a well-defined unilateral projection to the mammillary body. Radiofrequency heat lesions were generated with an electrode that was stereotaxically lowered to a point crossing the path of the post commissural fornix. Following removal of the electrode, a micropipette was then lowered to the lesion site and the cell suspension injected. In the final step the

fornix was labelled by injecting the subiculum with 2 µl of a 10 % solution of the tracer biotin dextran. For the main experiments, biotin dextran (BD)-labelling was performed shortly after the lesion had been generated, and the cell suspension had been injected. In some experiments, animals were labelled at the time of delayed grafting.

OECs and NSCs were transplanted into the fornix. The cells were identified with p75. Typically, a small column had formed at the dorsal site of the lesion, which ended in a somewhat spherical bolus of cells filling the lesion cavity. The bolus often had a central, necrotic core. In all cases, fornix fibres failed to advance into or past the lesion site. Regeneration into the bolus also failed when cells were transplanted with a 2 weeks delay. BD-labelled axons in close proximity to the lesion became thickened, exhibited many varicosities and often ended in growth-cone-like expansions. These axons resembled axons in pure lesions without grafting of cell suspensions, and just like them sprouted at the point were they came into contact with the lesion site.

Although axons were unable to advance into the lesion site, cells were seen to migrate from the graft into the proximal and distal ends of the severed fornix. At the proximal end cells clearly intermingled with the BD-labelled fibres. Interestingly, NF-immunoreactive axons were seen in both column and bolus but their origin could not be determined.

Embryonic rat brain cells obtained from whole brain preparations of 14 day old embryos failed to enable regeneration past the lesion site just like in the other cell types. These cells had a heterogeneous distribution and differentiated into various cell types. They sometimes appeared to be organised in subpopulations. They did neither express p75 nor GFAP with the exception of cells adjacent to surviving fibres of the fornix which expressed p75 weakly and diffusely.

Introduction

CNS injury

Damage to the central nervous system (CNS) as in stroke, head and spinal cord injury has devastating effects on the affected individual. The main problem exemplified by spinal cord injury is the disruption or severance of white matter tracts. After disruption, these fibre tracts fail to regenerate spontaneously. Severed nerve fibres in the adult CNS sprout in response to injury but do not elongate along their original pathways. Injury to the adult CNS is essentially an irreversible event. In the peripheral nervous system (PNS), the developing CNS, fish and amphibians the situation is quite different and cut fibres there are able to re-establish their original pathways and form synaptic connections with their former targets. This observation gave rise to the idea that the properties of a more permissive environment for regeneration, like the PNS, could be transferred to the adult CNS. Unlike the CNS, fibres in the PNS are able to regrow to their original destination and restore function. The striking differences between the PNS and CNS environments are highlighted by injury to the dorsal root fibres. Following axotomy, fibres are able to grow back along their original pathway outside the CNS but once they reach the CNS/PNS interface they fail to advance into the CNS.

Regeneration of cut axons requires several steps in succession. Firstly, severed fibres have to advance into the tissue bridge or cell transplant at the lesion site. They then have to extend through the graft and eventually leave the graft to re-enter the host CNS. In the last step, the axons have to trace their original way back to the target area and establish new synaptic connections. Functional regeneration will also require remyelination of the reconnected fibres.

Schwann cells

In 1928 Ramón y Cajal published the experiments of his pupil Tello who in 1911 was the first to attempt the transplantation of a conditioned sciatic nerve into the adult CNS (Cajal, 1928). It took 70 years before this idea was re-explored and the experiment replicated by Aguayo and co-workers (Richardson et al., 1980). Aguayo investigated the regenerative abilities of a sciatic nerve grafted into the spinal cord extensively. Horseradish peroxidase (HRP) and radioautographic axonal tracing in the thoracic spinal cord revealed that axons were innervating the graft but had failed to re-enter the rostral spinal cord stumps (Richardson et al., 1982). Some axons in the grafts originated from intrinsic CNS neurons with their cell bodies in nearby segments of the spinal cord, whereas others arose from the dorsal root ganglia. However, the corticospinal tract did not contribute any fibres.

In an extension of these earlier experiments, Schwann cells were cultured from peripheral nerve and transplanted as cell suspensions into the CNS. This enabled a less traumatic transplantation procedure and a more accurate cell placement. Such grafts transplanted into the spinal cord are able to attract fibres into the graft, but once again the axons are unable to leave the transplant and make contact with the CNS (Li and Raisman, 1995). Even genetically engineered Schwann cells, designed to secrete brain-drived neurotrophic factor (BDNF), were unable to mediate re-entry of fibres into the spinal cord (Menei et al., 1998). Newer studies however, seem to indicate that limited host re-entry is possible under special circumstances (Xu et al., 1999). While Schwann cells seem to have a limited potential for regeneration in the spinal cord, some as yet unconfirmed reports claim that they guide back axons to their original destination at other sites of the CNS (post-commissural fornix; Stichel et al., 1996, and the septo-hippocampal cholinergic pathway; Montero-Menei et al., 1992).

Neural stem cells

Neural stem cells are traditionally defined by their ability either to renew themselves thereby replenishing a pool of stem cells (symmetrical division) or to differentiate into mature cell types (asymmetrical division). Neural stem cells are defined as having the potential to generate all the major cell types found in the CNS but it is

thought that once the cells have differentiated into progenitors of either neuronal or glial lineage they are restricted to a specific cell fate and cannot revert to an earlier state.

In modification of this original concept of stem cells there is increasingly evidence to support a more dynamic concept (Blau et al., 2001) of stem cells. Cell that would be considered as progenitor cells (immature cells that have a more lineage-restricted differentiation potential than stem cells) have the ability to self-replicate and cells that have apparently reached maturity (Dupin et al., 2003) might de-differentiate again under certain circumstances and even trans-differentiate to a different lineage (Koshizuka et al., 2004). Nevertheless, it is useful at least for working purposes to consider stem cells as cells capable of both self-renewal and differentiation into lineage-restricted progenitors that give eventually give rise to specific mature CNS cells of different classes.

Phenotypically, both stem cells and progenitor cells stain for the marker nestin (Dahlstrand et al., 1995). There are a growing number of other stem cell markers like Presenilin, Notch, and Numb but none of them appear to be uniquely specific for stem cells (Maslov et al., 2004;Cai et al., 2002;Cai et al., 2003).

Proof for a given cell being a neural stem cell is normally obtained from functional in-vitro assays. Neural stem cells can be expanded

as clones if they are cultured as neurospheres (Reynolds and Weiss, 1992) in serum-free medium. Single cells obtained from neurospheres can form new neurospheres or they can be differentiated into glia and neurones.

Various parts of the postnatal and adult CNS contain cells capable of forming new cells. Most notably are the dentate gyrus of the hippocampus, the subventricular zone (SVZ) (Levison et al., 2003) and the olfactory bulb (Liu and Martin, 2003) as well as the olfactory epithelium (Chuah and Au, 1991). The developing neural crest is a source of stem cells but these cells appear to be more restricted in their lineage commitment (Mujtaba et al., 1998) (Stemple and Anderson, 1993) (Kruger et al., 2002) and cannot differentiate into all types of CNS cells.

It is surprising that despite the existence of stem cells in the adult brain there is very little active repair after CNS injury. This may reflect inhibitory conditions of the mature CNS that suppress the development of mature CNS cells and/or the lack of a large enough stem cell pool whereby the generation of replacement cells is exceeded in number by cell loss.

The great attraction of neural stem cell grafts relates to their potential use for a number of different therapeutic purposes. They can form neurons that could either replace lost neurons in degenerative

conditions, or act as relay bridges to restore circuits. If they formed glia they could act as bridges for axon regeneration, or replace oligodendrocytes and re-myelinate fibre tracts. Neural stem cells may also support axon regeneration through the secretion of neurotrophic factors (Lu et al., 2003) in animal models where axons are disconnected.

Protocols exist to expand the number of stem cells *in vitro* (Gottlieb, 2002). Much hope is pinned on the possibility that they might respond to local tissue cues and differentiate exactly into the kind of tissue needed at the injury site or even migrate to it (Leavitt et al., 1999;Imitola et al., 2004). Damaged areas in the CNS might release factors that attract and influence the development of stem cells. Since stem cells can turn into more than one cell type they have a theoretical advantage over simply transplanting a single more differentiated cell type.

Olfactory ensheathing cells

The olfactory system (Figure 1) is the only site in the central nervous system (CNS) where neurons and axons are continuously replaced during adult life (Huard et al., 1998;Graziadei and Graziadei, 1979). Specialised sensory neurons responsible for odour perception are located in the olfactory epithelium of the nasal cavity. The olfactory mucosa is a specialised pseudostratified epithelium made up of various cell types. The globose basal cells (a putative stem-cell)

(Mackay-Sim and Kittel, 1991), sustentacular (supporting) cells and the olfactory receptor neurons represent the more important cellular elements of this system. The globose basal cells give rise to new neurons (Sicard et al., 1998;Murrell et al., 1996). These neurons migrate apically in the epithelium where they extend one apical dendrite and a basal axon. On their way from the olfactory mucosa to the olfactory bulb neurites have to grow through the basal cell layer and connective tissue and traverse the cibriform plate of the ethmoidal bone. From there they continue within the bundles of olfactory nerves, enter the olfactory bulb and finally establish synapses in the glomerular layer of the olfactory bulb. When air-borne molecules are inhaled and carried in the air-stream to the nasal cavity they come into contact with the olfactory receptor cells. Smell is perceived whenever a specific group of molecules is recognised by the ciliated dendrite triggering an action potential that spreads along the axon to the first relay station in the olfactory bulb.

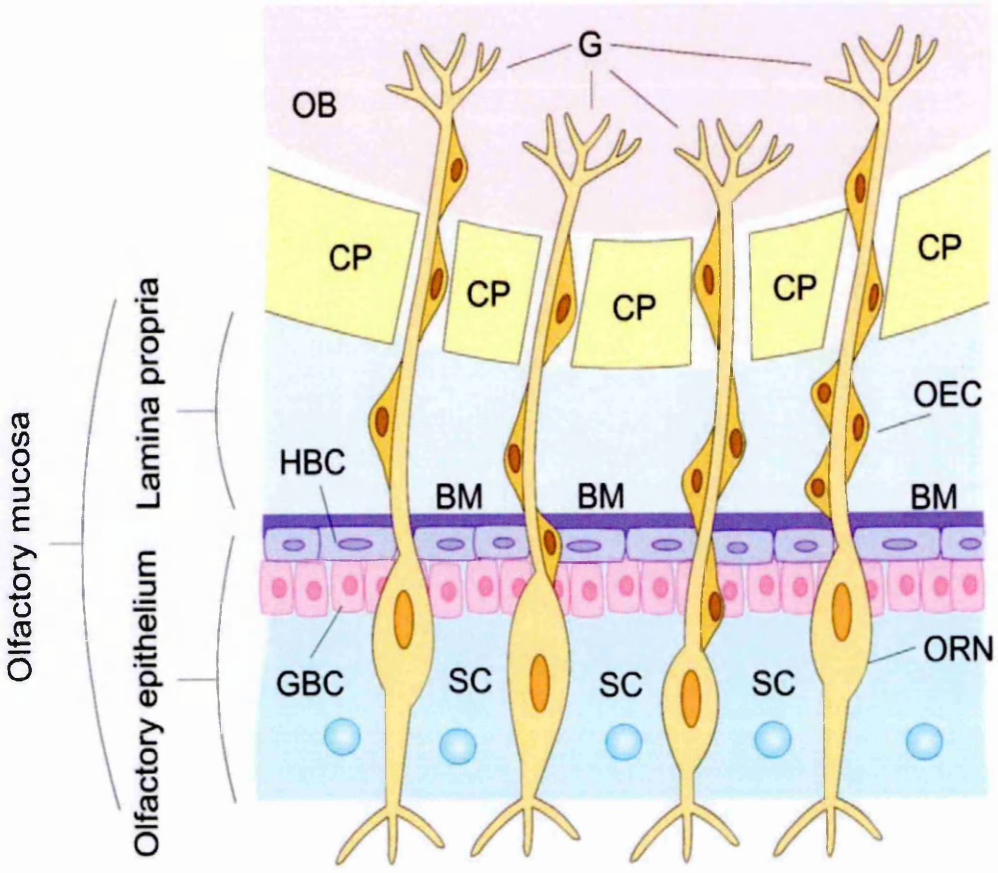

Figure 1 Schematic representation of the olfactory system.

The olfactory system is the only site in the central nervous system (CNS) where neurons and axons are continuously replaced during adult life

The olfactory mucosa is divided into an epithelium and a lamina propria. The epithelium is separated from the underlying lamina propria by a basal lamina (**BM**). The main cellular constituents of the epithelium are the horizontal (**HBC**) and the globose basal cell (**GBC**) and the sustentacular cell (**SC**). The lamina propria is made up of loose connective tissue. Typical cellular constituents are fibroblasts and cells associated with blood vessels and also macrophages.

Olfactory receptor neurones (**ORN**) are located in the olfactory epithelium of the mucosa (**M**). Their axons traverse the lamina propria of the mucose and then the cribriform plate (**CP**) and eventually form synapses in the glomeruli (**G**) of the olfactory bulb (**OB**).

Olfactory ensheathing cells (**OEC**) accompany and ensheath olfactory nerves along their path from the mucosa to the bulb. When the olfactory nerve is injured they also provide guidance channels for regenerating axons. The globose basal cell (**GBC**), a putative stem cell (Goldstein and Schwob, 1996), gives rise to new neurones.

The olfactory nerve fibres are accompanied and ensheathed by a unique Schwann cell-like cell type, the olfactory ensheathing cell (OEC). This cell is found beneath the olfactory epithelium in the lamina propria (Au and Roskams, 2003). Rather than enfolding individual axons, like a non-myelinating Schwann cell, the OECs ensheathe whole bundles of olfactory axons and cover them to the glomerular layer of the olfactory bulb. Olfactory neurones subjected to damage die at once and are immediately replenished from the stem cell pool. The regeneration of their axons to the olfactory bulb is associated with OECs. Local OECs provide a guidance channel for regenerating olfactory axons. They do not migrate or divide under these circumstances (Li et al., 2005), a feature that sets them apart from Schwann cells involved in the repair of damaged peripheral nerve. Olfactory neurones only have a short life-span and the turnover rate is about 28 days (Graziadei and Graziadei, 1979). Experiments aimed at obliterating the olfactory mucosa or olfactory bulb have demonstrated the enormous potential for self-repair in the olfactory system (Chuah et al., 1995). This unique ability of the olfactory system for self-regeneration drew the attention to OECs as potential candidate repair cells in CNS injury. OECs were able to achieve axon regeneration in a dorsal root transection model (Ramon-Cueto and Nieto-Sampedro, 1994). Just like Schwann cells OECs induce axon elongation but unlike Schwann cells they also allow re-entry into the CNS both in the olfactory bulb and in the dorsal root (Li et al., 2004). Experiments at our laboratory

demonstrated that it is possible to regenerate the severed corticospinal tract in the spinal cord by micro-injecting OEC suspensions into the lesion site (Li et al., 1997;Li et al., 1998). Other groups were able to corroborate these findings (Ramon-Cueto et al., 1998). Whereas Schwann cell transplants induce highly tortuous axons with interspersed varicosities and multiple branching points, OECs recruit axons running in well-aligned parallel fascicles. And although axons in the olfactory system are unmyelinated, OECs are capable of myelinating axons in the spinal cord (Imaizumi et al., 1998). Most importantly, OECs facilitate actual host re-entry of axons, the crucial prerequisite for functional recovery. Rats that had been given OEC grafts regained forepaw reaching function after spinal cord lesions (Li et al., 1997). More recent experiments have shown that even elementary functions like breathing can be restored following transplantation of OECs to lesions in the cervical spine (Li et al., 2003). Most researchers use OECs from the glomerular layer of the olfactory bulb but OECs can also be found in a clinically more accessible location, namely the olfactory mucosa where they are derived from a precursor cell (Chuah and Au, 1991) in the mucosa. Both cultured OECs from the olfactory mucosa as well as pieces of lamina propria promoted functional recovery and axon regeneration in spinal cord transection (Lu et al., 2001). Delayed studies using these cell types some time after causing the spinal cord injury were likewise successful (Lu et al., 2002;Keyvan-Fouladi et al., 2003).

OECs are derived from the olfactory placodes. Without using purification procedures (as in this study), OEC cultures contain contaminating cell types, principally meningeal cells. The olfactory ensheathing cells resemble Schwann cells and express several typical Schwann cell markers such as p75 and S100. They also express GFAP and weakly express fibronectin. Meningeal cells express fibronectin strongly and fail to react with p75. OECs and meningeal cells co-operate in remyelination. Meningeal cells often enclose bundles of OEC-myelinated axons, an arrangement reminiscent of the perineurium seen in peripheral nerves (Lakatos et al., 2003b). A similar interplay between Schwann cells and fibroblasts is involved in the formation of the perineurium of peripheral nerves. The signalling molecule Desert Hedgehog (Dhh) is secreted by Schwann cells and controls the organisation of the surrounding connective tissue (Mirsky et al., 1999). Dhh is also strongly expressed by transplanted OECs (Smith et al., 2001). Both OECs and Schwann cells are capable of myelinating axons as demonstrated by the presence of P_0 mRNA , the gene for the major peripheral myelin protein. Despite the fact that there are no myelinated axons in the olfactory system OECs are able to myelinate axons in spinal cord injury models.

Both OECs and Schwann cells express an impressive range of neurotrophic factors (Boruch et al., 2001;Taylor and Bampton, 2004;Friedman et al., 1999) and respond to the same growth-

promoting molecules in culture. However, in specific culture conditions, Schwann cells (Mirsky et al., 2002) unlike OECs (Lipson et al., 2003) have been shown to express also neurotrophin 3 (NT3).

Despite these obvious similarities between them, OECs and Schwann cells seem to differ in their response to CNS injury. Schwann cells increase sprouting at the lesion site while OECs, in contrast, reduce sprouting and promote host re-entry. Transplanted OECs also appear to have superior migratory abilities in the CNS than Schwann cells. Most notably are the differences observed between OECs and Schwann cells when they come in contact with host astrocytes. In the olfactory bulb OECs co-exist with astrocytes unlike the peripheral nervous system which is devoid of astrocytes. Both OECs and astrocytes contribute to the glia limitans in the olfactory bulb. In CNS injury, OECs seem to suppress astrogliosis whereas Schwann cells induce astrocytic hypertrophy. Moreover, Schwann cells induce apoptosis in astrocytes. In culture, OECs freely intermingle with astrocytes and even migrate into areas containing astrocytes (Lakatos et al., 2000). Although Schwann cells are able to migrate across astrocytes monolayers they generally avoid contact with astrocytes and induce hypertrophy in astrocytes, corresponding to the *in vivo* situation. OECs and Schwann cells transplanted into the uninjured white matter of the adult rat spinal cord evoke very different reactions. Transplanted OECs lead to a milder expression of GFAP and chrondroitin sulfate proteoglycans

(Lakatos et al., 2003a) in the host tissue than do transplanted Schwann cells. OECs reduce the expression of proteoglycans, a group of growth-inhibiting molecules, in reactive astrocytes (Verdu et al., 2001) unlike Schwann cells that increase the deposition of proteoglycans at the lesion site (Plant et al., 2001). Much of the unique effects of OECs probably depend on direct cell-to-cell interactions. OEC-conditioned medium, containing OEC-specific neurotrophic factors, does not appear to stimulate neurite outgrowth of embryonic chick ganglia in culture whereas co-cultures with OECs do (Lipson et al., 2003).

The situation *in vivo* is probably more complicated since most culture studies were comparing pure OECs or Schwann cell cultures but there is evidence to suggest that mixed cell transplants have different properties from pure suspensions. It appears that the meningeal cells restrain the migratory behaviour of the OECs and that the two cell types together are more effective in axon regeneration than OECs alone. Recent experiments have also shown that pure cultures of OECs are less effective at remyelination than mixtures of this cell type with meningeal fibroblasts (Lakatos et al., 2003b).

The astrocytic response to injury

An important impediment to axon regeneration is the so-called 'glial scar', characterised by a reactive gliosis that forms in the wake of CNS injury (Silver and Miller, 2004). This scar is heterogeneous in

its composition and made up of reactive astrocytes, macrophages, fibroblasts, oligodendrocytes, endothelial cells, leucocytes and various non-cellular elements in the extracellular matrix like proteoglycans (Asher et al., 2001) and a well-defined laminated basal membrane (BM) in the lesion centre (Reier and Houle, 1988). Fibroblasts derived from the meninges migrate to the injury site and aid in the formation of this basement membrane (Carbonell and Boya, 1988). The BM represents a well-defined extracellular matrix (ECM) with collagen IV and laminin as the main components (Timpl and Brown, 1996). The typical response to CNS injury is characterised by hypertrophy of both astrocytic cell bodies and re-arrangement of their cell processes. Astrocytes actively migrate towards the injury site. They strongly express GFAP and interdigitate their processes (Norenberg, 1994). They also participate in the phagocytosis of cellular debris, occupy the spaces left behind by degenerating cells and together with fibroblasts reconstitute a new glial limiting membrane. In addition, astrocytes can also act as antigen-presenting cells (Dong and Benveniste, 2001) and present antigens in an MHC-restricted manner.

The significance of the astrocytic response to CNS injury has been validated by a number of experiments. The potential for axon regeneration depends to a great deal on the extent of CNS injury characterised by the astrocytic response. Cell suspensions of dorsal root ganglia neurones microinjected into the corpus callosum of rats

were capable of extending neurites over a long distance provided the injection site was only minimally perturbed (Davies SJ et al., 1996). Fibre regrowth was reduced if, however, the injection procedure disturbed the cytoarchitecture profoundly (Davies SJ et al., 1999).

To improve regeneration various attempts have been made to ablate reactive astrocytes. Most ablation methods employed either chemical means (ethidium bromide) (Moon et al., 2000) or X-irradiation (Trotman et al., 2004). These experiments largely support the view that astrocytes impede regeneration and therefore that axons regenerate better in the absence of astrocytes. Recently, a more elegant method for the selective ablation of reactive astrocytes has been introduced. A transgenic mouse was created that had a thymidine kinase (HTK) gene inserted downstream of the GFAP promoter region. Reactive astrocytes activate the GFAP gene and thereby up-regulate the expression of the HTK enzyme. These animals were given systemic ganciclovir which was then converted into a cytotoxic metabolite by the HTK enzyme (Bush et al., 1999;Delaney CL. et al., 1996). The reactive astrocytes were hence selectively destroyed by ganciclovir administration. The animals received stab wounds to the cortex and hippocampus. Expression of neurofilament M was increased in the path of the stab wound, an area that had become devoid of astrocytes. Interestingly, this area was also lacking neuronal cell bodies.

To some extent, this scar tissue acts as a physical barrier that obstructs the growth of axons and blocks the diffusion of chemoattractive molecules from the injury site. Studies based on calculating the diffusion coefficients with tetramethyl ammonium-sensitive electrodes were able to demonstrate decreased diffusion in regions of astrocytic hypertrophy and increased chondroitin sulphate expression (Roitbak and Sykova, 1999).

However, the recent emphasis is on inhibitory molecules expressed by the extracellular matrix (Filbin, 2003). The available options are hence directed at removing these inhibitory molecules or inhibiting their effects. Various inhibitory molecules have been identified at the injury site. These include the chemorepellant semaphorin III (De Winter et al., 2002), chondroitin sulphate, keratin and the proteoglycan NG2 to name but a few.

One major class of inhibitory molecules found in the extracellular matrix are the chondroitin sulphate proteoglycans. Chondroitinase ABC is a bacterial enzyme that can cleave glycosaminoglycans from the chondroitin sulphate core. Experiments conducted in a crush-model of the dorsal column in rats treated with chondroitinase ABC revealed axon elongation originating from the sensory neurons in the dorsal root ganglia and cranial extension of the fibres for up to 4 mm in the spinal cord (Bradbury et al., 2002). In a similar fashion, the corticospinal fibres regenerated downwards from the site of injury.

The basement membrane (BM) situated at the centre of CNS injury has been singled out as another target for pharmacological intervention. One of the major constituents of the BM is collagen IV (Coll IV) amongst about 50 other constituents like the proteoglycans. Coll IV is formed by an interaction of astrocytes with fibroblasts or endothelial cells. Coll IV forms a stable triple helix only after hydroxylation of newly synthesized collagen molecules. The deposition of Coll IV at the BM can be reduced by the topical application of α,α'(2,2')-dipyridyl (DPY), an iron chelator, that inhibits a key enzyme in this process. This approach was successfully employed to lesions of the transected post-commissural fornix (Stichel et al., 1999c). Axons were able to traverse the injury site and elongate up to their normal target, the mamillary body. Astrocytes and their processes intermingled with the regenerating fibres. This technique also enabled transected nigrostriatal dopaminergic axons to reinnervate the striatum in adult mice and mice at postnatal age 14 suggesting that type IV collagen is required for the development of the fibrotic response to adult brain injury (Kawano et al., 2005). However, the same regeneration paradigm failed in the thoracic spinal cord (Weidner et al., 1999b).

Myelin-associated inhibitory molecules

The normal function of oligodendrocytes is to envelope axons with myelin sheaths to provide electrical insulation and enable an increase in the propagation speed of action potentials along the Ranvier nodes. Myelin contains molecules that impede axon regeneration. In a landmark experiment (Schwab and Thoenen, 1985) dissociated newborn rat sympathetic or sensory neurons were plated in the presence of sciatic nerve or optic nerve segments. It was then shown that dorsal root ganglions extended their axons across Schwann cells from the sciatic nerve but avoided contact with myelin and oligodendrocytes from the optic nerve (Schwab and Caroni, 1988). This observation gave rise to the concept that myelin was responsible for regenerative failure in the CNS. Mice immunised with myelin showed extensive regeneration of large numbers of axons of the corticospinal tracts after dorsal hemisection of the spinal cord and recovered certain hind limb motor functions (Huang et al., 1999). Likewise, antisera taken from immunized mice were able to block myelin-derived inhibitors and promote neurite growth on myelin *in vitro*. Schwab identified two inhibitory protein fractions associated with myelin (Caroni and Schwab, 1988). An antibody raised against these proteins could overcome the inhibitory effects of myelin and oligodendrocytes. This antibody, called IN-1, was subsequently injected in rats subjected to experimental spinal cord injury (Bregman et al., 1995). The rats regained a degree of their normal function

after the operation and about 5 % of the fibres regenerated across the lesion site. The molecules recognised by IN-1 were unknown for a long time. More recently, a gene named Nogo encoding an inhibitory molecule recognised by IN-1 has been discovered (Chen et al., 2000). The gene has 3 alternative isoforms, designated as Nogo-A, -B and –C (Schwab, 2004). Nogo A has the strongest inhibitory properties and is highly expressed by oligodendrocytes but not by Schwann cells.

Rats that had undergone complete transections of the cervical corticospinal tract and were subsequently treated with the anti-Nogo-A antibody mAb IN-1 recovered their ability to perform precise forelimb and finger movements (Raineteau et al., 2001). Another specific monoclonal antibody (7B12) directed against Nogo A has been created. This antibody was successfully employed in a rat stroke model to improve forepaw function 24 hours after the initial lesion (Wiessner et al., 2003). Corticospinal fibres from the uninjured sensorimotor cortex crossed the midline in the cervical spinal cord and bypassed the lesion site. Their number correlated positively with the behavioural outcome. The antibody did not improve the size of the infarct volume. The results therefore suggest that an improvement in behaviour was solely the result of uninjured fibre tracts forming new synapses with spinal motor neurones, thereby establishing alternative pathways. More recently, the extensively used anti-Nogo-A antibody mAb IN-1 was effective in achieving axon

growth through the lesion site in a primate model of unilateral lesioning of the thoracic corticospinal tract (Fouad et al., 2004).

Nogo, however, may not be the only inhibitory molecule recognised by IN-1. There are other yet un-identified inhibitory proteins associated with myelin (Filbin, 2003).

Requirements for an assay system

Our experience with human olfactory bulb samples has shown that cells with similar properties to the rat OECs can be obtained from tissues removed surgically as part of another operation, or material up to several hours post mortem. However, neither source is abundant, and the numbers of cells obtained from a single human olfactory bulb, given its small size, is very limited, and would not be sufficient to repair any substantially sized human lesion. Therefore it is important to look for other sources of candidate repair cells. The olfactory mucosa is hereby of particular interest since it is easily accessible from a surgical point of view (Feron et al., 1998) and could be grafted into the same patient without the need for immunosuppression. Adult Schwann cells (ASCs) either genetically modified or enhanced with OECs could be another potential source for candidate repair cells, as could be certain stem cell populations like OECs derived from stem cells in the olfactory mucosa or the neural crest stem cells (NCSCs).

To carry out the large number of tests (ability to enhance regeneration, dose response, toxicity etc) needed to validate the use of any one of the many candidates for reparative cells and their enhancement, it is essential to have an assay system capable of screening various types of cells and procedures preparatory to the

much more time consuming tasks of trying out these cells in microlesions of the corticospinal tract. Dissociated cell cultures such as dorsal root ganglia (Scott, 1977) and retinal ganglia cells (Baehr and Bunge, 1990) have been used in the past to investigate the properties of certain growth factors and cells like Schwann cells. Cell cultures, unfortunately, do not necessarily allow results to be related to the in-vivo situation, as the cellular elements are analysed in isolation from their environment in the living animal.

Any assay system would have to address a number of specific points. How well do transplanted candidate repair cells survive after transplantation? Do they integrate well into the host environment and are they aligning and co-operating with existing tissue structures? Do the transplanted cells display any migratory behaviour? What is the host response to the recipient cells? To what extent are axons recruited into the graft and what is their arrangement in relation to astrocytic processes and candidate repair cells? Do these fibres manage to leave the graft and re-enter the host environment? In addition, a number of other requirements need to be fulfilled by an assay system. Chief among them is the need for reliable and reproducible results that allow careful comparison of different candidate repair cells. Moreover, the assay system should enable quick screening of multiple cell lines.

Creation of cell columns in the thalamus

The technique of stereotaxic microinjection of cells into the thalamus was originally introduced in this laboratory by Gary Brook (Brook et al., 1994;Brook et al., 2001). He demonstrated the possibility of laying a column of cells into the thalamus, thereby in effect creating an artificial white matter tract to support the recruitment of axons from the host CNS into the graft. He was able to study host axons entering the graft and their response to various cell types. The relative simplicity of this approach and the speed with which it can be performed lend itself ideally for use as an assay system to study various candidate repair cells. Operations on the spinal cord are time-consuming and require substantial technical expertise, whereas microinjections to the thalamus owing to its large size and accessibility can be accomplished in a short space of time. The microinjection technique is relatively atraumatic (Raisman et al., 1993) and thereby largely avoids the negative impact of the glial scar on the regeneration process. Another important advantage is that the animals subjected to this procedure do not sustain any functional neurological deficits and hence do not require any special post-operative care requirements. This screening assay only assesses the anatomical changes in response to cell transplantation. The behavioural tests can later be properly conducted in a spinal cord model once a suitable candidate repair cell has been identified by the assay.

Transplanting human cells into the rat CNS

Translating animal studies into therapeutic approaches

Animal models can provide useful information on the reparative capacities of candidate repair cells. For potential clinical applications, however, one cannot automatically assume that the human counterparts of suitable animal candidate repair cells would also be able to accomplish fibre regeneration in humans. To bridge the knowledge gained from the animal model to actual clinical applications, it has become necessary to extend the thalamus model to human candidate repair cells. The most promising source for human candidate repair cells lies in the olfactory nasal mucosa, an area that is easily accessible to the ear nose throat surgeon and would allow auto transplantation of cultured cells into the site of CNS injury.

If it could be shown that human OECs from the olfactory mucosa provide the same benefits in the rat model as rat OECs of mucosal origin with regard to axon recruitment and fibre regeneration, then most likely the same cells would also work in humans. Unfortunately, such an undertaking does not come without certain difficulties since humans and rats are very different species and xenografts are quickly and forcefully rejected by the host immune system.

Mechanisms of rejection in syngeneic, allo- and xenografts

The CNS has traditionally been regarded as an immunologically privileged site. Its unusual immunological status is explained in part by the blood brain barrier (BBB) formed by endothelial cells and astrocytes, the weak expression of major histocompatability complex antigens (MHC) of class I and II, the lack of a classical lymphatic drainage and strong anti-inflammatory properties of the brain parenchyma. However, this privilege is not absolute and allografts (Lawrence et al., 1990) and xenografts in particular are invariably rejected. Although a lymphatic drainage for the brain has not been described anatomically, tracer substances and cells that are injected into the brain are detected within a few hours to days in the deep cervical lymph nodes in rodents (Bradbury and Westrop, 1983;Oehmichen et al., 1979). The cervical lymph nodes are capable of antigen-specific B-cell proliferation and antibody production in response to an intracerebral deposition of antigen (Larsson et al., 2001;Cserr and Knopf, 1992). The intact BBB is impenetrable to immunoglobulins and naïve T-cells but activated T-cells can traverse this barrier (Wekerle, 1986). Furthermore, injury and inflammation disrupt the integrity of the BBB (Pachter et al., 2003;Gloor et al., 2001) allowing the influx of molecules that would normally not cross the BBB.

Neural xenografts are generally quickly rejected by the recipient with perhaps one known exception; studies with human adult Schwann

cells (ASCs) in our laboratory (Li, unpublished observations) revealed survival of these donor cells in the rat spinal cord without the need for immunosuppression. These unexpected findings are supported by an earlier study in Wistar rats suggesting that both human ASCs and NSCs can survive without any overt signs of rejection for up to 10 weeks after implantation (Hermanns et al., 1997). Experiments using xenogeneic grafts of mouse sciatic nerve to bridge excised segments of facial nerve in rat recipients (Choi and Raisman, 2003) demonstrated that short segments could lead to restoration of the blink reflex without the need for immunosuppression whereas immunosuppression was required to restore function in longer segments. These observations point at a low-grade rejection of Schwann cells by the host immune system. There are no reports in the literature that would explain this apparent anomaly. One has to assume that Schwann cells either have a lower immunogenenicity or that they are able to reduce the strength of rejection by some unknown mechanism. There are a few reports that ascribe immunomodulatory functions to Schwann cells (Bonetti et al., 2003) (Colomar et al., 2003) which may account for the impaired immune response.

Grafts can be classified as syngeneic, allogeneic and xenogeneic. Syngeneic transplants are derived from the same animal or cloned or inbred animals with the same genotype. They only elicit a very weak

non-specific inflammatory response that largely depends on the extent of tissue trauma and immunosuppression is not required.

The term allogeneic refers to tranplantation of tissue between animals of the same species. The need for immunosuppression depends on the extent of host-graft strain mismatch. Incompatability at both class I and II MHC loci leads to vigorous rejection (Mason et al., 1986;Lawrence et al., 1990).

Xenografts can be divided into concordant (between closely related species), and discordant grafts (between distantly related species). In general, the less two species are related to each other the stronger is the response by which the xenograft is rejected. In practise this means that mouse nerve cells will survive far better than porcine neurones transplanted into the rat CNS. It has been speculated that the poorer survival of discordant xenografts may be attributed to a higher susceptibility to humoral (antibody-mediated) rejection. As the xenograft becomes vascularised over time antibodies gain access to the graft. A study in normal mice and immunoglobulin deficient (IgKO) mice revealed better survival of embryonic porcine ventral mesencephalic cells in IgKO mice (Larsson et al., 1999). The majority of IgKO mice had surviving grafts for up to 4 weeks, whereas survival was minimal in control mice beyond the 4 day horizon. Interestingly, the late rejection response in IgKO mice was largely CD8 T-cell mediated.

MHC class II antigens play an important role in xenograft rejection. This was shown in MHC class II-deficient mice (Duan et al., 2002) serving as xenograft recipients for dissociated embryonic ventral mesencephalic tissue from Sprague-Dawley rats. All of the MHC class II-deficient mice had surviving grafts in the striatum 4 weeks post-grafting. In contrast, only a few of the MHC class I-deficient mice exhibited surviving grafts and none of the wild-type mice had any surviving grafts. These results suggest that the indirect pathway of foreign antigen recognition mediated by host MHC class II molecules and helper T cells is crucial for the rejection response to intracerebral xenografts.

The importance of MHC may be surprising, since MHC antigens are scarcely expressed by neuronal cells in the CNS. However, class-I antigens are present on endothelial cells. Other investigations have demonstrated MHC class-II antigens on microglia (Lawrence et al., 1994) and astrocytes (Dong and Benveniste, 2001). Furthermore, MHC antigens are inducible by injury and surgical trauma. Neural xenograft cell suspensions are often not pure and contain 'contaminating' cells like endothelial cells and microglia which are known to express MHC antigens. These non-neural cells are assumed to contribute to the immunogenicity of the graft. In an attempt to reduce the immune response to porcine donor tissue, microglial cells were removed with antibodies (anti-Gal) against the α–galactosyl epitope and complement (Brevig et al., 2001). This pre-

treatment reduced the microglial content to 11-24% of the control group. Purified human CD4 T-cells were co-cultured with porcine embryonic brain cells. Human CD4 cells did not proliferate in porcine embryonic brain cells pre-treated with anti-Gal but did proliferate in a control culture treated only with complement. These experiments suggest that it is not primarily the neural cells but other accompanying cells that induce a strong immune response.

Similar observations were made in immunocompetent rats with 6-hydroxydopamine induced hemiparkinsonism receiving dissociated ventral mesencaphalic (VM) tissue from pig embryos pre-treated with anti-Gal and complement or medium and complement (control group; (Brevig et al., 2001). In five out of eight rats receiving pre-treated VM cells, a reduction of amphetamine-induced circling behaviour by more than 50 % was observed whereas improvement was not seen in the control group.

Xenograft rejection is mediated by T-lymphocytes which ultimately infiltrate the graft. The role of T-cells is supported by several lines of evidence; xenografts survive better in T-cell deficient hosts and in animals receiving immunosuppressive drugs like cyclosporine (CsA) and tacrolimus (FK506) (Castilho et al., 2000). Monoclonal antibodies directed against $CD4^+$ T-cells prolong the survival of both concordant (rat fetal neocortex) and discordant (human fetal forebrain tissue) neural xenografts in a mouse model (Wood et al.,

1996). These findings are consistent with previous investigations showing that the rejection of skin xenografts depends critically on the presence of $CD4^+$ lymphocytes.

All the available data support the concept, that neural xenografts are predominantly rejected by the indirect pathway, whereby a foreign peptide is presented to T lymphocytes by an antigen-presenting cell in the context of self major histocompatability complex antigens (MHC) although the direct pathway (direct stimulation of T lymphocytes by foreign MHC) may also play also a role, at least in non-neural grafts (Chitilian et al., 1998). Graft antigens, in the form of cell debris and shed molecules, are drained to the cervical lymph nodes where they are processed by host dendritic cells and presented in the context of MHC class-I and class-II molecules to CD4 and CD8 T-cells. CD4 T cells transform into helper T cells, which as their name implies, help to activate B cells and CD8 T-cells. CD4 T cells also turn into inflammatory cells that act on macrophages in the graft thereby initiating a delayed-type hypersensitivity-like response. CD8 T-cells become either cytotoxic cells, lysing cells bearing MHC class-I molecules on their cell surface, or downregulate the immune response in their capacity as suppressor cells.

Markers of rejection

The immune response to xenografts is characterised by the involvement of various immune cells over time as shown in a study with dissociated mesencaphalic tissue from syngeneic, allogeneic and xenogeneic origin transplanted into the striatum of adult rats (Duan et al., 1995). Hosts were sacrificed at 4 days, 2 weeks or 6 weeks after surgery. Their brains were processed for MHC class I and II antigens, complement receptor 3 (CR3) antigens on microglia and macrophages, helper T-lymphocyte antigen-cluster of differentiation (CD4), cytotoxic T-lymphocyte antigen (CD8) and tyrosine hydroxylase immunohisto-chemistry.

Animals with syngeneic grafts expressed low levels of MHC class I and II antigens at all times. CR3 positive cells were initially found in the graft area but by 2 and 6 weeks their numbers had fallen and they were mainly located at the graft-host interface. The numbers of CD4 and CD8 immunopositive cells were low by 4 days and 2 weeks and fell to undetectable levels by 6 weeks.

Xenogeneic grafts displayed signs of rejection from an early stage onwards. These animals had not received any drugs to stem rejection. At 4 days post operation (post OP) small cavities were visible in a number of grafts and at 2 weeks and beyond scarring and necrosis became more apparent. At 6 weeks all transplants had become rejected. Large numbers of MHC class I-positive cells of

round morphology were noted as early as 4 days post OP and continued to become more pronounced at the later time points. In contrast, MHC class II-positive cells were low at 4 days post OP but increased markedly in number by 2 and 6 weeks. These cells displayed mostly round morphology in the graft and resembled microglia at the graft periphery. MHC class II-positive Cells were often found in blood vessels located in close proximity to the graft. Perivascular cuffing by both MHC class I and MHC class II-positive round cells was also observed. This was most pronounced by 2 weeks after transplantation. Activated CR3-positive microglia and macrophages were seen at all time points. At 4 days there were only small numbers of lymphocytes but by 2 weeks grafts were heavily infiltrated with CD4 and CD8-positive T-cells. Perivascular cuffing was also noted.

Reducing graft rejection/ immunosuppression

Cyclosporine A (CsA), an inhibitor of T-cell activation (Masri, 2003), can delay and sometimes even completely abolish rejection. Previous studies have shown its effectiveness in neural xenotransplantation (Brundin et al., 1985). CsA is a cyclic polypeptide consisting of 11 amino acids produced as a metabolite by the fungus species *Beauveria nivea*. The $CD4^+$ T-lymphocyte is the main target but CsA also affects $CD8^+$ T-cells and the release of interleukin 2 (Il-2) and other lymphokines. Similar properties have been ascribed to tacrolimus (FK 506), a more potent

immunosuppressant than CsA. FK 506 was isolated from the Streptomyces tsukubaensis strain. It can inhibit Il-2 at concentrations almost 100 times lower than CsA. Like CsA it affects an early phase in the T-cell activation pathway but has chemically a very different molecular structure.

Both CsA and FK 506 act through inhibition of the T-cell enzyme calcineurin (Castilho et al., 2000). They form specific complexes with cytoplasmic molecules. Calcineurin is thereby prevented from dephosphorylating specific nuclear factors. As a result, further downstream of the cascade, T-cells produce insufficient amounts of interleukin-2 (Il-2), a cytokine essential for full T-cell activation.

Recently, a new form of administration for FK 506 has been described for neural transplantation. Liposomes can be prepared and used as vehicle for FK 506 administration. Like CsA, FK 506 is nephrotoxic and neurotoxic in a dose-dependent manner. Lipid micelles offer a new way of reducing these toxic side effects due to their altered biodistribution (Lee et al., 1995) (Ko et al., 1994).

The fornix system as a potential assay system

The fornix (Stanfield et al., 1987) has some unique properties which lend itself ideally to the study of host re-entry and target re-innervation. From an anatomical point of view, the fornix is a very accessible white matter tract with a well-defined projection. Tracers can be injected into the subiculum and followed all the way to its target area, the mamillary body. The tract represents essentially a unilateral projection from subiculum to mamillary body although it carries both afferent and efferent fibres at various points.

The fornix projects from the subiculum to the ipsilateral mamillary body. Fibres originating mainly from the septal two thirds of the subiculum extend obliquely over the surface of the hippocampus. These fibres unite in a bundle, the so-called fimbria. Once they have left the hippocampus, they become known as the columns of the fornix. At the anterior commissure the fornix splits into a precommissural component, which innervates various basal forebrain structures, among them the septal nuclei, and gives rise to the postcommissural tract which innervates predominantly the medial nuclei of the mamillary body. The projections to the mamillary body are topographically organised.

The arrangement of fibres in the fornix is very useful for lesioning studies. This has been demonstrated by Stichel who carried out

transections of the postcommissural fornix in adult Wistar rats (Stichel et al., 1996). A tungsten wire was lowered stereotactically into the brain lateral to the left fornix at a distance of about 0.6 – 1.3 mm proximal to the target, the mamillary bodies. The wire was extended 3 mm in a semicircle ventrally to the tract and withdrawn 2.5 mm to sever the fornix. Finally, the wire was retracted and the knife removed. Immediately after transection animals received either a transplant of NSCs pre-labeled with a fluorescent dye or a DMEM injection as control. The cells were stereotactically injected into the centre of the lesion. Regenerating axons were anterogradely traced via injection of horseradish peroxidase into the subiculum. Animals were allowed to survive from 4 days up to 8 months. Stichel's group observed a substantial fraction of fornix fibres emanating from the proximal fornix stump and traversing the lesion site to re-enter host territory and advance toward their normal target, the mamillary body (Stichel et al., 1996). In all animals that displayed regeneration, labelled cells were found extending from the injection site to the target area. Regenerating fibres persisted for up to 8 months following the grafting procedure.

Material and Methods

Culturing and preparation of candidate repair cells

Adult Schwann cells

Schwann cells (ASCs) were isolated from adult peripheral nerve and maintained in tissue culture by a modification of the method described by Morrissey (Morrissey et al., 1991). Sciatic nerves were dissected out from adult AS rats and transferred into a Petri dish containing phosphate buffered saline (PBS) enriched with antibiotics (penicillin and streptomycin, internal store) and rinsed 4 more times by transfer to the next Petri dish with above solution. Subsequently, nerves were cut into small pieces of about 1 mm with a tissue chopper and then placed in a culture dish containing growth medium, Dulbecco's Modified Eagle Medium (DMEM, Gibco) with 10 % foetal calf serum (FCS, internal store) and 1 % antibiotics (penicillin/streptomycin, internal store)). Initially, only fibroblasts were migrating out of the explant. When the outgrowth around the explants had reached a near-confluent monolayer, the explants were transferred (1. passage) to a new culture dish. After 2 weeks explants were passaged once more. Mostly ASCs migrated from the explants 6 weeks after starting the cultures. Explants were then placed in 60 mm Petri dishes and incubated overnight in growth medium (DMEM with 15 % FCS containing dispase I (1:6, Roche Molecular Biochemicals) and collagenase (0.5 %, Sigma)). The

following day explants were dissociated by gentle trituration. Dissociated ASCs were then washed out with medium and centrifuged at 1200 revolutions per minute (RPM) for 5 mins. The pellet was re-suspended with growth medium and centrifuged a second time. The pellet was re-suspended, triturated and the cells finally plated down in the culture dish. Medium was replaced after 2 days by a chemically defined medium (Verdu et al., 2000) to limit fibroblast proliferation. ASCs were ready for transplantation once they had grown to confluence.

Olfactory ensheathing cells

Olfactory ensheathing cells (OECs) were isolated from adult olfactory bulbs and cultured according to a modification of the method described by Ramon-Cueto (Ramon-Cueto and Nieto-Sampedro, 1992). Olfactory bulbs were removed from adult AS rats and collected in PBS. The glomeruli were dissected out from the bulbs under the microscope and transferred into 60 mm dishes. Glomeruli were washed in PBS and then incubated with 0.1 % trypsin for 15 min. Cells were re-suspended in growth medium (DMEM-F12/ Glutamax with 10 % FCS and antibiotics) twice thereafter. DNAse was added, the cells triturated and centrifuged for 5 min at 1200 RPM. Cells were then plated down and the above medium was changed initially after 4-5 days and thereafter every 3-4 days. Passaging times varied according to cell density in culture.

Neonatal Schwann cells

Neonatal Schwann cells (NSCs) were obtained from neonatal day 1-2 rat pups and cultured by a modification of the method described by Brockes (Brockes et al., 1979). Rat pups were culled by decapitation and both sciatic nerves were removed and collected in L-15 medium (Gibco). The nerves were cut into small segments of about 100 µm with a tissue chopper and incubated for 30 min with a solution containing trypsin (0.1 %, Sigma) and collagenase (0.03 %, Sigma) to digest the extracellular matrix. Digestion was stopped by triturating the cells with a solution containing 30 mg of bovine serum albumin (BSA, Sigma), 5 mg of trypsin inhibitor (Sigma) and 20 µl of DNAse (Sigma) in 10 mls of Hank's Balanced Salt Solution (HBSS, Gibco).

In the next step the cell suspension was centrifuged at 1200 RPM for 5 mins. The supernatant was removed and the cells re-suspended in 1 ml of growth medium (10 % foetal calf serum (FCS) in DMEM (Gibco) enhanced with a 1 % solution of antibiotics (streptomycin/ penicillin, internal store)). Cells were triturated again, made up to a volume of 1.5 ml per dish in culture medium and plated down onto 35 mm dishes. From the next day on, they were treated for 3 consecutive days with cytosine arabinoside (Sigma) to eliminate fibroblasts. After about 6 days NSCs were ready for transplantation.

Human and rat ensheathing cells from the olfactory mucosa

Human OECs were obtained from biopsy samples taken from patients, after providing informed consent, who had undergone various surgical procedures including removal of skull base tumours and naso-pharyngeal carcinomas. All biopsies were taken from areas which were considered as unaffected by malignant growth at the time of surgery. Biopsies from the posterior region of the mucosa were collected in saline solution supplemented with antibiotics. All biopsy samples were later histologically examined; none of them had been infiltrated by tumour tissue.

Rat mucosal OECs were obtained from the olfactory mucosa of adult AS rats. Briefly, lamina propria from the dorsal part of the septum and the superior turbinates was dissected free after enzymatic pre-treatment of the mucosa and collected in L15 (Invitrogen, UK) medium.

For tissues from both human and rat sources an identical cell culture protocol was followed. Olfactory mucosa was chopped and plated on to poly-D-lysine (PDL, Sigma; 10μg/ml.) coated dishes and maintained in Dulbecco's modified Eagle medium/ Hams F12 (50:50) (DMEM/F12; Invitrogen) with 10% FCS (DFF10) for 7 days. At day 8, the medium was enriched with fibroblast growth factor-2 (human Recombinant FGF-2, R&D Systems, UK; 20ng/ml). To generate enough cells for transplantation, cells were sub-cultured by

trypsinising cells and re-seeding on to freshly PDL-coated dishes. At between 14-20 days *in vitro*, rat mucosal cells were prepared for transplantation.

For human material, it was necessary to freeze cells in cell freezing medium and store in liquid nitrogen so that they could be retrieved for transplantation when necessary. Frozen stocks of cells were thawed and re-suspended in excess DMEM/F12. After a brief spin at 300 g for 3 minutes, the pellet was re-suspended and the cells were plated to 100 mm PDL coated plastic dishes. The cells were fed with DFF10 supplemented with FGF-2 and maintained under optimal conditions for use in transplantation.

Neural crest stem cells

Neural crest stem cells (NCSCs) were retrieved by dissecting out neural tubes from 10 ½ day old rat embryos as described by Stemple (Stemple and Anderson, 1992). Briefly, neural tubes from embryos were explanted on a dish coated with fibronectin. Culture medium contained chick extract to supplement growth factors. Neural crest cells migrated from the dorsal aspect of the neural tube explant onto the surface of the culture dish. The explants were removed from the culture dish after 24 hours and the migrating neural crest stem cells transferred to a fibronectin coated dish. The population was left to expand (passage 1) and then transferred to another dish for further expansion. This procedure was repeated three more times until passage 4 had been reached. The population density was

deliberately kept low to prevent cells from differentiating. Cells were examined under phase contrast and an estimate of the three main cell lineages derived from NCSSs was made.

Foetal brain cells

Pregnant AS rats were culled by intraperitoneal injection of 0.5 ml phentobarbitone, an approved Schedule I killing method. Uterine horns were removed by caesarean section, dissected free from their blood supply and the peritoneum, and immediately stored in ice-cold L-15 (Leibovitz 15) solution with added antibiotics.

Individual uterine horns were incised with a microscissor and embryos of age 14 to 15 were delivered by gentle compression of the uterine horns. An incision was made to separate the upper half of the head (roughly above the level of the future skullbase) from the lower half of the head, the body and the trunk, which were subsequently discarded.

The brains were stripped of all their coverings; the precursor structure to become the future skull and the meninges, characterised by their rich supply of blood vessels. The brains were then washed two more times in L-15 to rinse off tissue debris.

A modification of an established protocol at this laboratory to obtain cortical neurons from embryos at age 18 to 19 was used for further processing. Briefly, up to three brains were pooled and placed under

a tissue chopper to yield tiny pieces of brain in the order of 100 μm by 100 μm.

The tissue pieces were placed in a 60 mm dish and incubated at 37° C in a filter-sterilized solution of 10 ml of Earls balanced salt solution (EBSS) containing 60 mg papain, 10 mg cysteine, 100 μl EDTA solution and and 20 μl β-mercaptoethanol. The reaction was stopped 30 min later by adding 10 ml of growth medium (with horse serum), 20 μl of DNAse (Sigma) and 10 ml of filter-sterilized DMEM containing 10 mg chicken egg white trypsin inhibitor and 2 mg DNAse. The solution was gently shaken and then spun down in a centrifuge for 5 min at a speed of 1200 RPM. The supernatant was removed and discarded. Finally, after adding 1 ml of growth medium the tissue was triturated with a Kwill tube and a 5 ml plastic syringe followed by a fire polished Pasteur pipette. Cells were counted, re-suspended in L-15, centrifuged another time and subsequently, after removal of the supernatant and addition of a small volume of L-15, stored on ice before being grafted into the host.

Labelling with green fluorescent protein

Selected cultures of OECs and NCSSs were transfected for 24 hours with an adenovirus (gift of Dr Doorbar in Virology, NIMR) carrying the sequence for GFP. The cultures were further processed as described previously. Tissue had to be routinely perfusion-fixed to avoid leakage of GFP into the surrounding tissue.

Preparation of cell suspensions

For transplantation, the following procedure was followed for both rat and human OECs from the olfactory mucosa. Subconfluent cells were digested with trypsin. After inactivating trypsin in DFF10 and triturating cells to give a single cell suspension, the total cell count was estimated using a haemocytometer. Following a brief spin (300g 5 min), the pellet was re-suspended using DMEM/F12. One further spin in DMEM/F12 was necessary to remove traces of serum. Pellet was resuspended in DMEM/F12 and transferred to an Eppendorf tube and kept on ice. An overall cell yield of 8-12 $x10^6$ was obtained.

All other cell suspensions were prepared by replacing culture medium with Hanks' balanced salts devoid of Ca^{++} and Mg^{+} ions to reduce cell adhesion to the dish. Thereafter, cultures were exposed in the incubator for 2 min to 0.125 % trypsin. The reaction was stopped by adding medium (according to the cell type used) containing 10 % FCS. The cell suspension was then transferred into a tube for centrifugation (Econospin, Sorvall Instruments, DU Pont) at 1,000 RPM for 5 min. Following centrifugation, DNAse was added at a concentration of 1:100 to the cell suspension to reduce cell aggregation, the suspension was triturated and cells were counted in a haemocytometer chamber. Medium was added and the cells spun down a second time. The volume was then made up to a final concentration of approximately 1 x 10^8 cells/ml. Cell suspensions were kept on ice prior to grafting.

All cell types were transplanted into the adult rat thalamus at a concentration of 100 x 10^6/ml. NSCs and OECs were grafted into the postcommissural fornix at the same concentration of 1 x 10^8 /ml.

Immunosuppression of xenograft recipients

Oral cyclosporine

Oral cyclosporine (CsA) at a concentration of 100 mg/L (a 250 ml ampoule of CsA was dissolved in 2.5 L tap water) was contained within the drinking water freely available to the rats. This is based on an average daily fluid consumption of 100 ml/kg bodyweight or 20 ml/day in a typical 200 mg rat yielding 10 mg CsA/kg.

Intraperitoneal cyclosporine

Intraperitoneal CsA was administered at a concentration of 15 mg/kg bodyweight. Injections commenced 24 hours before surgery and continued on a daily basis for the lifetime of the animal.

Liposomal tacrolimus

The preparation of liposomal tacrolimus was based on the protocol described by Alemdar (Alemdar et al., 2001). 100 mg tacrolimus (Fujisawa Inc), 2.5g phospholipon 90 H (Natterman Phospholipid GmbH/ Rhone-Poulonc), 250 mg cholesterol and 2.5 ml absolute ethanol were mixed and heated to 55-60 °C. The components were mixed with 47.5 ml of normal saline. The preparation underwent 5

freeze/thaw cycles to achieve a spontaneous pre-formation of liposomes. Liposomes were sized by filtration through a filter with a pore size of 0.45 µm. This solution yields a concentration of tacrolimus of 2mg/ml.

To achieve a final concentration of tacrolimus of 1mg/ml in the cell suspension, OECs from the human mucosa were mixed with liposomal tacrolimus at a ratio of 1:1. Likewise, The final solution for intraperitoneal injection was diluted 1:1 in normal saline.

Animals received 1mg tacrolimus per kg bodyweight i.e. 0.2 ml for a typical 200g rat. Injections commenced 1 day prior to surgery and continued on a daily basis for the lifetime of the animal (2 weeks). The cell suspension was stereotactically grafted into the thalamus as previously described.

For control purposes, a cell culture with human OECs was treated with liposomal tacrolimus at a concentration of 1 mg/ml (equal parts of liposomal tacrolimus and medium). The culture was derived from the same preparation and was at the same stage as those cultures that were used for grafting purposes.

Surgery

Preparation and anaesthesia

All animals were deeply anaesthetised by intraperitoneal injection of Avertin. Avertin was prepared by mixing 2 g of 2,2,2-tribromethanal (Aldrich Chem Co., USA.) and 2 ml 2-methylbutan-2-01 and adding 100 ml distilled water and 8 ml absolute ethanol. Avertin was stored at 4°C prior to use. Rats received 1 ml Avertin per 100 g body weight. The skin of the operating area was shaved, disinfected with 70 % alcohol and the rats mounted in a stereotaxic frame.

Extrusion of columns in the thalamus

The scalp was incised, the bone exposed by removing periosteum and a burr hole made according to the chosen co-ordinates. The edge of the burr hole was then cleared of sharp bone fragments and the dura carefully lifted up with a pair of fine forceps and opened to expose the underlying brain.

A micropipette with an internal diameter (Figure 2) of approximately 300 μm was loaded with 3-5 μl of cell suspension. It was centred 2.5 mm lateral and 3.3 mm posterior to the bregma aiming at the thalamus. The pipette was then lowered to a depth of 7 mm into the brain measured from the surface of the closed dura mater, and gradually withdrawn while injecting the cell suspension over a distance of 3-4 mm. The cell suspension was injected with the pulse generator set to a pulse frequency of about 1 pulse/sec and a pulse

duration of about 0.1 sec. The generator controlled the air flow rate from the pressurised air cylinder via an electromagnetic valve. Following injection, the micropipette was left *in situ* for another 5 min to allow for pressure equilibration before the micropipette was carefully retracted

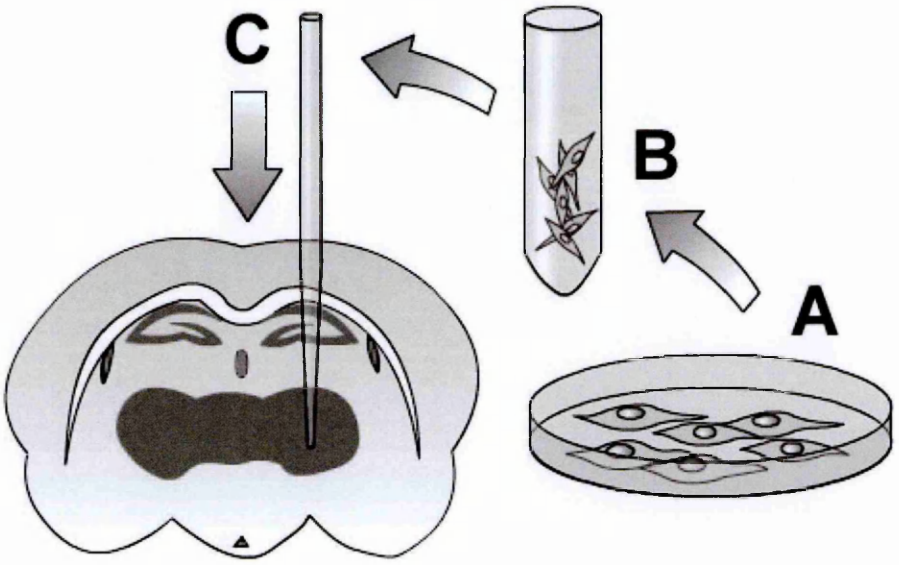

Figure 2 Schematic representation of the steps involved in cell transplantation into the thalamus.

A. Preparation of tissue culture

Cells are cultured according to defined standard protocols. They go through several stages of feeding with growth medium and reseeding onto new plates (depending on the cell type used and the appropriate protocol) until a large enough number of cells has become available.

B. Preparation of cell suspension

Cells are enzymatically digested and finally processed into a cell suspension and stored in a small vial. The cell suspension is kept on ice until the final moment of transplantation.

C. Microinjection into the thalamus

The skull is surgically exposed and a burr hole is created using a stereotaxic frame. The pipette is loaded by aspirating 3-5 µl of cell suspension from the vial. The pipette is then positioned according to the chosen co-ordinates and lowered into the thalamus. The cells are then deposited into the target area (the thalamus) by short-lasting pulses controlled by a pulse generator connected to a pressurised air cylinder. The pipette is left for 5 min in place before gentle retraction to allow for pressure equilibration.

Generating a lesion and microinjection of cells into the fornix

Animals were prepared for surgery and anaesthetised as previously described. The skull was exposed with a midline incision and the periosteum stripped off the underlying bone.

Radiofrequency heat lesions were generated with an electrode that was stereotaxically lowered to a point crossing the path of the postcommisural fornix (Figure 3). Prior to insertion the tip of the electrode was cleansed of debris and charred particles with a fine sand paper. The resistance of the electrode was determined in PBS solution and would typically be about 400 Ω. The electrode was then mounted into the stereotaxic frame. The co-ordinates chosen for the centre of the radiofrequency heat lesion were 2.6 mm posterior, 1.0 mm lateral and 8.6 mm ventral to the bregma. The co-ordinates were based on Paxinos' atlas (George Paxinos, 1997) of the rat brain but had to be adjusted by trial and error to account for the different proportions of the female AS rats used in this setting.

A burr hole was made and the electrode lowered to its target point. The electrode was connected to a lesion generator (model RFG-3C RF, Radionics. INC. Cambridge, US) which allowed control of voltage and time and displayed resistance and wattage. The brain resistance at the target point varied from 4 kΩ to just above 5 kΩ. Resistances above 5 kΩ were outside the displayed range of the

lesion maker and prompted a message by the lesion maker indicating that the circuit was open. Despite this problem, it was possible in most case to initiate a current flow. A duration of 60 seconds was found to give an acceptable lesion size in most cases. The resistance changed with the onset of current flow. It often fell initially, even for resistances outside the displayed range, to reach a plateau value but in some cases it rose again towards the end of the 60 seconds period. The electrode was then withdrawn, removed from the stereotaxic frame and replaced by a micropipette. The micropipette was readjusted with reference to the bregma and loaded with the cell suspension. The micropipette was lowered into the brain but only to a depth of 8.4 mm to allow the cell suspension to fill the cavity left behind by the electrode. A volume of 2 μl was slowly injected and the micropipette left *in situ* for another 5 min to allow for pressure equilibration. Finally, the micropipette was gently retracted. A subgroup of animals only received cell suspensions but no lesion and yet another subgroup received the cell suspension 2 weeks after lesioning.

The fornix was labelled by injecting the subiculum with 2 μl of a 10 % solution of the tracer biotin dextran (BD, Molecular Probes Inc, US). In the initial stages the labelled animals had only a lesion. For the main experiments, BD-labelling was performed shortly after the radiofrequency heat lesion had been generated, and the cell

suspension had been injected. In later experiments, animals were labelled at the time of delayed grafting.

The chosen co-ordinates were 6.4 mm posterior, 3.5 mm lateral and 4.2 mm ventral to the bregma. As for the cell suspension, the tracer was slowly injected and the pipette left in place for several minutes before it was retracted.

For surgical procedures on the fornix, the preparation of NSCs and OECs suspensions and cell suspensions from 14 to 15 day old embryos followed the protocols outlined previously.

Skin closure and recovery

Skin and scalp were sutured with 4.0 Vicryl and the animals allowed to recover from anaesthesia under a warm lamp to prevent hypothermia. All animals were carefully checked for vital signs and adverse reactions following surgery until they had regained consciousness.

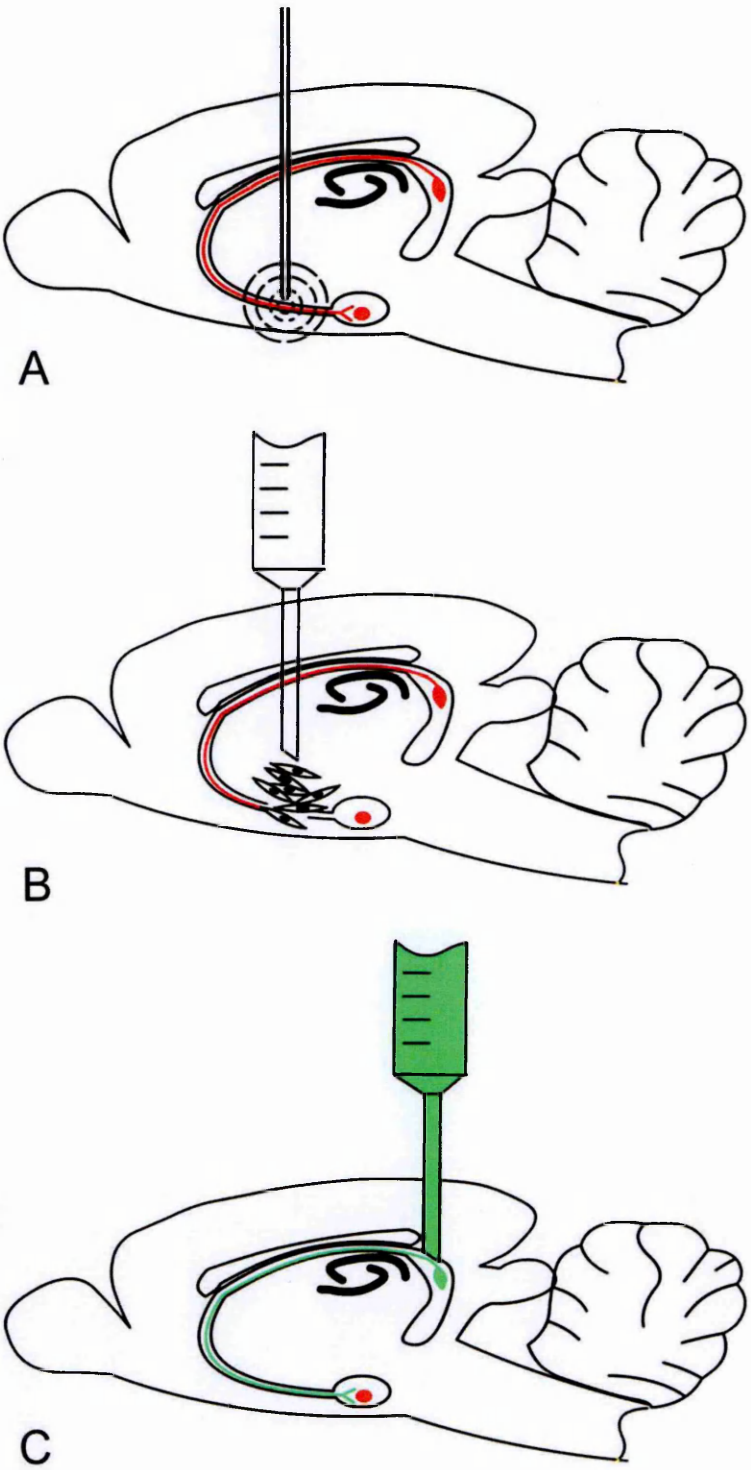

Figure 3 Surgery on the post-commissural fornix.

The diagram is a schematic representation of the fornix system.

A radiofrequency heat lesion (**A**) is generated to interrupt the post-commissural fornix (pathway highlighted by red colour).

Cells (**B**) are microinjected into the lesion site, either immediately or after a delayed and specified period of time.

The surviving and regenerating fornix fibres (**C**) are labelled by microinjection of biotin-dextran (BD, green colour) into the subiculum. BD is a colourless substance which can be detected by a streptavidin-conjugated fluorochrome probe.

Tissue fixation

Intracardial perfusion

All animals were culled under terminal anaesthesia by intraperitoneal injection of 0.5 ml Euthanal (Pentobarbitone). Following apnoea, a cruciate incision with a scissor was made into the abdominal wall just below the ribcage to provide access to the diaphragm. The lateral edges of the diaphragm were incised on both sides to gain access to the chest cavity. The incisions were then upwards extended, cutting the rib cage open and leaving a ribcage flap in the middle which could then be hinged back on itself. The chest cavity was now fully exposed. Clamps were applied to the descending aorta and the apex of the heart was nicked with fine scissors. A cannula with a syringe attached was gently advanced into the left chamber until the cannula became lodged into the ascending aorta. Perfusion could then begin. All protocols commenced with the perfusion of 100 ml of PBS over a 5 min period. Blanching of the ears and eyes indicated successful filling of the vascular system with PBS.

At the end of the perfusion procedure the skin over the skull was incised and the head separated from the trunk. The skull was then further cleared of skin and muscle attachments. The skull was subsequently removed piece by piece to gain access to the underlying brain. Finally, the dura was removed and the brain cut into a small tissue block. The orientation of the tissue block

depended on the surgical procedure used, i.e. a frontally oriented block was required for thalamus operations and a sagittal block was necessary for fornix procedures. Further processing depended on the chosen perfusion protocol.

Simple PBS perfusion

This was the initial method of choice for samples destined for simple light microscopy. The animals were intracardially perfused with 100 ml PBS over 5 min using a syringe. Brains were removed and frozen in dry ice. Unprocessed frozen tissue blocks were stored at –80° C.

Perfusion with 4% paraformaldehyde

This was the initial protocol for animals that had received fornix operations. Perfusion fixation rather than simple PBS perfusion was always necessary for animals that had received cells labelled with green fluorescent protein (GFP) to prevent GFP from leaking into the surrounding tissue. Samples obtained through this procedure could only be cut on the vibratome and could not be much thinner then 25-50 µm.

Animals were intracardially perfused, initially with 100 ml of PBS followed by 4 % paraformaldehyde over 30 min. Paraformaldehyde was drained from a bottle situated about 80 cm above the level of the sample. From there it drained via gravity into a plastic tube attached

to the cannula lodged into the aorta. A small valve allowed adjustments of the perfusion rate. Following perfusion, brains were cut along the desired plane and trimmed to a smaller size. The trimmed blocks of brains were stored overnight in 4 % paraformaldehyde and processed the next day.

Perfusion with 4% paraformaldehyde suitable for cryostat sections

This procedure overcame the shortcoming of the previous one, allowing 10 µm sections and obviated the need for immediate tissue sectioning. The procedure followed the steps outlined above but the tissue block was re-immersed in 10 % sucrose (in a PBS solution) after an overnight storage period in 4 % paraformaldehyde. Once the sample had sunk to the bottom of the container, it was immersed in 20 % sucrose until it had stopped floating again and then quickly frozen in dry ice.

Tissue sectioning

Cryostat sections

Coronal sections of 10 µm thickness were cut on a cryostat (Leica CM3050). Frozen sections were mounted on coated slides and air-dried for 30 min. They were stored at 4°C over a short period of time (1-4 weeks), and at –20°C for longer periods, prior to final processing for immunohistochemistry.

Vibratome sections

50 μm coronal sections were cut on a vibratome (Leica VT1000S).

Staining procedures

Staining for light microscopy

Sections were fixed in either acetic alcohol or 4 % paraformaldehyde for 30 min depending on the antibodies used. Paraformaldehyde was used in the majority of cases since it gave better results with the notable exception of p75 that gave clearer pictures with acetic alcohol.

Slides were washed in PBS followed by blocking in 5 % defatted milk in PBS, each step lasting 30 min. They were then incubated overnight at 4°C with the primary antibody. Antibodies were diluted in a solution of 0.05 % azide (NaN_3) and 1 % BSA in PBS.

The following monoclonal primary mouse antibodies were used:

- anti-glial fibrillary acidic protein (GFAP) diluted 1:400 (Sigma), a marker of rat astrocytes and glial cells
- anti-low affinity nerve growth factor-receptor (p75) diluted 1:20 (MAB 365, Chemicon), detects rat Schwann cells and Schwann-like OECs

- anti-low affinity nerve growth factor-receptor (p75) diluted 1:100 (MAB 5264, Chemicon), detects human Schwann cells and Schwann-like OECs
- anti-nestin diluted 1:500 (MAB 353, Chemicon), a marker of immature neuroepithelial cells of rat and mouse origin; detects Schwann cells and OECs
- anti-human mitochondria (MIT) 1:300 (MAB 1273, Chemicon); stains the mitochondria of all human cells
- anti-S-100 (Sigma) 1:1000

The following polyclonal primary rabbit antibodies were used:

- anti-neurofilament L 1:500 (the 70 kD lightchain, Serotec)
- anti-neurofilament H 1:500 (the 200 kD heavychain, Serotec), the 2 anti-neurofilament antibodies were always used in conjunction to stain nerve cells and their axons
- anti-fibronectin (Chemicon) 1:500
- anti-nestin 1:500 (Chemicon), reacts only with human nestin

The following polyclonal goat antibody was used:

- anti-peripherin 1:200 (Santa Cruz Biotechnology Inc, US), marks mostly nerve cells of peripheral origin and a few cells of central origin

Sections were washed for 40 min the following day and incubated for 30 min with a secondary biotinylated antibody directed against the

primary antibody used (Vector Laboratories Ltd). The anti-mouse secondary antibody was diluted 1:300 and the secondary anti-rabbit antibody was diluted 1:500. Following a further 30 min wash, sections were incubated with avidin-biotin complex conjugated with horseradish peroxidase (Vectastain ABC Kit, Vector Laboratories Ltd.). After a last washing cycle in PBS slides were transferred into acetate buffer and then visualized using the glucose oxidase-nickel 3,3'-diaminobenzidine (DAB) method. Where required, slides were counterstained with neutral red or thionine. Finally, slides were dehydrated in ascending concentrations of ethanol, defatted in Histoclear (Novara), and finally mounted in DPX mounting Medium (Raymond A Lamb Ltd.).

Staining for confocal microscopy

Sections were washed, and subsequently incubated overnight with the primary antibodies (mouse and rabbit in conjunction) and 0.2 % Triton in antibody diluent (1 % bovine serum albumin and 0.05 % azide in PBS). The primary antibodies were used at the same concentrations as for light microscopy processing.

In the second step, slides were washed several times again and then simultaneously incubated with two different fluorochrome-conjugated secondary antibodies depending on the primary antibody:

- Alexa 488 goat anti-rabbit IgG 1:500 (A-11008, Molecular Probes, Inc)

- Alexa 546 goat anti-mouse IgG 1:500 (A-11003, Molecular Probes, Inc)
- Alexa 568 donkey anti-goat 1:500 (A-11057, Molecular Probes, Inc) for samples where anti-peripherin had been used as primary antibody

No primary antibody was required for immunostaining the BD-labelled fornix. Instead, streptavidin, Alexa Fluor 647 (S-21373, Molecular Probes, Inc) with its known affinity for biotin was employed in the second step together with another secondary antibody.

Slides were examined under the fluorescence (Zeiss Axiophot) and the confocal microscope (Leica TCS SP). Selected slides were counterstained with DAPI (4',6'-diamidino-2-phenylindole dihydrochloride) diluted 1:1000. Confocal images were digitally captured for up to 3 different wavelengths across the thickness of the sample. Vibratome sections (50 µm) were usually scanned in 5 µm increments and frozen sections (10 µm) in 2 µm increments. Channel colours were arbitrarily selected for any given wavelength. Coloured images were finally overlaid to aid in assessing the relationship of differently stained tissue structures. Images were stored on standard write-once compact discs.

Staining for markers of immunorejection

10 µm frozen sections were cut and mounted on to slides. Frozen sections were gently fixed for 5 min in 96 % alcohol and washed

several times in PBS over a 30 min period. Slides were then pre-incubated with horse serum diluted in PBS at a concentration of 1:30.

The following monoclonal mouse antibodies from Serotec (Oxford, UK) were used for detection of immune cells at a concentration of 1:100:

- anti rat class I (OX-18), recognises rat MHC class I antigen
- anti I-A mouse/rat (OX-6), recognises MHC class II antigen
- anti rat CD4 (W3/25) recognises the CD4 receptor expressed by helper T-cells and to a lesser degree by microglia and macrophages
- anti rat CD8 (OX-8) recognises mainly the CD8 receptor expressed by suppressor T-cells

Slides were incubated for 1 hour at 4°C with above primary antibodies and subsequently rinsed with PBS for 30 min. Thereafter, they were incubated with secondary biotinylated horse anti-mouse antibody at a concentration of 1:300 for 1 hour at 4°C. After another 30 min PBS wash cycle, slides were covered with avidin-biotin complex conjugated with horseradish peroxidase for 30 min, washed another 30 min in PBS and finally visualised with the DAB reaction as previously described. Counterstaining was carried out with neutral red solution.

Quantitative analysis

Only the ventral part of the column, lying in the lateral ventroposterior thalamic nucleus (VPL) in close proximity to the internal capsule was taken into consideration for a quantitative analysis. Sections were chosen if they clearly demonstrated the central part of the graft since fibres in this part of the graft were most likely recruited fibres. Slides showing numerous short axons without any apparent orientation most likely represented the area of the column/host interface and were therefore excluded. Axons in close vicinity to the graft/host interface that did not appear aligned to the direction of the column were also disregarded. The area of the column with the highest apparent density of axons was selected for counting. The width of the column at this point was measured and the number of axons counted that crossed an imaginary line representing this width. Axon density was defined as the number of axons per mm. The average axon density and the corresponding standard error of mean (SEM) for a given number of axons at survival times of one, two, and three weeks were calculated. The SEM was obtained by dividing the standard deviation by the square root of the sample size. The SEM was chosen since it is a measure of how close the sample mean is to the real population mean. For each column the longest axon was selected, and its length approximated by drawing a line connecting its two ends. The mean length for the sample and the SEM were calculated.

Results

Columns extruded into the thalamus

General observations

Columns were of consistent appearance in approximately 80 % of cases. Consistency was judged by uninterrupted continuity of the cell column and correct position in the thalamus. Extensive tissue damage was rarely seen in the thalamus, but in some cases a haematoma or cavity had formed at the entry point of the micropipette into the cortex. Neovascularisation was observed in the graft, as well as elongation and alignment of transplanted cells, and migration of cells along induced blood vessels. Blood vessels from the host entered the graft at various point to line up with the transplanted cells. Blood vessels were frequently branching and running slightly obliquely across the parallel bundles of cells.

Donor cells, host axons and astrocytic processes ran in parallel to each other in the graft. Astrocytic processes and axons were often intertwined with each other and followed the same path into the graft.

The following data are shown as mean value ± standard error of mean (SEM). The average width of the column measured 70.8 ± 3.4 μm (n=119). The length of the column varied a lot and could not be precisely attained due to the fact that the column was often obliquely intersected by the section plane. However, based on measurements

of the column visible on the slides, columns extended for a distance of up to 1.5 mm through the thalamus. The column ended in most cases in a round or ellipsoid bolus at its ventral end. Occasionally, cells had become dispersed along a disrupted tissue plane between the thalamus and the internal capsule, forming another column perpendicular to the main column.

All of the cell grafts investigated (olfactory ensheathing cells (OEC), adult Schwann cells (ASC), neonatal Schwann cells (NSC), neural crest stem cells (NCSCs) and human OECs) were able to recruit axons as demonstrated by immunostaining for NF. Axon recruitment was most pronounced at the ventral end of the graft. Also, grafts which accidentally lay more lateral extending into the reticular thalamic nucleus (RTN) generally induced ingrowth of a greater number of axons than grafts lying in the desired position, the ventral posterolateral nucleus (VPL), regardless of the cell type employed (Zhang et al., 1995). These transplants, however, had to be disregarded for counting, as they did not correspond to the desired position within the thalamus.

A control group of animals (n=5) that had only received medium (DMEM) but no cell suspension showed only small numbers of short axons within the column. The mean axon density (Figure 4) was 35 $\pm$ 11.3 mm^{-1} at 14 days and the mean fibre length was 0.05 $\pm$ 0.01 mm. These columns were generally very thin and often

discontinuous. Given the thin width of the transplants and the short length of fibres it became difficult to decide whether fibres had actually been recruited into the graft or simply ran in parallel for

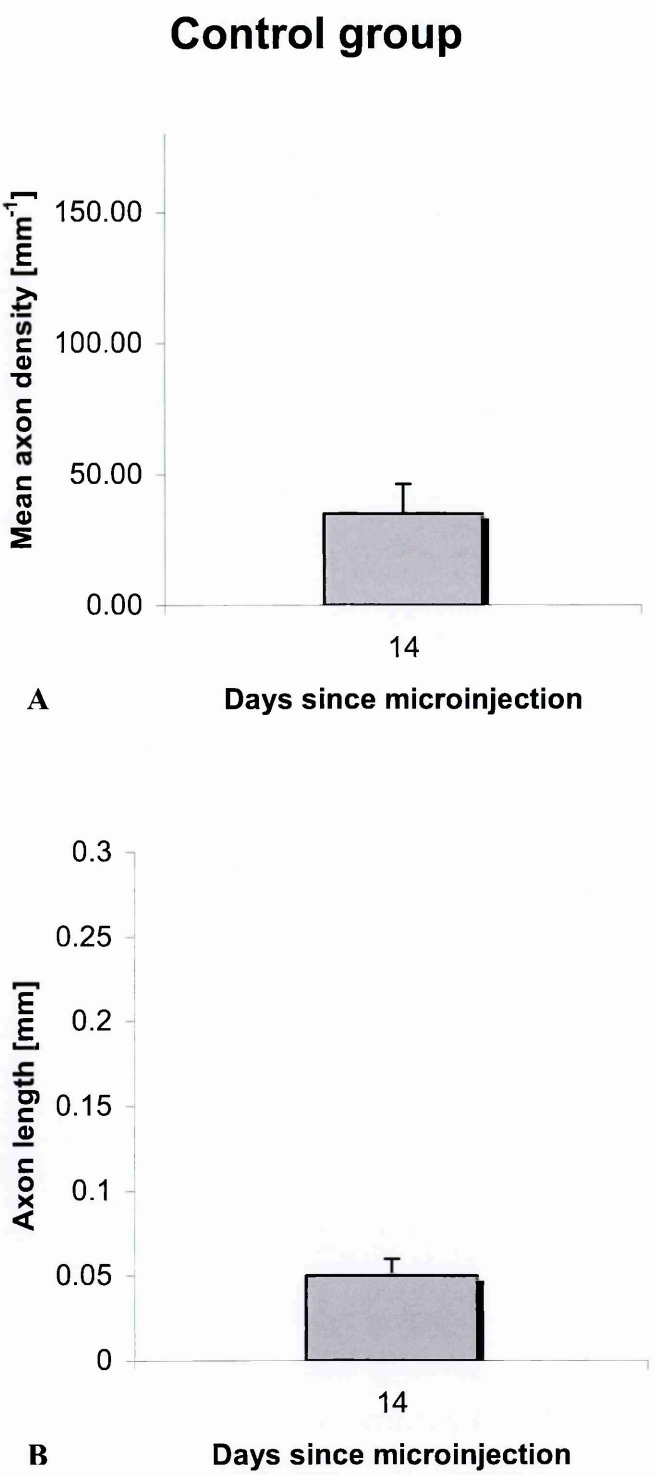

Figure 4 Quantitative analysis of axon recruitment in the control group.

The control group of animals (n=5) had only received medium (DMEM) but no cell suspension. There were only small numbers of short axons within the column. Axons in the control group did not recruit any substantial number of axons. All cellular transplants led to the ingrowth of a larger number of fibres and this was shown to be statistically significant. The axons that were counted were probably artefacts derived from the periphery of the very thin columns.

(**A**) The mean axon density is about 35 mm^{-1}.

(**B**) The mean axon length is about 0.05 mm. Error bars represent standard errors of mean.

Mean axon density and mean axon length are much lower in the control group than in all the groups that received a cell transplant.

mechanical or any other reasons. In normal cell grafts, it was relatively easy to identify fibres in the centre of the transplant and recognise genuine recruitment but in the thin control columns proportionally more fibres at the border of the graft were counted and this probably introduced a positive bias. Nevertheless, the control group provided some sort of benchmark measurement against which cellular transplants could be compared.

Olfactory ensheathing cells

Cell nuclei often looked oval and plump, and were scattered over the entire length of the column. Both subtypes of olfactory ensheathing cells (OECs) could be identified in roughly equal proportions by staining for p75 and fibronectin (Figure 5). The cells were all organised in parallel tiers and both astrocyte- and Schwann-cell like OECs freely intermingled with each other. Grafts were often observed to contain large numbers of cell debris and macrophages. OECs were capable of recruiting axons at the 7, 14 and 21 day stage (Figure 6). A number of grafts (Figure 7) failed to facilitate any ingrowth of axons and those grafts that did recruit axons were marked by only localised axon recruitment that did not extend across the whole length of the column. Axons were most numerous at the ventral end of the graft. Axon recruitment at 7 and at 14 days (Figure 8) was sparse but had improved considerably in number by 21 days (Figure 9 and Figure 10). Axons and astrocytic processes were noted for their close spatial alignment (Figure 7 and Figure 10).

Where axon recruitment had failed a paucity of astrocytic processes within the graft was also noted on a number of occasions (Figure 7). Not only astrocytic processes and axons were aligned but cells and axons also ran in parallel oriented tiers (Figure 9).

The axon density (Figure 11) increased from 29.3 ± 2.6 mm^{-1} (n=21) at 7 days and 31 ± 4.6 mm^{-1} (n=9) at 14 days to 91.4 ± 18 mm^{-1} (n=9) at 21 days post-operation. The mean length of axons (Figure 11) changed from 0.082 ± 0.007 mm (n=21) at 7 days and 0.138 ± 0.027 mm (n=9) at 14 days to 0.108 ± 0.018 mm (n=9) at 21 days.

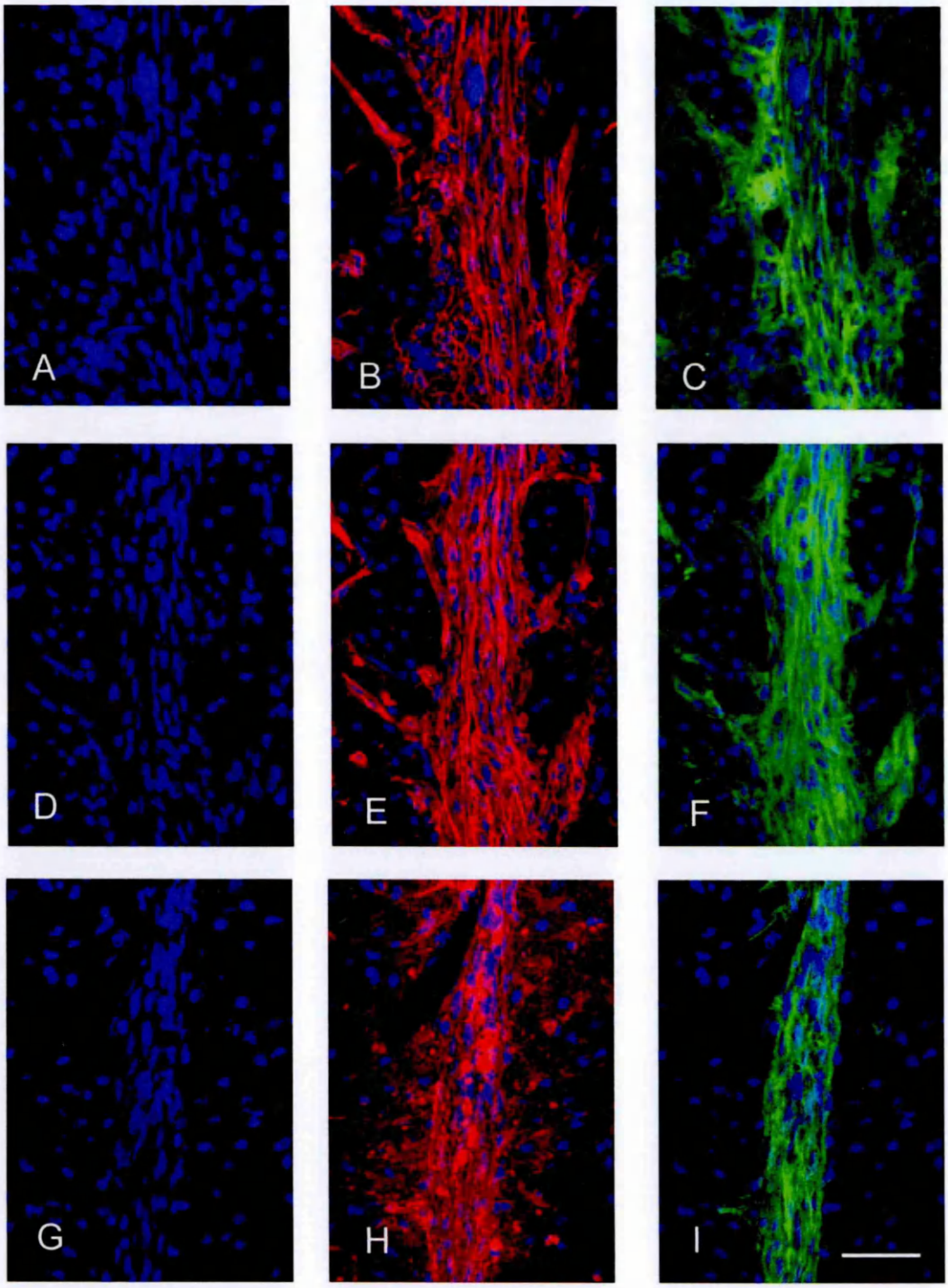

Figure 5 Comparison of cell-type characteristics in mucosal OECs, NSC and bulbar OECs.

Confocal images of olfactory ensheathing cells (OECs) derived from the rat mucosa (**upper row: A,B,C**), of neonatal Schwann cells (NSCs) (**middle row: D,E,F**) and OECs derived from the olfactory bulb (**lower row: G,H,I**). The scale bar represents 50 μm. All animals were culled at 14 days post-OP. Cell nuclei were marked with a blue-fluorescent dye (DAPI stain). The p75 Schwann cell receptor was stained with a red-fluorescent dye and the green marker shows the fibronectin distribution.

Cell nuclei (**A**) of mucosal-derived OECs are highly organised, of slender shape and run in parallel bundles. The fibroblast-like cells (**B**) are fibronectin- and the Schwann cell-like OECs (**C**) are p75 (low affinity nerve growth factor receptor) -immunoreactive. Cells can be seen migrating away from the column.

Neonatal Schwann cells (NSCs) display a similar appearance: Cell nuclei (**D**) are well aligned. Fibroblasts (**E**) are fibronectin-positive and NSCs stain positive for p75 (**F**).

Cell nuclei of OECs from the bulb (**G**) are more oval in shape and look less organised. The staining pattern for fibronectin (**H**) and p75 (**I**) is much like in the other 2 cell types.

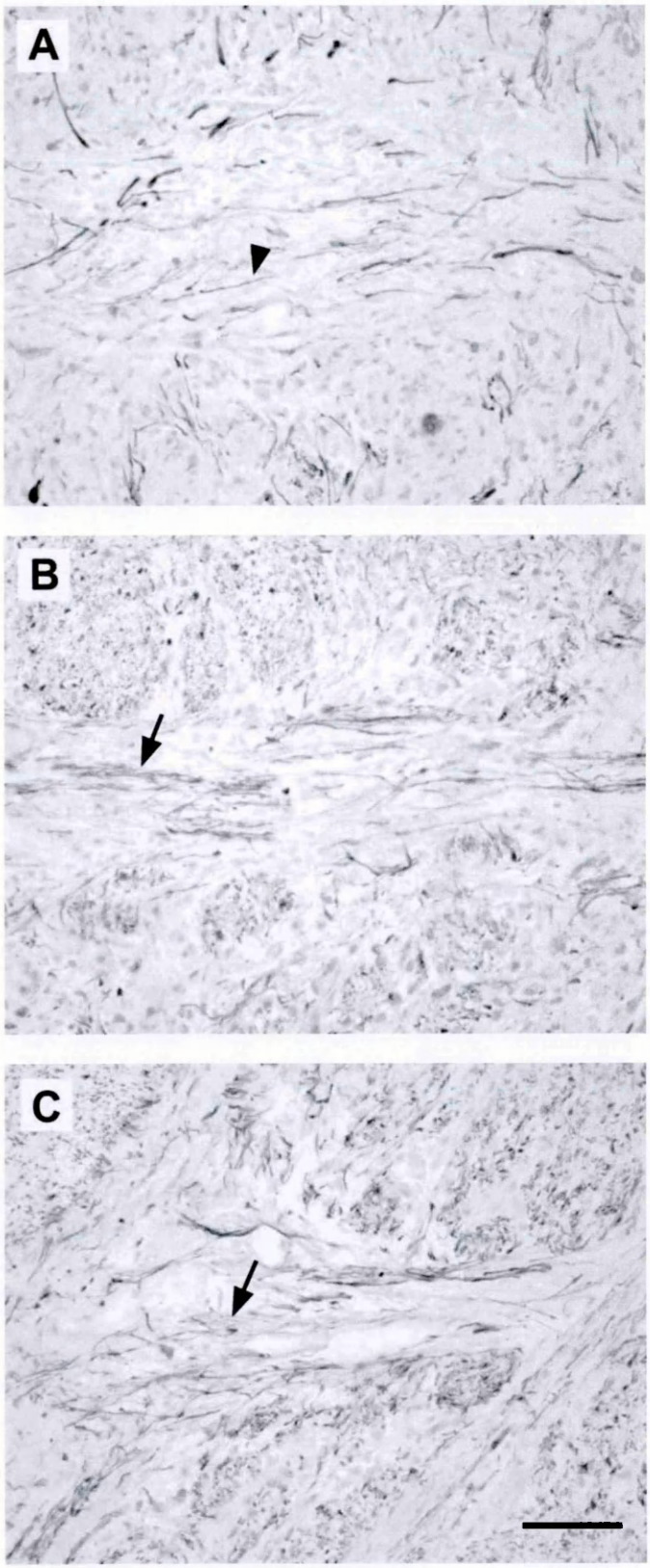

Figure 6 Axon recruitment by OEC grafts transplanted into the thalamus.

Light microscopy of olfactory ensheathing cells (OECs). Animals were culled at 7, 14 and 21 days post operatively. Axon recruitment was detected by immunostaining for neurofilament (NF). Cell nuclei were counterstained with thionin. The scale bar represents 50 μm. The photographs show how nerve fibres are recruited by OECs.

A. At the 7 day stage NF-positive nerve fibres (arrow head) are still relatively short.

B. At the 14 day stage nerve fibres have become more abundant and an increase in fibre length can be noted. In addition, fasciculating bundles (arrow) of nerve fibres have emerged.

C. At 21 days post operatively, NF-positive axons (arrowhead) remain organised in fasciculating bundles (arrow). The axon arrangement is more irregular than in NSC grafts.

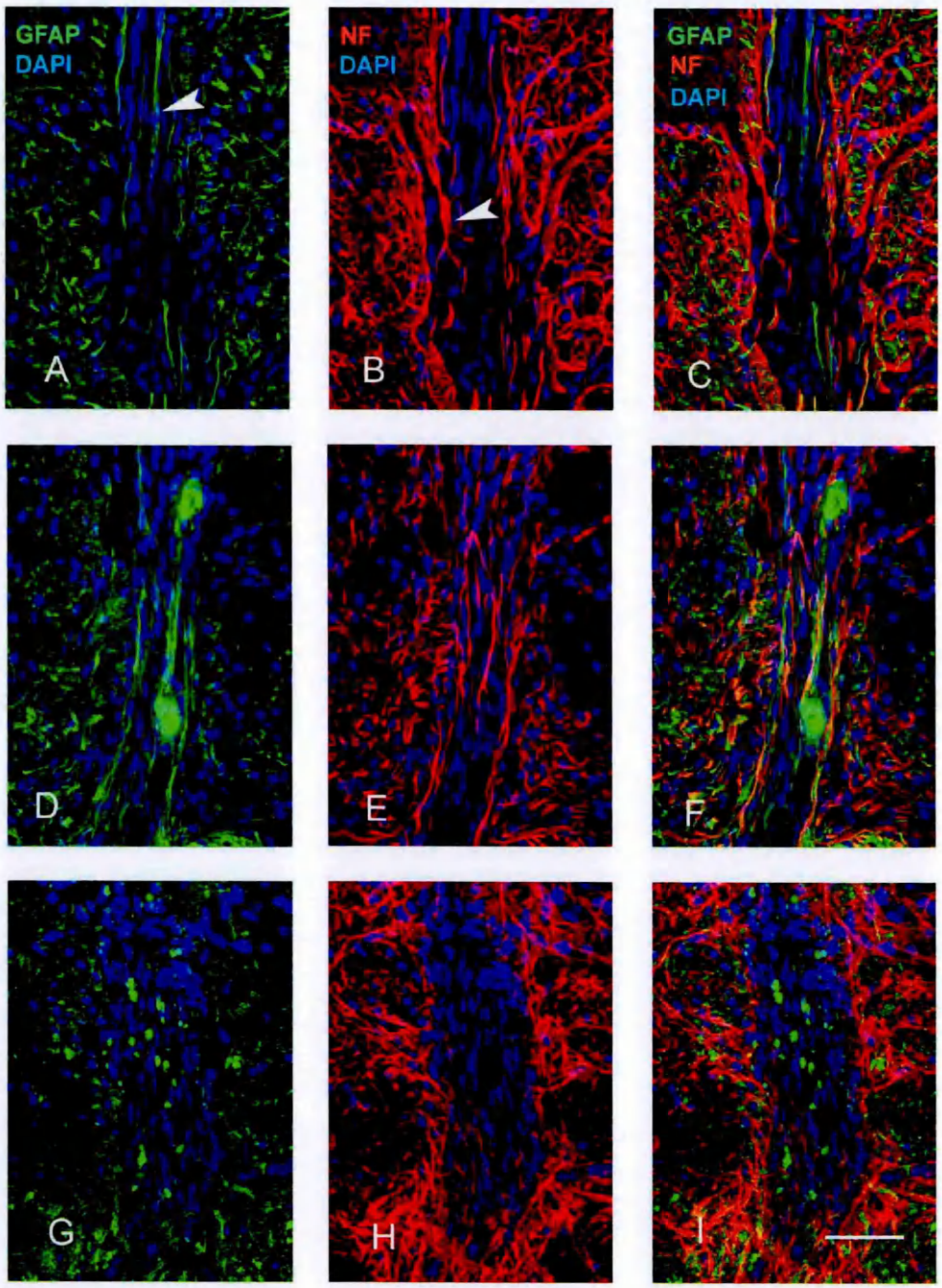

Figure 7 Comparison of axon recruitment by mucosal OECs, NSCs and bulbar OECs.

Confocal images of olfactory ensheathing cells (OECs) derived from the rat mucosa (**upper row: A,B,C**), of neonatal Schwann cells (NSCs) (**middle row: D,E,F**) and OECs derived from the olfactory bulb (**lower row: G,H,I**). The scale bar represents 50 μm. All animals were culled at 14 days post-OP. Cell nuclei were marked with a blue-fluorescent dye (DAPI stain). The glial fibrillary acidic protein (GFAP) positive astrocytes and their processes were stained with a red-fluorescent dye and the distribution of neurofilament (NF) positive fibres was highlighted with a green fluorescent colour.

Olfactory ensheathing cells (OECs) from the rat mucosa: **(A)** NF-positive axons (arrowhead) run in parallel with the column, as do **(B)** GFAP-positive fibres originating from astrocytes (arrowhead). **(C)** All 3 structures (axons, astrocytic fibres and cells) are aligned and establish contact with each other.

Neonatal Schwann cells (NSC) recruit more axons **(D)** than mucosal OECs and more astrocytic processes **(E)** enter the graft. The overlay picture **(F)** shows to what extent axons and astrocytic processes are intertwined with each other.

OECs from the bulb fail to attract any axons in this sample **(G)**. Green spots mark the presence of autofluorescent macrophages. This OEC graft is also devoid of astrocytic processes **(H)**. Cell nuclei (blue) appear scattered and disorganized. The overlay picture **(I)** demonstrates the lack of fibres and astrocytic processes in the graft.

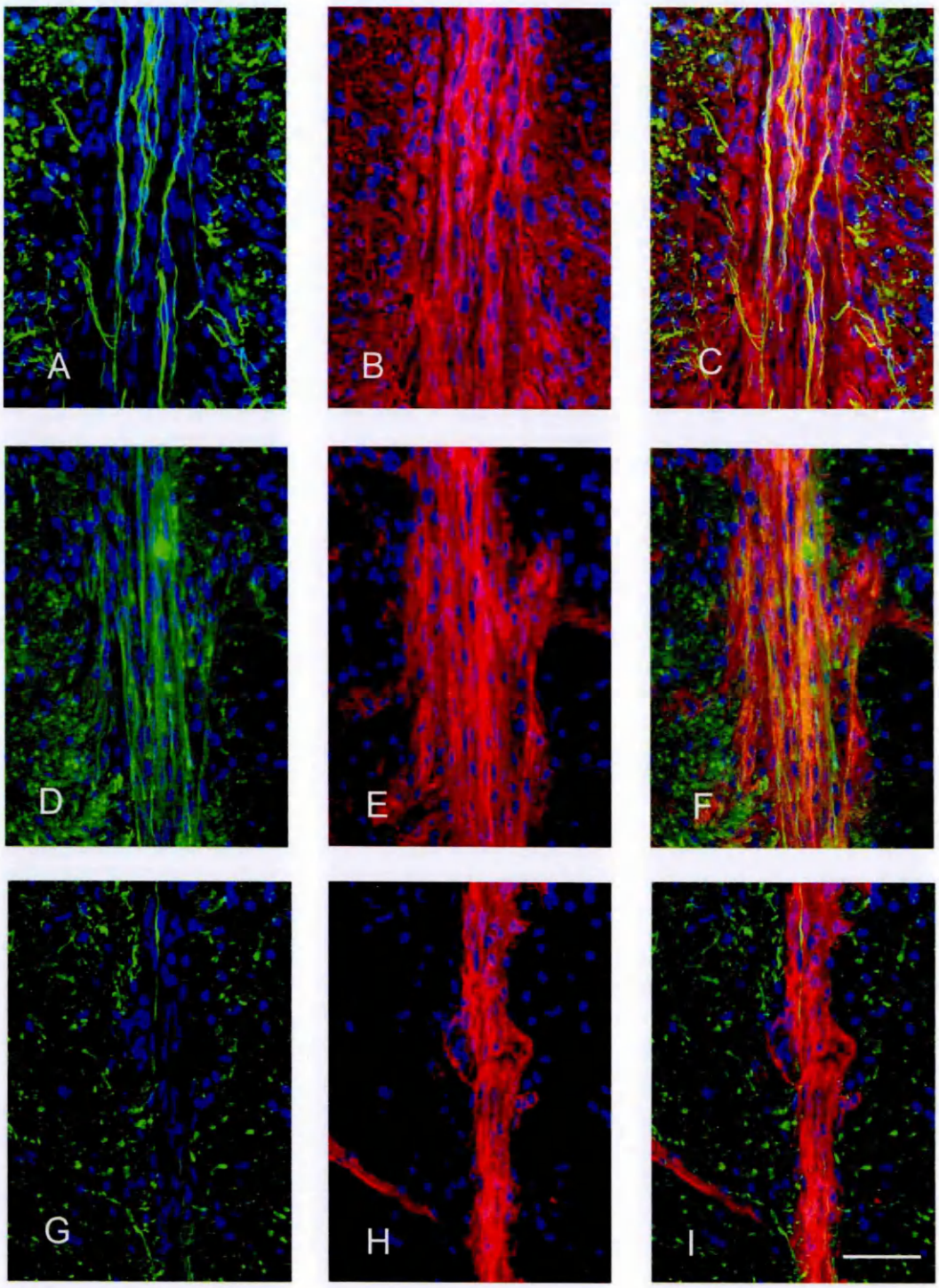

Figure 8 Comparison of axon recruitment by mucosal OECs, NSCs and bulbar OECs 14 days post operatively.

Confocal images of olfactory ensheathing cells (OECs) derived from the rat mucosa (**upper row: A,B,C**), of neonatal Schwann cells (NSCs) (**middle row: D,E,F**) and OECs derived from the olfactory bulb (**lower row: G,H,I**). The scale bar represents 50 μm. All animals were culled at 14 days post-OP. Cell nuclei were marked with a blue-fluorescent dye (DAPI stain). The p75-positive cells were marked with a red-fluorescent dye and the distribution of neurofilament (NF) positive fibres was highlighted with a green fluorescent dye.

NF-positive Axons **(A)** are recruited into a column **(B)** comprised of p75-positive OECs derived from the olfactory epithelium. Both OECs and axons form a regular arrangement of parallel-running bundles **(C)**.

NSCs recruit axons at a high density **(D)** than OECs. The staining pattern of NSCs **(E)** is very similar to OECs of mucosal origin. Axons and NSCs **(F)** intermingle extensively.

OECs from the bulb **(H)** are seen in smaller numbers than the other 2 cell types. OECs recruit only few axons **(G)**. The overlay picture **(I)** demonstrates the spatial relationship between axons and cells.

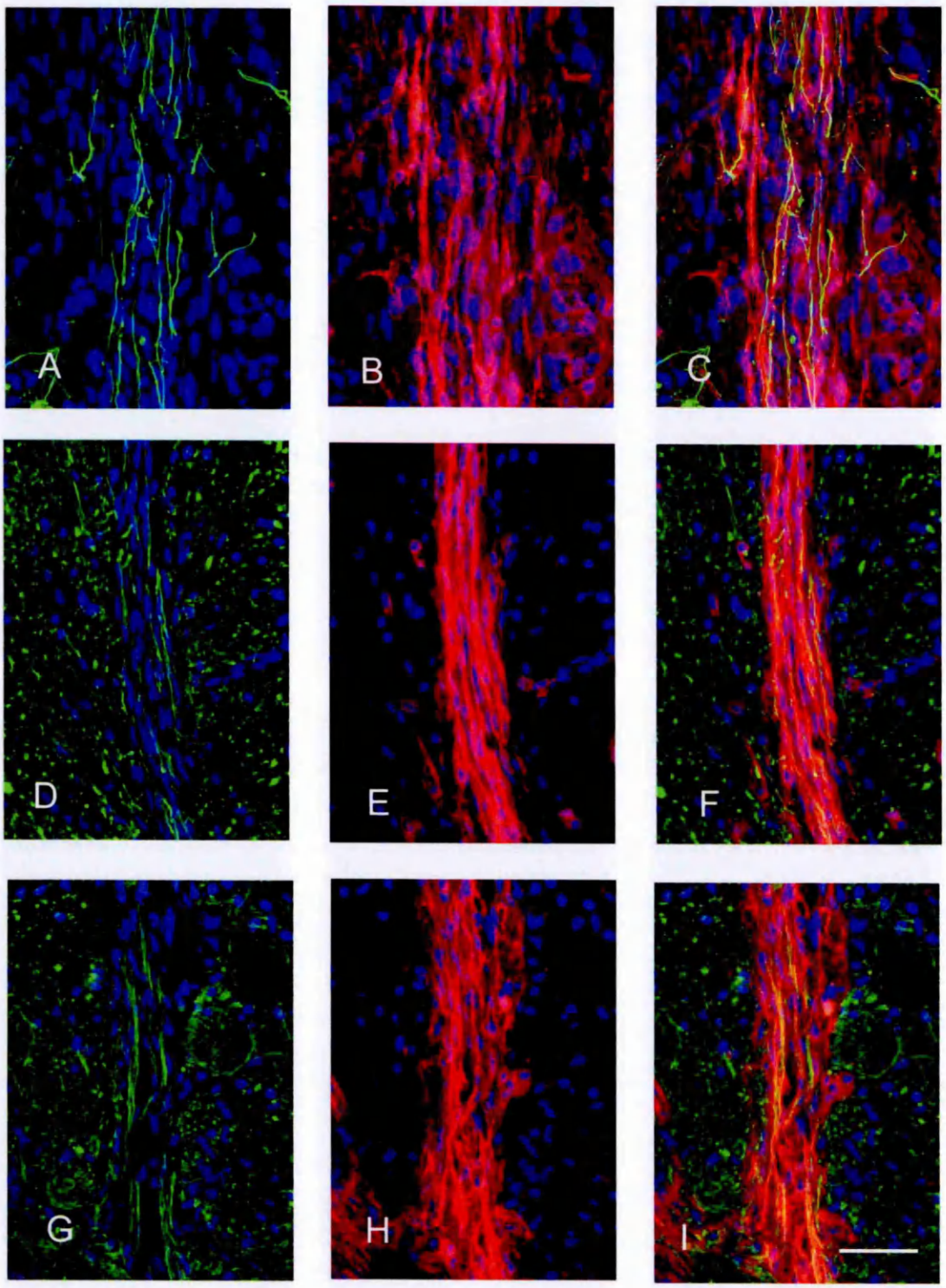

Figure 9 Comparison of axon recruitment by mucosal OECs, NSCs and bulbar OECs 21 days post operatively.

Confocal images of olfactory ensheathing cells (OECs) derived from the rat mucosa (**upper row: A,B,C**), of neonatal Schwann cells (NSCs) (**middle row: D,E,F**) and OECs derived from the olfactory bulb (**lower row: G,H,I**). The scale bar represents 50 μm. All animals were culled at 21 days post-OP. Cell nuclei were marked with a blue-fluorescent dye (DAPI stain). The p75-positive cells were marked with a red-fluorescent dye and the distribution of neurofilament (NF) positive fibres was highlighted with a green fluorescent dye.

At 21 days post-OP all cell types facilitate axon recruitment (**A, D, G**) demonstrated by NF-immunoreactivity. Transplanted cells are identified by immuno-staining for p75.

OECs of mucosal origin (**B**) and NSCs (**E**) appear more organised than OECs from the bulb (**H**). The latter are also less numerous than the other 2 cell types. NSCs **(E)** are densely packed and aligned in regular parallel tiers; a feature that distinguishes them from the other 2 cell types. The overlay images (**C,F,I)** shows how cells and axons align in regular tiers in all 3 cell types.

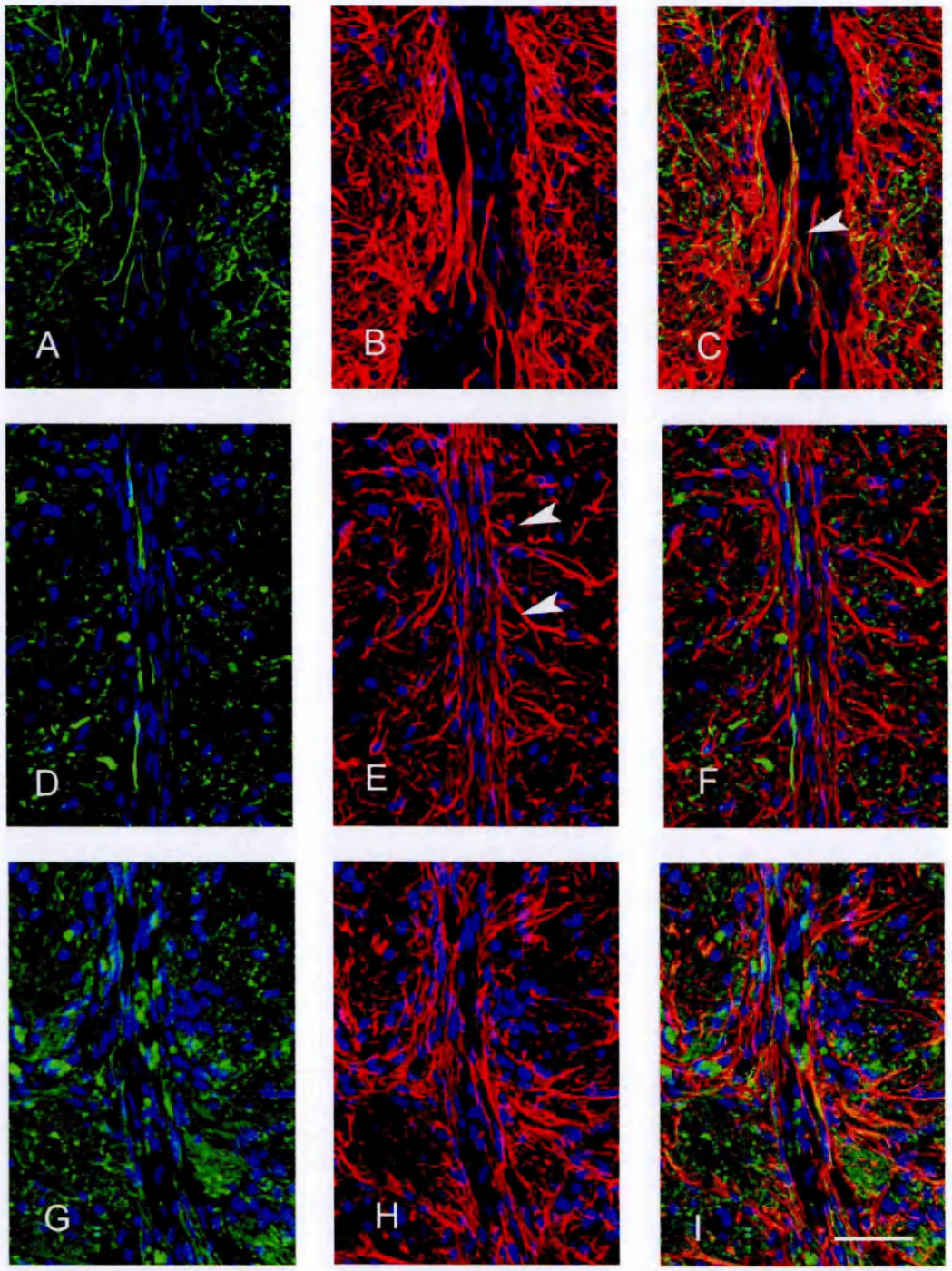

Figure 10 Comparison of astrocytic behaviour and axon recruitment in mucosal OECs, NSCs and bulbar OECs at 21 days post operatively.

Confocal images of olfactory ensheathing cells (OECs) derived from the rat mucosa (**upper row: A,B,C**), of neonatal Schwann cells (NSCs) (**middle row: D,E,F**) and OECs derived from the olfactory bulb (**lower row: G,H,I**). The scale bar represents 50 μm. All animals were culled at 21 days post-OP. Cell nuclei were marked with a blue-fluorescent dye (DAPI stain). The glial fibrillary acidic protein (GFAP) positive astrocytes and their processes were stained with a red-fluorescent dye and the distribution of neurofilament (NF) positive fibres was highlighted with a green fluorescent colour.

Axons entering a graft made up of mucosal-derived OECs (**A**) are guided by (**B**) astrocytic processes. The overlay image **(C)** shows how both structures come in close contact with one another (arrowhead).

NSCs achieve a high degree of order; cell nuclei are elongated and spindle-shaped. Axons (**D**) run in parallel bundles and astrocytic processes (**E**) enter the graft at almost regularly spaced intervals (arrowheads) and align with the other structures (**F**) once they are inside the graft. The appearance of these astrocytic processes bears a resemblance to a branching tree.

In contrast, OECs from the bulb appear more disorganised but still manage to attract some axons (**G**). Astrocytic processes (**H**) stay in close contact with axons (**I**). Autofluorescent macrophages (green specs) are commonly encountered.

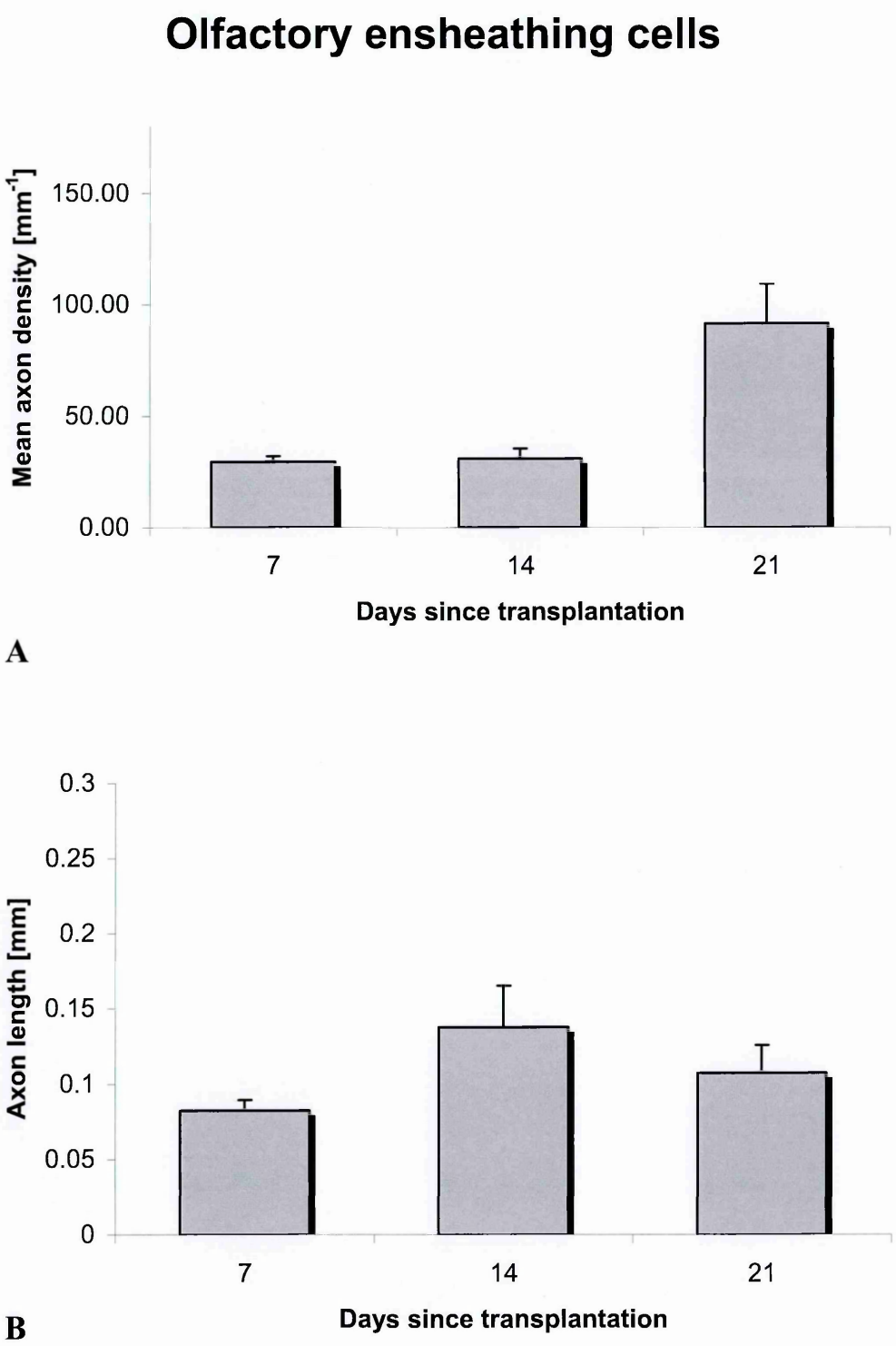

Figure 11 Quantitative analysis of axon recruitment by olfactory ensheathing cells from the bulb.

Olfactory ensheathing cells derived from the bulb (OECs) (**A**) attract small numbers of axons at 1 and 2 weeks post-OP and the actual axon density at this point in time is of the same order as in the sham group. However, at 3 weeks after transplantation fibre density has increased to about 90 mm^{-1}.

Axon length (**B**) varies over the observed time period but stays close to 0.1 mm.

Error bars represent standard errors of mean.

Adult Schwann cells

Adult Schwann cells (ASC) were capable of recruiting axons (Figure 12). Abortive sprouting characterized by numerous short thickened axons turning away from the graft was sometimes seen at the host/graft interface. ASCs (Figure 12) only recruited small numbers of axons and sometimes no axons at all. The distribution of axons was often patchy and restricted to certain areas of the graft. The ventral end of the transplant was most successful at recruiting axons. At day 7 the mean axon density (Figure 13) was 53.8 ± 13.6 mm^{-1} (n=15). At day 14 post operation (post OP) the average axon density was measured as 68.7 ± 9 mm^{-1} (n=13), and 63.1 ± 13.5 mm^{-1} (n=6) at day 21 post OP. The average maximal axon length (Figure 13) at day 7 post OP was 0.13 ± 0.024 mm (n=15), 0.139 ± 0.022 mm (n=12) at day 14 post OP and 0.127 ± 0.02 mm (n=6) at day 21 post OP.

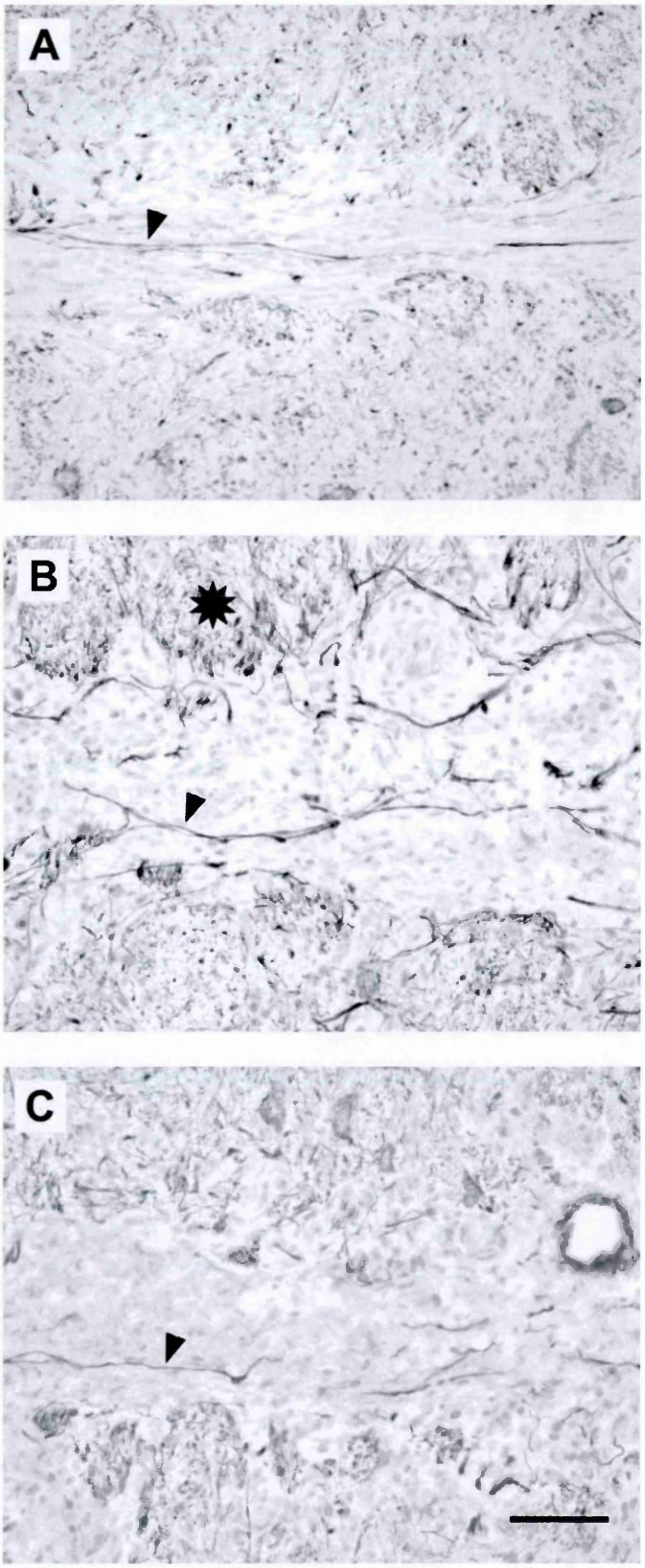

Figure 12 Axon recruitment by ASC grafts in the thalamus.

The photomicrographs are showing adult Schwann cells (ASCs) 7 (**A**), 14 (**B**) and 21 (**C**) days after surgery and grafting of cell suspension. Axons have been marked with neurofilament (NF). The scale bar represents 50 μm.

The NF-positive axons (arrowheads) line up in parallel within the column. Only small numbers of axons are seen in these samples.

Reactive axon sprouting can be seen at the periphery of the graft (asterix).

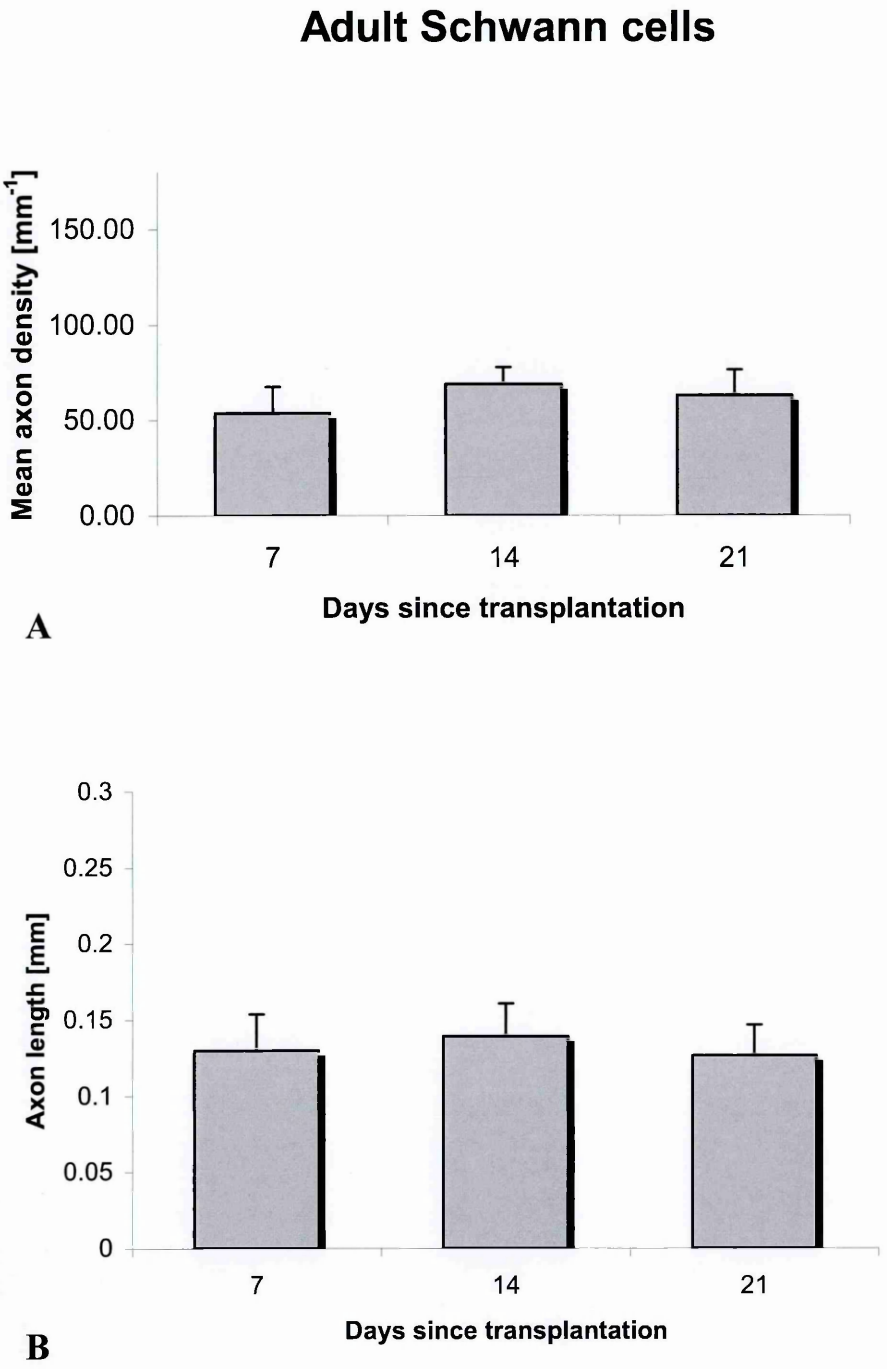

Figure 13 Quantitative analysis of axon recruitment by adult Schwann cells.

Adult Schwann cells (ASCs) (**A**) recruit axons at a density of 50 – 60 mm^{-1}. The axon length (**B**) is about 0.13 mm. There is little change over the observed time period of 3 weeks for either the mean axon length or the mean axon density.

Error bars represent standard errors of mean.

Neonatal Schwann cells

The survival of neonatal Schwann cells (NSCs) was superior to that of adult Schwann cells (ASCs). Their nuclei were mostly elongated and spindle-shaped, forming chains of cells and running in parallel with the direction of the column. All in all, the cell nuclei appeared highly organised and the cytoplasm of NSCs stained positive for low affinity nerve growth factor receptor (p75). An approximately equal number of fibronectin-positive (Figure 5) fibroblasts accompanied the NSCs. Both cell types intermingled freely. NSCs columns were characterised by their regular arrangement of cells in parallel tiers. Bundles of fasciculating NF-positive axons (Figure 9 and Figure 10 and Figure 14) were recruited into the graft and seen along the entire length of the transplant. Some of the axons also displayed varicosities. Astrocytic processes were often seen to enter the column at almost regular intervals (Figure 10) and observed to establish close contact with axons (Figure 7 and Figure 10). All 3 structures; astrocytic processes, axons and cells (compare Figure 7 to Figure 10) were noted to run in parallel oriented tiers. Small von Willebrand factor-(vWF) positive blood vessels entered the column at various points to line up with the other structures within the graft (Figure 15). Blood vessels were also seen to enter the bolus and often divided into branches.

The axon density (Figure 16) increased from 76.9 ± 5.6 mm^{-1} (n=6) at 7 days and 91.7 ± 10.9 mm^{-1} (n=10) at 14 days to 126.7 ± 27.4 mm^{-1} (n=3) at 21 days post OP. The mean length of axons (Figure 16) changed only slightly from 0.185 ± 0.03 mm (n=6) at 7 days and 0.217 ± 0.027 mm (n=10) at 14 days to 0.21 ± 0.047 mm (n=3) at 21 days.

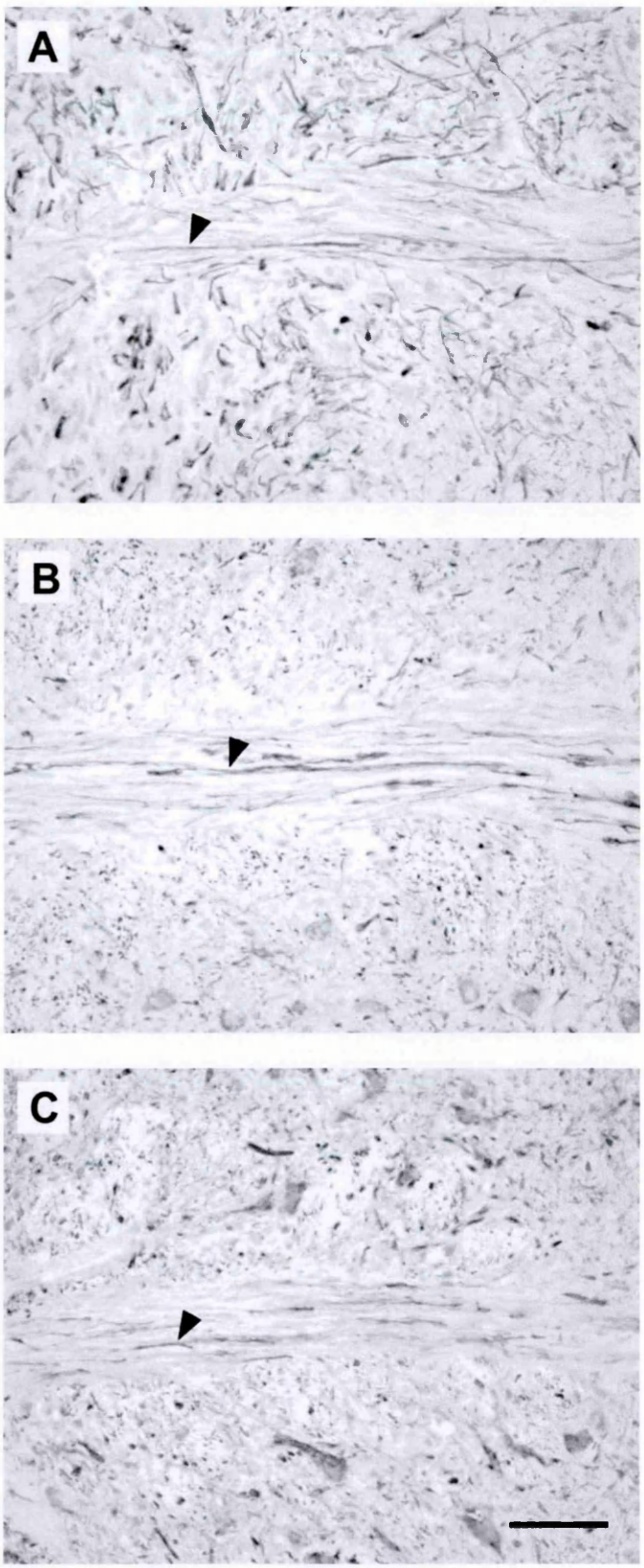

Figure 14 Axon recruitment by NSC grafts in the thalamus.

Neonatal Schwann cell (NSC) grafts 7 (**A**), 14 (**B**) and 21 (**C**) days post OP. Numerous NF-positive axons (arrow-heads) are seen. Axons extend throughout the graft. The axon density increases over time.

Scale bar represents 50 μm.

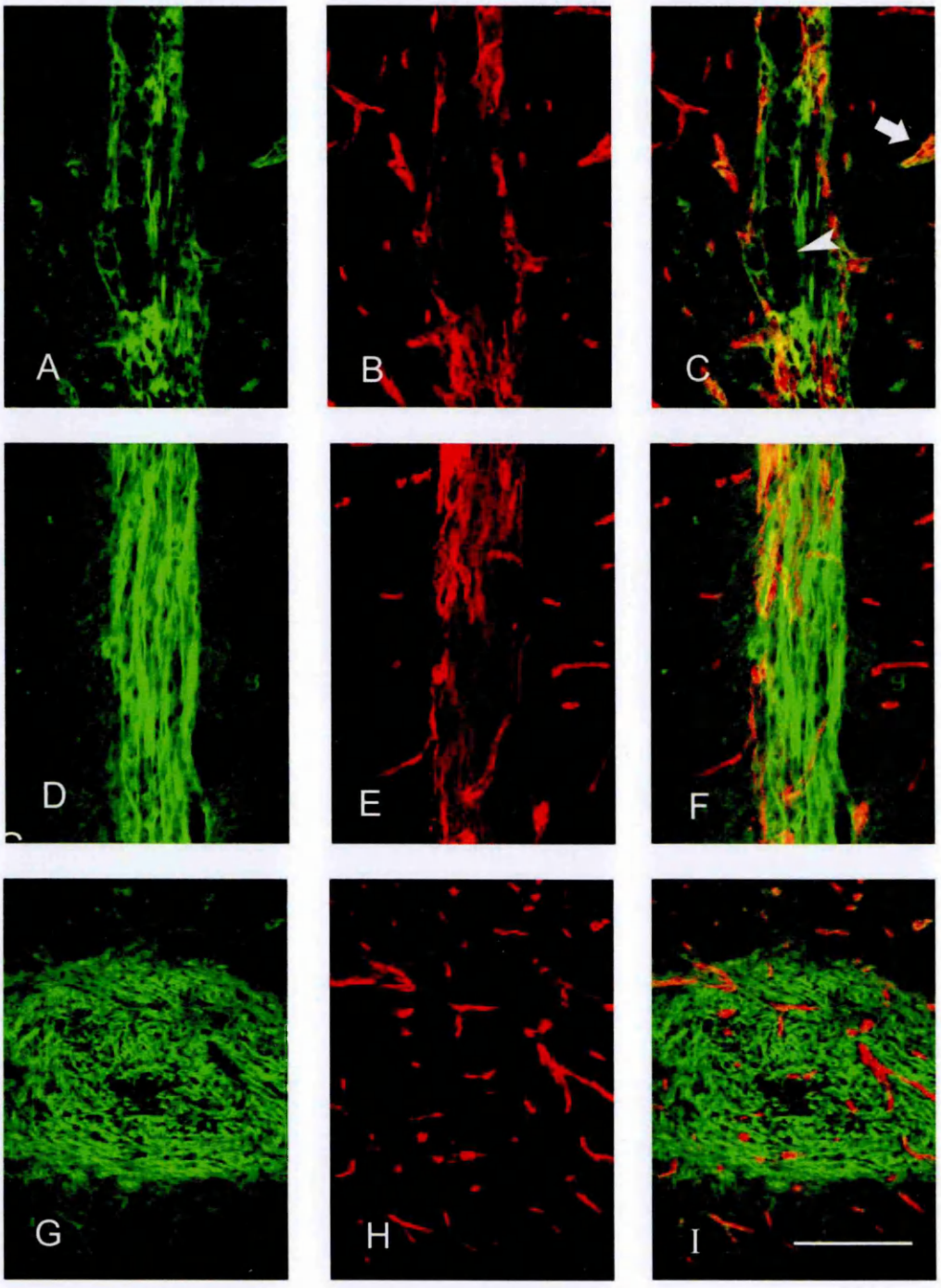

Figure 15 Neovascularisation of the graft.

Confocal images of olfactory ensheathing cells (OECs) derived from the rat mucosa (**upper row: A,B,C**) and neonatal Schwann cells (NSCs, **middle and lower row: D,E,F,G,H,I**) . The scale bar represents 50 μm.

All animals were culled 2 weeks after surgery. Cells immunoreactive for p75 are marked with the green fluorescent dye while von Willebrand factor (vWF)-positive blood vessels display red fluorescence. These images show the relationship of cells and blood vessels.

P75-positive OECs from the mucosa (**A**) form a column. The graft (**B**) is supplied by (vWF)-positive bloodvessels. The overlay image (**C**) shows the spatial relationship of OECs and blood vessels. It is apparent that blood vessels and OECs are aligned to some extent. The graft has not taken in all places and large empty spaces lacking a blood supply (**arrowhead in C**) are visible in the column. Elsewhere, vWF-positive bloodvessels correspond to more cellular areas. Cells migrate away from the column along preformed blood vessels (**arrow**).

NSCs (**D**) survive better then mucosal OECs and the graft also has a more extensive blood supply (**E**). Cells and blood vessels align with each other (**F**).
In this sample, NSCs form a bolus (**G**) with blood vessels entering in a radial fashion (**H**). The overlay image (**I**) depicts NSCs and blood vessels together.

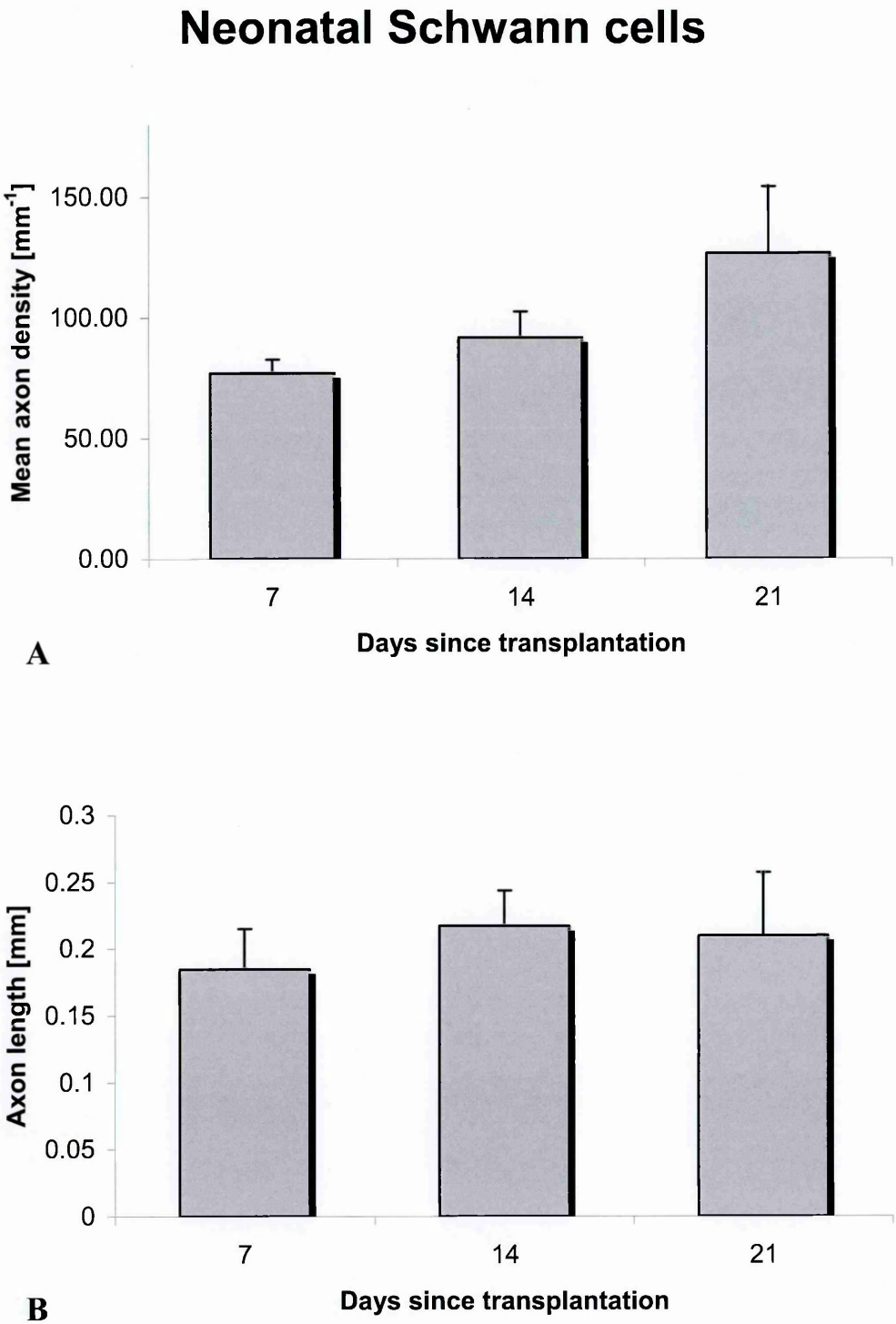

Figure 16 Quantitative analysis of axon recruitment by neonatal Schwann cells.

Neonatal Schwann cells (**A**) recruit increasing numbers of axons over time up to a density of about 130 mm^{-1} at 3 weeks.

(**B**) The axon length varies little over time and stays close to 0.2 mm.

Error bars represent standard errors of mean.

Olfactory ensheathing cells from the rat olfactory mucosa

Mucosal-derived OECs displayed spindle-shaped cell nuclei and p75- and fibronectin-positive cells were aligned in parallel strands (Figure 8). Axons (Figure 17) were seen in an equal distribution throughout most of the graft and integrated well in the graft. Astrocytic processes and axons intermingled with each other. Occasionally, astrocytic processes appeared to provide a guidance structure to axons (Figure 7 and Figure 10) enabling axons to run piggybacked into the centre of the graft. Axon recruitment was observed along most of the graft (compare Figure 7,8 and 9). Axons lined up between the tiers of cells. Columns were vascularised (Figure 15) by newly formed blood vessels originating from the host tissue. These blood vessels were seen to supply the column in a patchy distribution. Certain areas of the column were devoid of both donor cells and blood vessels. Newly formed blood vessels also provided a pathway for migrating donor cells to leave the column.

The axon density (Figure 18) decreased from 101.9 ± 16.1 mm^{-1} (n=5) at 14 days to 79 ± 11.4 mm^{-1} (n=8) at 21 days post-operation. The mean length (Figure 18) of axons stayed practically unchanged at 0.156 ± 0.028 mm (n=9) at 14 days and 0.159 ± 0.029 (n=9) at 21 days.

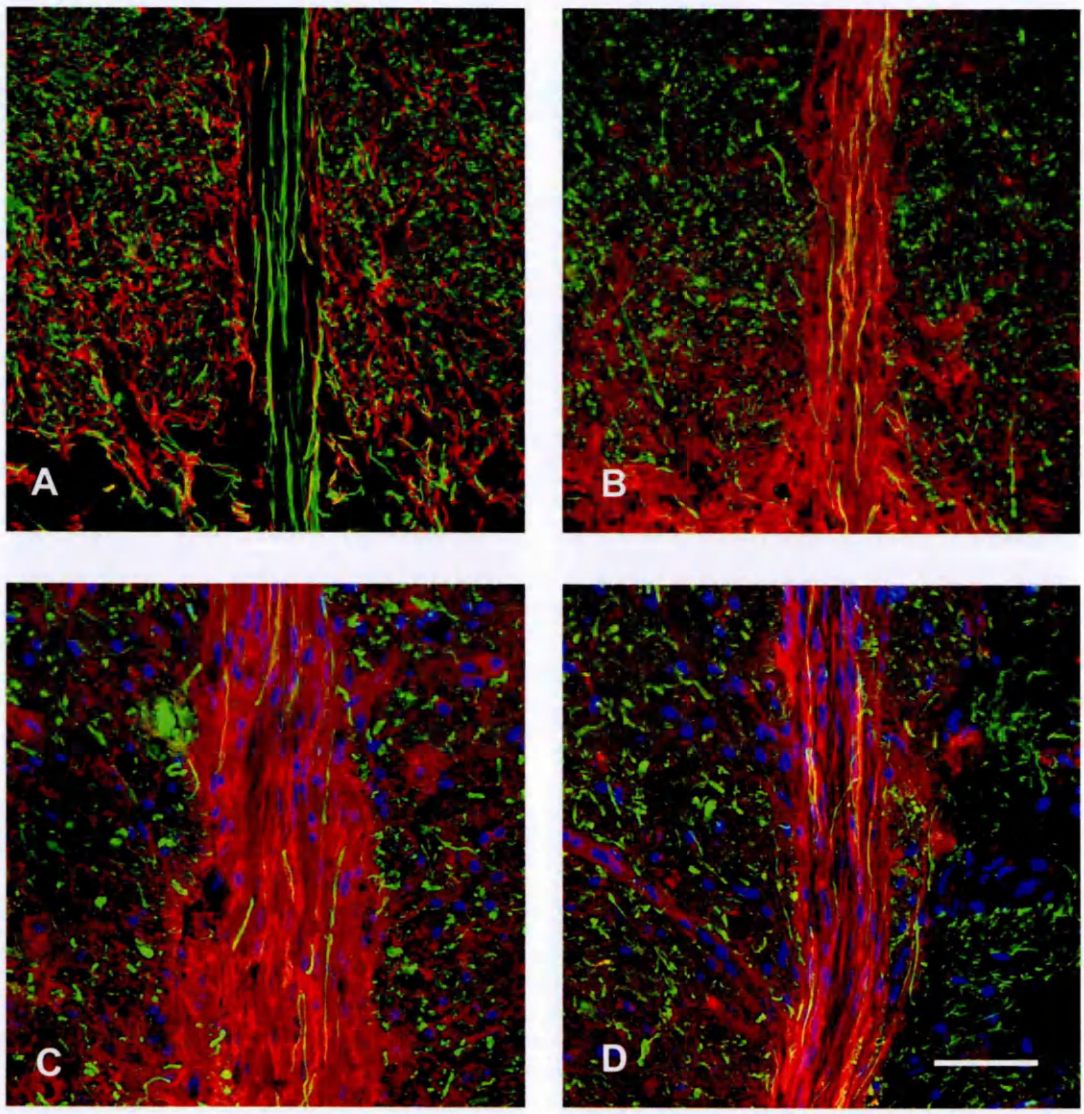

Figure 17 Mucosal-derived OECs 14 days post-OP in the thalamus.

Confocal images of mucosal-derived olfactory ensheathing cells (mucosal OECs). All animals were culled 14 days after microinjection of cells into the thalamus. Cell nuclei were counter-stained with a blue-fluorescent dye (DAPI). The scale bar represents 100 μm for the top row and 50 μm for the bottom row.

Mucosal OECs (**A**) recruit large numbers of NF-positive axons (green staining on all pictures). The fibres align with and often run in conjunction with GFAP-positive astrocytic processes (red fluorescence).

Same sample (**B**) showing p75-positive cells (red fluorescence) filling the column and attracting axons (green colour).

The high power magnification shows p75-immunoreactive cells (**C**: red fluorescence) and nestin-positive cells (**D**: red fluorescence). The staining pattern for nestin is less diffuse than the one observed for p75.

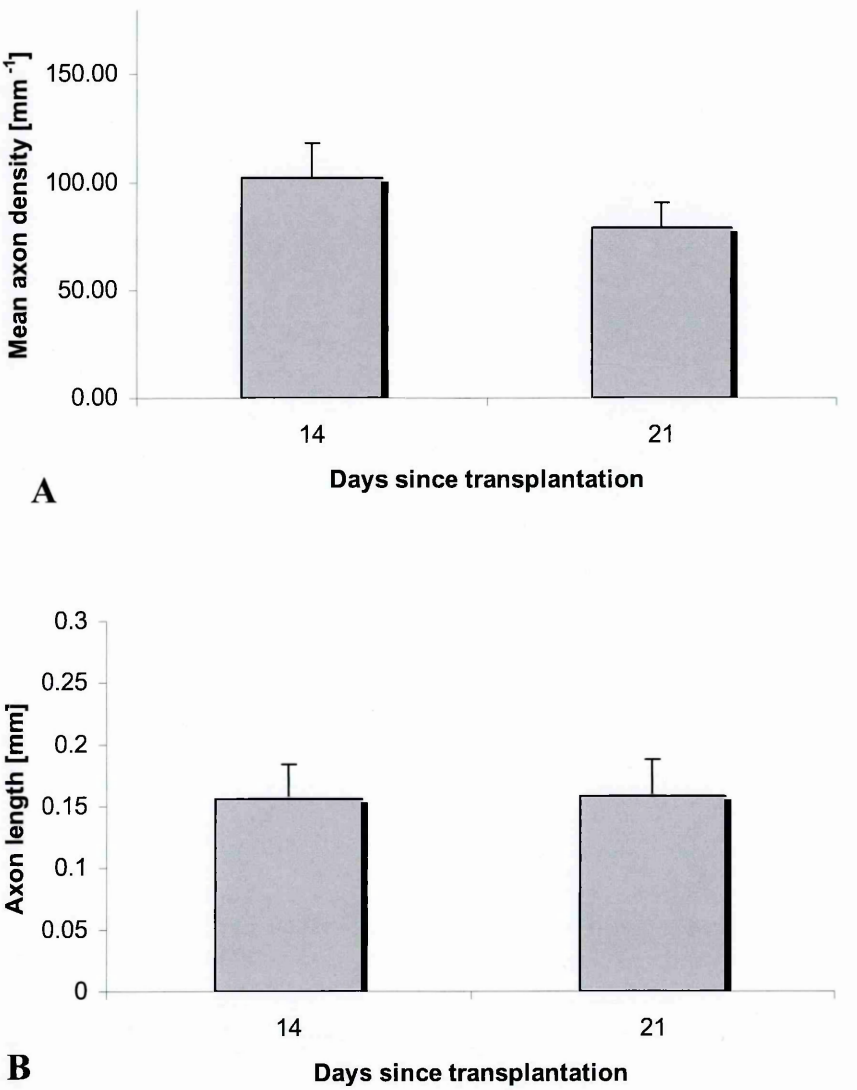

Figure 18 Quantitative analysis of axon recruitment by olfactory ensheathing cells from the mucosa.

Mucosal olfactory ensheathing cells (mucosal OECs: **A**) recruit fewer axons than NSCs. The mean density at 14 days is about 100 mm^{-1} and falls to 80 mm^{-1} at 21 days.

The fibre length (**B**) stays constant at about 0.15 mm over the observed time period.

Error bars represent standard errors of mean.

Olfactory ensheathing cells from the human olfactory mucosa

These animals were only investigated at the 7 and 14 days time interval. In the initial stages animals received only oral cyclosporine. However, this was not sufficient to suppress the loss of the grafted cells accompanied by the perivascular cuffing characteristic of immune rejection. The grafts became necrotic in a patchy distribution leaving islands of surviving tissue in between. Staining with mouse anti-human mitochondria monoclonal antibody (MIT) revealed a honey comb-like appearance of the cells but did not did not show the typical spindle-like shape of OECs. Recruitment of axons was rarely seen. The transplants were heavily infiltrated by both CD4 and CD8 positive cells. A typical sign of immunorejection, perivascular cuffing (Figure 19) of T-cells in blood vessels supplying the graft, was clearly seen in a number of grafts.

In contrast, transplanted cells survived better in rats receiving systemically administered cyclosporine. Human cells expressing MIT displayed the typical morphology of OECs; cells had a long spindle-shaped cytoplasm with an oval nucleus occupying most of the width of the cell (Figure 20). However, MIT was not always expressed across the whole of the graft although a number of nuclei had a shape suggestive of OEC-morphology. Generally speaking, MIT expression was localised to a few cells only. Axon recruitment was sparse (Figure 20) and varied along the course of the graft.

Mean axon density (Figure 21) increased from 49.9 ± 22.4 mm^{-1} (n=5) at 7 days to 90 ± 10 mm^{-1} (n=2) at day 14. Axon length (Figure 21) was comparable to the sham group (Figure 4) with 0.07 ± 0.01 mm (n=3) at 7 days and 0.06 mm ± 0.01 (n=2) at 14 days.

One graft (Figure 20 H) had formed in the potential space between the thalamus and the internal capsule as previously described for the other cell types. Despite large numbers of MIT-positive cells no axons could be identified in this particular graft.

Staining for immune markers revealed that systemic cyclosporine did not completely abolish the immune response against the xenograft. Mild infiltration by CD4 and (Figure 19) and CD8-positive cells was seen at 7 days but diminished (Figure 20 and Figure 22) by 14 days. Perivascular cuffing was never seen in systemically treated animals. MHC I-complex was only mildly detectable and diffusely expressed but MHC II-positive cells were seen surrounding the graft in close vicinity. Most of the cells (Figure 22) expressing MHC-II complex had an appearance suggestive of microglia.

Experiments with liposomal tacrolimus were unsuccessful. All control cells in culture treated with liposomal tacrolimus died within a 48 hour period. No cells could be detected in any of the animals that had

received cells suspensions mixed with liposomal tacrolimus. Only an empty cavity was found at the transplantation site.

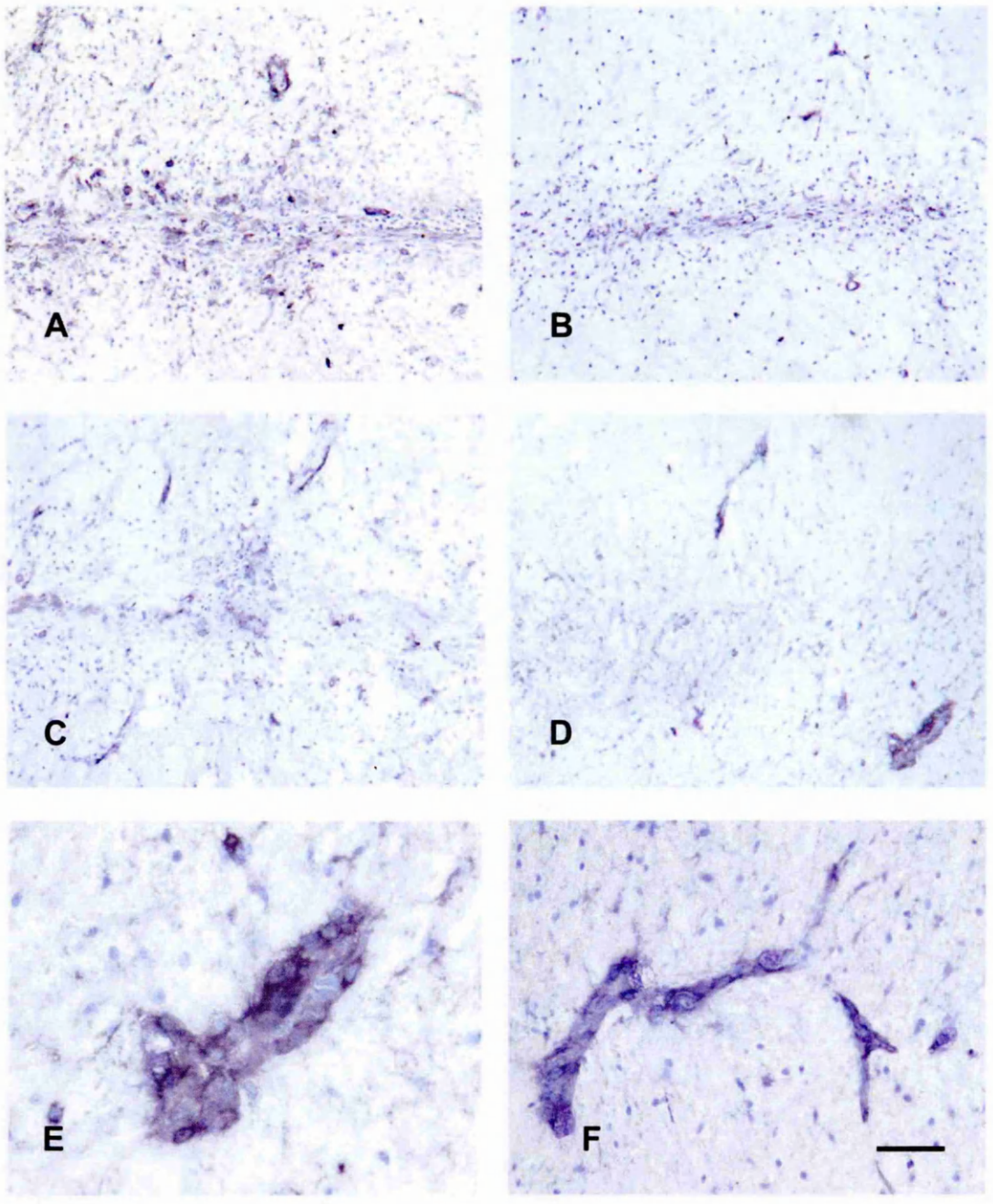

Figure 19 Immunorejection of human olfactory ensheathing cells in rats receiving oral or intraperitoneal cyclosporine.

Photomicrographs of CD4 expression in animals receiving intraperitoneal cyclosporine for 1 week (**A**) and 2 weeks (**B,C**) following microinjection of olfactory ensheathing cells derived from the human olfactory mucosa into the rat thalamus.

Infiltration with CD4 is variable even among animals of the same survival time. Generally speaking, infiltration of the graft is strongest after 1 week (**A**) and becomes much reduced after 2 weeks (**B,C**) in animals having systemic immunosuppression.

In contrast, oral administration of cyclosporine fails to prevent perivascular cuffing (**D**; low magnification, **E** and **F**; high magnification), a hallmark of intense rejection.

Scale bar represents (A,B,C) 100 μm, (D) 200 μm, (E,F) 50 μm.

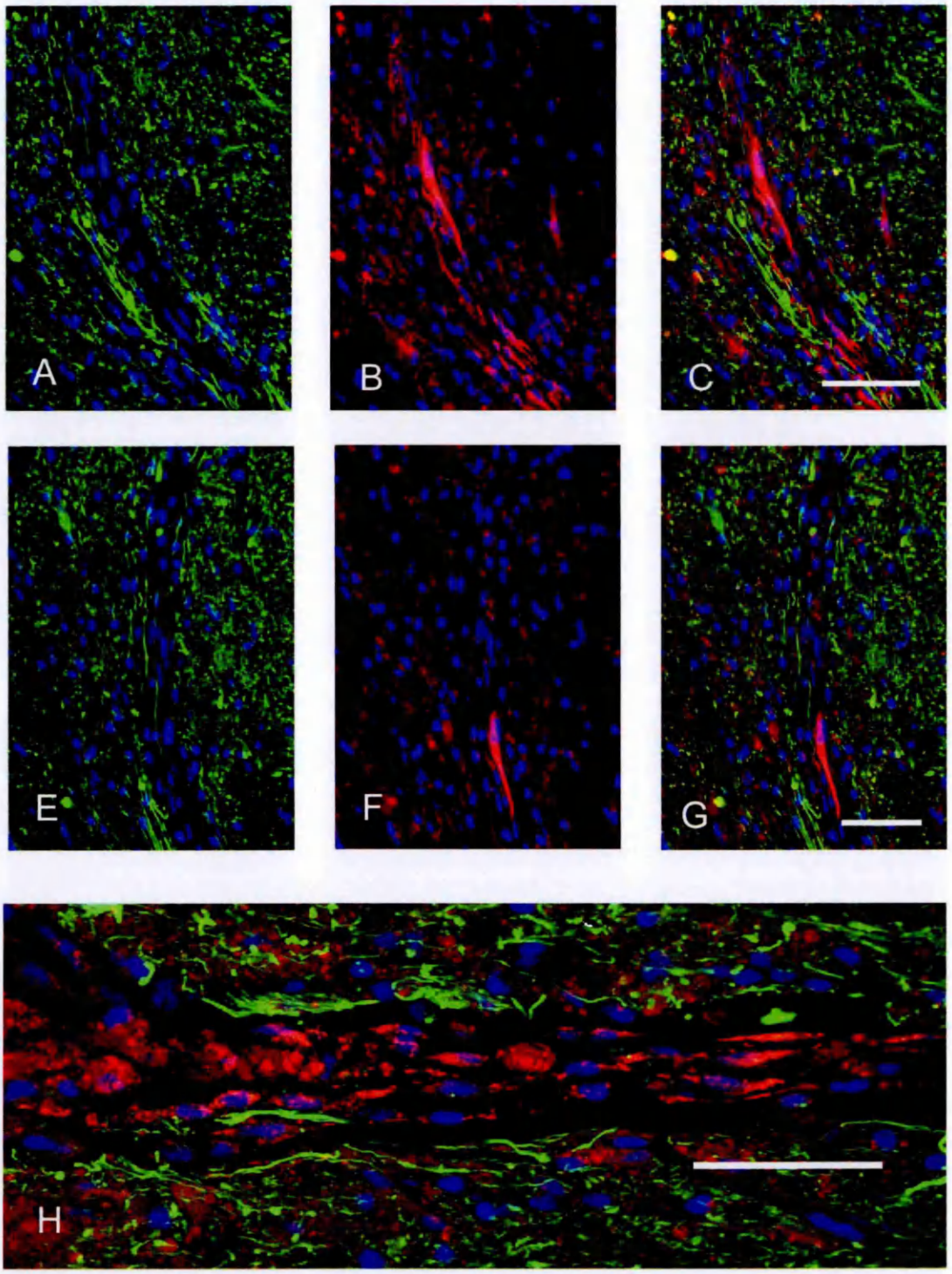

Figure 20 Human OECs from the mucosa transplanted into rat thalamus.

Confocal images of olfactory ensheathing cells (OECs) from the human mucosa 14 days after microinjection into the rat thalamus. All animals received intraperitoneal cyclosporine. The scale bars all represent 50 μm.

Red fluorescent human OECs (**B,F**) identified by human anti-mitochondrial antibody (MIT) recruit small numbers of green-fluorescent axons (**A,E**). Both axons and OECs are sparse in numbers. The overlay image (**C,G**) depicts the relationship between cells and axons.

The bottom image shows a graft occupying the distal end of the thalamus (**H**) whereby the cells have extended horizontally along a weak tissue plane between thalamus and surrounding tissue rather than forming the typical bolus. Very few axons are recruited in this case even though large numbers of transplanted cell have apparently survived and become aligned.

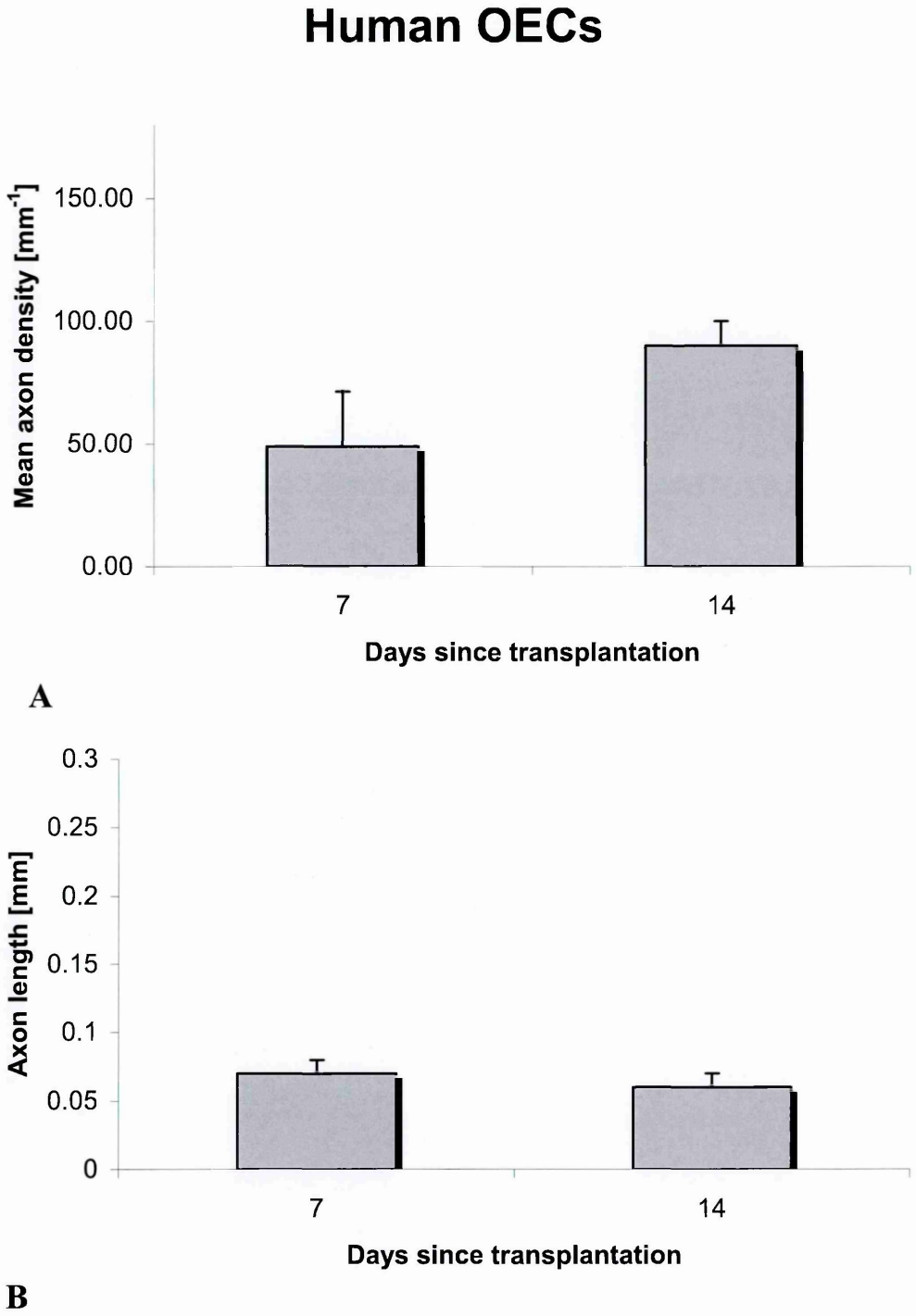

Figure 21 Quantitative analysis of axon recruitment by human mucosal olfactory ensheathing cells.

Human mucosal olfactory ensheathing cells (OECs) in animals receiving systemic cyclosporine recruit small numbers of axons (**A**) which seem to approach a density of about 100 mm^{-1} over time.

Axon elongation (**B**) is severely stunted and is indistinguishable from the control group.

Error bars represent standard errors of mean.

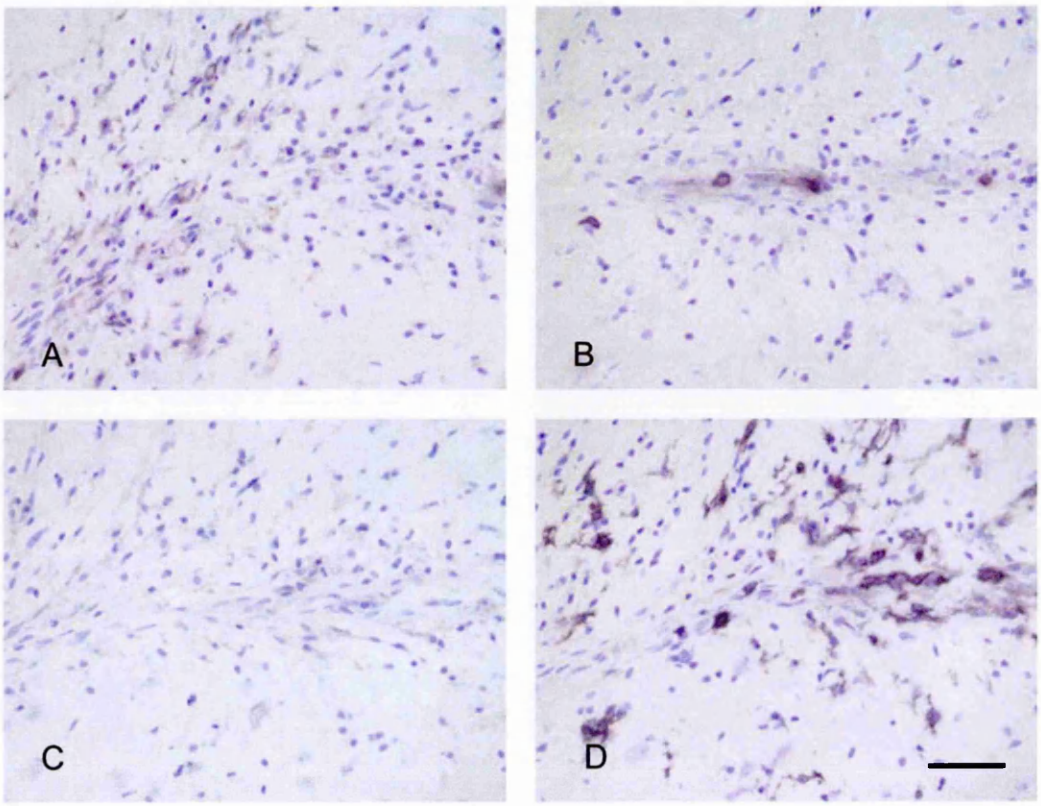

Figure 22 Immune response to human OECs in rats receiving intraperitoneal cyclosporine.

Photomicrographs of olfactory ensheathing cells (OECs) derived from the human mucosa 2 weeks after microinjection into the rat thalamus. Cyclosporine was systemically administered. The scale bar represents 50 μm.

In this sample CD4-positive T-cells (**A**) are not visible and only a few CD8-positive T-cells (**B**) can be detected. Expression of MHC I-complex (**C**) is undetectable in this sample and only weakly stained in other samples. MHC II-positive cells (**D**), mostly of microglial origin, surround the graft.

Neural crest stem cells

Prior to transplantation, cultured neural crest stem cells (NCSCs) were examined under phase contrast (Figure 23) to assess cells for viability and to count their numbers. Approximately 20 % of cells displayed stem cell morphology, 10 % had a Schwann cell-like appearance and the remaining 70 % were identified as smooth muscle cells. Stem cells had a bow-shaped appearance, Schwann cells were spindle-shaped and smooth muscle cells were flat elongated cells characterized by multiple filopodia.

All of the following results were obtained from animals culled 2 weeks (n=8) after transplantation. NCSCs formed columns similar in appearance to the ones seen in grafts employing ASCs, OECs and NSCs. A bolus was commonly seen at the ventral end, just ending close to, or actually abutting the fibre tract of the internal capsule. A number of cells were observed expressing both neurofilament (NF) and peripherin, a marker for neurones of peripheral origin. These cells, therefore identified as neurons, were mainly situated in the bolus or at the ventral end of the column (Figure 24 and Figure 25). They neither expressed nestin nor any of the other markers characteristic for cells of NCSC lineage. Occasionally, axons were observed leaving the cell bodies of these neurons. Those axons were thick and usually only spanned a short distance. The column was characterized by densely packed cells with long processes intermingling with each other. These cells expressed both nestin

(Figure 24 and Figure 25), an intermediate filament protein characteristic of immature neuroepithelial cells, and the glial marker p75. However, they did not express S-100. Although no double-labelling with p75 and nestin was performed, distribution and morphology of the cells identified by these two antibodies were strikingly similar. Numerous delicate NF-positive axons were seen inside the column (Figure 25). They were thinner than the axons observed in any of the other cell grafts previously tested, ran over long distances and were evenly distributed throughout the graft. The precise origin of these axons could not be established. They did not seem to arise from the transplanted neurones of NCSC origin and were not expressing peripherin, the marker for neurones of peripheral origin. Occasionally, the course of the axons could be traced back to the area of the host/graft interface.

The graft/host interface did not show any significant difference to its appearance in ASC, NSC or OEC grafts. Glial fibrillary acidic protein (GFAP) positive astrocytic processes (Figure 25)) entered the graft and aligned themselves with p75 positive/nestin positive cell processes inside the graft. Astrocytic processes only expressed GFAP but not nestin. A close relationship between astrocytic processes, p75/nestin-positive cells and the fine NF-immunoreactive axons could be seen with the three components preferentially running in bundles. At times some axons would part from their

original bundle only to intermingle with an adjacant bundle and follow its course.

NCSCs infected with a defective adenovirus (n=4) containing the DNA sequence for green fluorescent protein (GFP) were used to elucidate the differential fate of these cells *in vivo.* Approximately 80 % of cells in culture labelled positive for smooth muscle actin (SMA). Most of the cells also expressed GFP. None of the cells were observed to express GFP within the column or the bolus following a survival time of 14 days. Cells in the column weakly stained for peripherin, indicating a neuronal fate. However, a cell type of very unusual morphology (picture not shown) was seen at the margin of the graft but just within the host neuropil. These large cells strongly expressed GFP with their processes radiating out in all directions. Some of the processes entered the graft. They did not express any of the markers characteristic for cells of neuronal or glial origin and could hence not be detected by labelling for p75, nestin, GFAP, S100, peripherin or SMA. It is worth mentioning that further experiments in our laboratory have shown the poor survival of GFP-transfected cells at the 2 weeks stage which is possibly related to toxic properties of the vector.

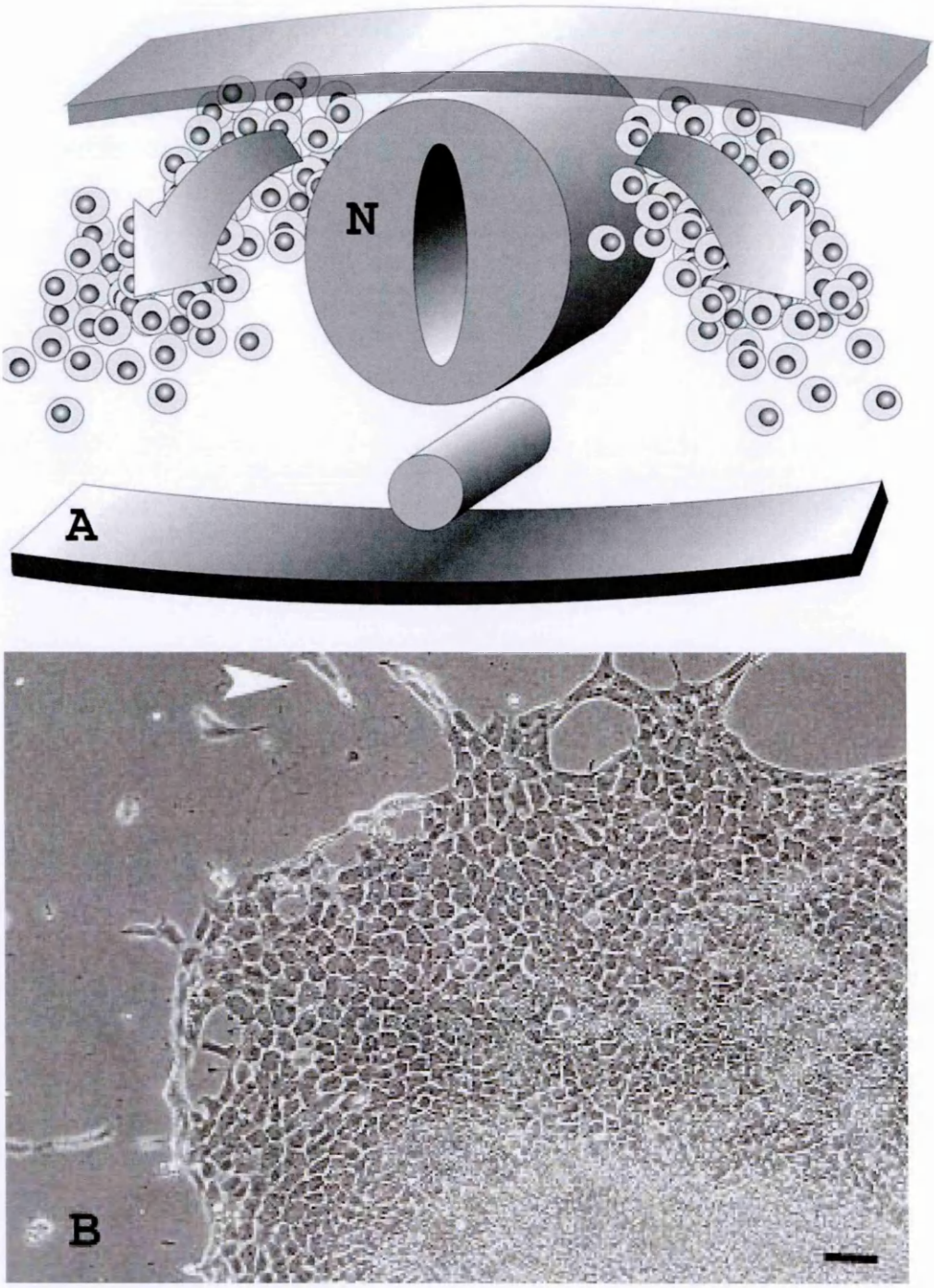

Figure 23 Migration of neural crest stem cells.

Schematic representation (**A**) of neural crest stem cells (NCSCs) migrating (arrows) from the neural tube (**N**) and differentiating into various tissue types.

The phase-contrast photomicrograph of an NCSC explant (**B**) at age 10.5 days (courtesy of Mrs. Harsha Jani) shows how migration also takes place *in vitro*. NCSCs proliferate and migrate (white arrowhead) in cell culture and have the potential to give rise to different cell types.

The scalebar represents 50 μm.

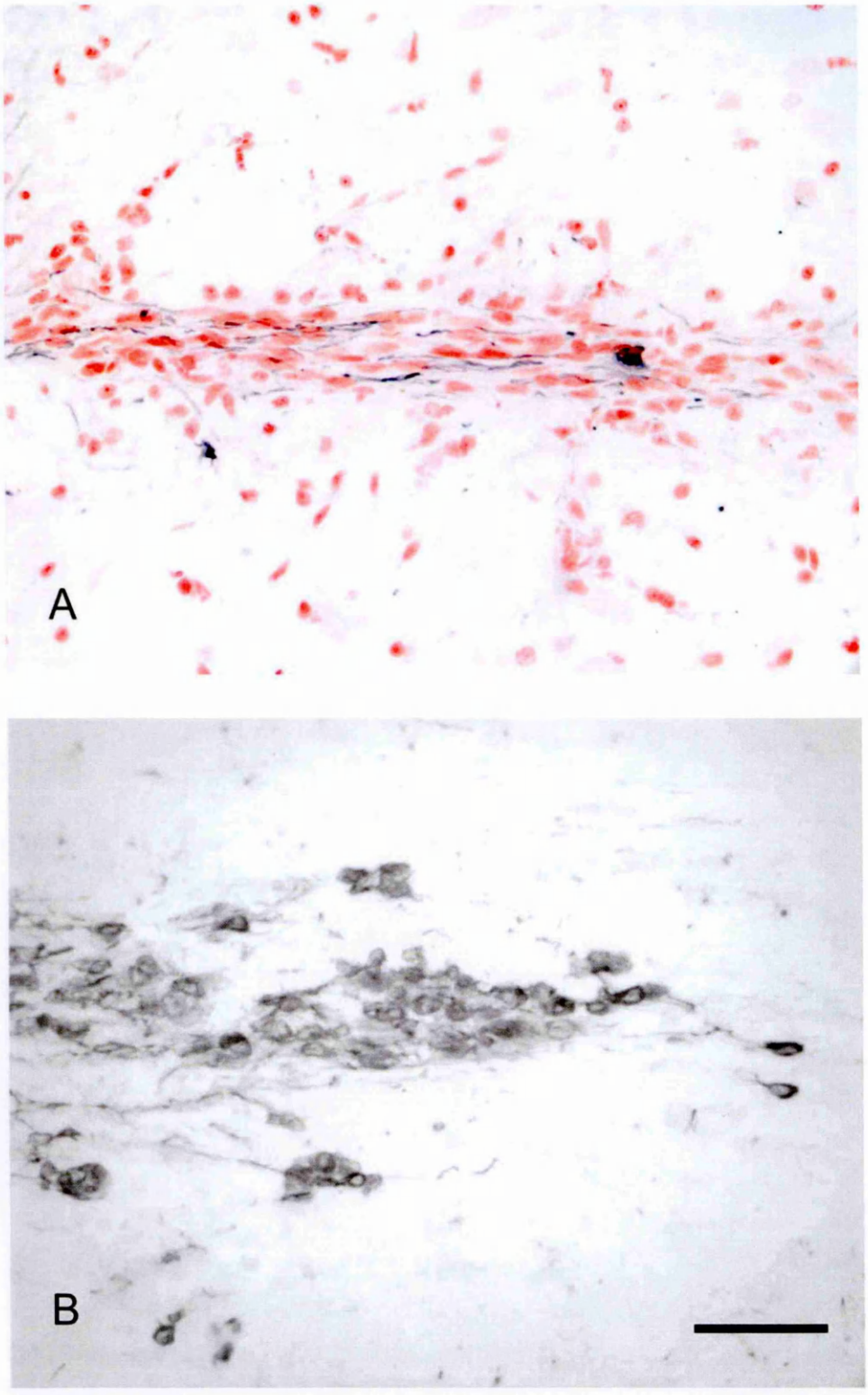

Figure 24 Cell fate of neural crest stem cells grafted into the thalamus.

Photomicrographs of neural crest stem cells (NCSCs) grafted into the thalamus. NCSCs can either adopt a glial or a neural fate depending on environmental cues. The Scale bar represents 50 μm.

Glial cells (**A**) express nestin (black streaks). They are found in the column portion of the graft where they run in parallel bundles. Cell nuclei (red) are counterstained by neutral red.

In the bolus portion of the graft NCSCs are more likely to differentiate into neurones (**B**). These cells stain positive for peripherin, a marker predominantly expressed by neurones of peripheral origin, and often resemble dorsal root ganglia in their appearance.

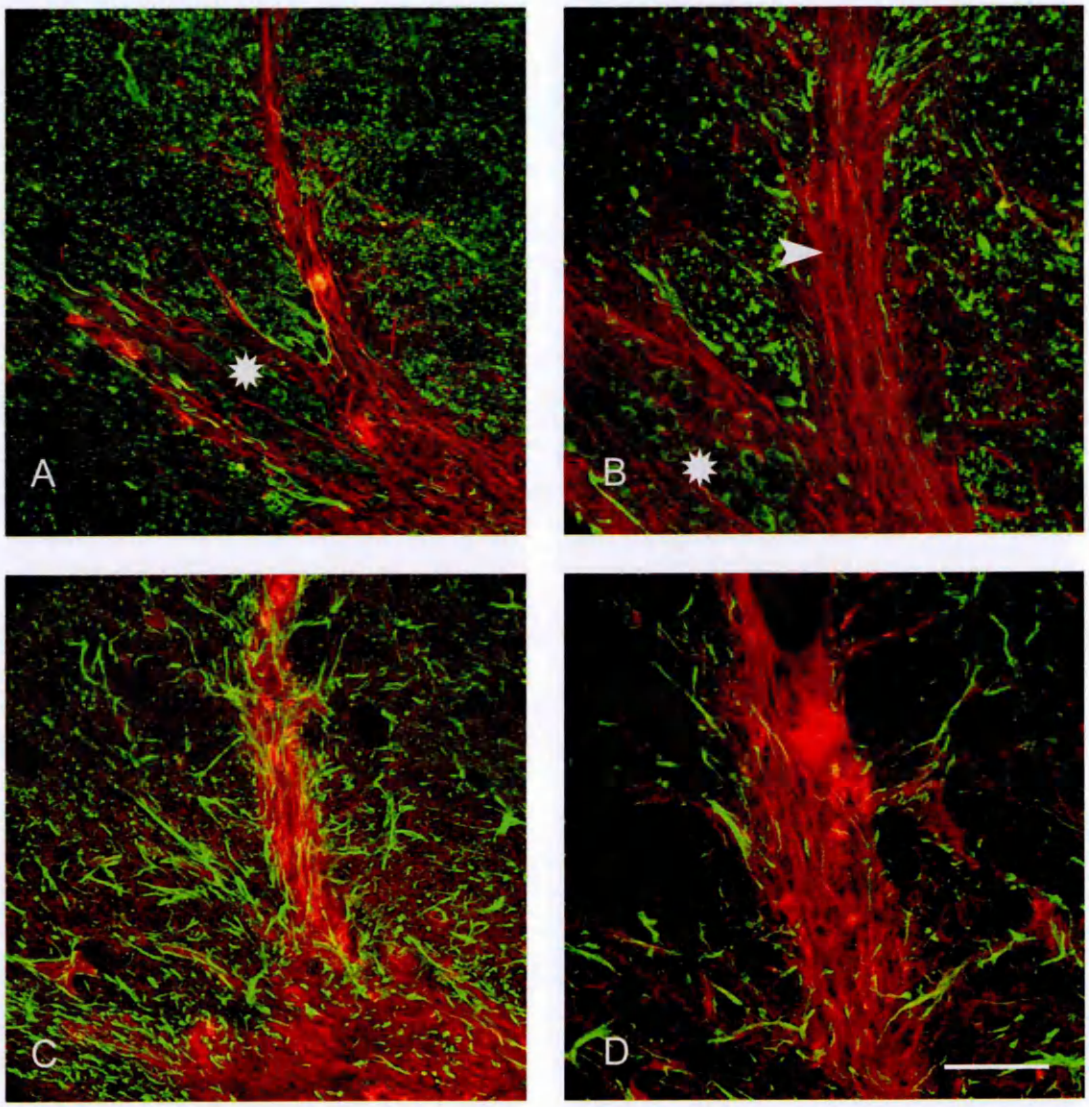

Figure 25 Axon recruitment by neural crest stem cells.

Neural crest stem cells (NCSCs) 14 days after microinjection into the rat thalamus. Scale bar represents 100 μm (**A,C**) and 50 μm (**B,D**).

Neurones and axons are stained for NF (green fluorescence). Glial cells are detected by nestin expression (red fluorescence).

NCSCs (**A**) adopt both a neural (asterix) and a glial fate. Very fine axons (**B**) are attracted into the graft (**arrowhead**). These axons do not seem to be derived from neurones (**asterix**) of NCSC origin.

NCSCs (**C**) differentiate into glial cells expressing p75 (red fluorescence) and intermingling with GFAP-positive (green fluorescence) astrocytic processes. (**D**) The staining pattern of these glial cells is similar for nestin (red fluorescence). Astrocytic processes (green fluorescence) align in the graft.

The fornix system

Pure lesions

It proved to be difficult to achieve a complete lesion transecting the whole of the postcommisural fornix (Figure 3). The lesion size was deliberately kept small not exceeding 1 mm in diameter to avoid a large gap in the fornix that might have had a detrimental affect on fibre regeneration. The initial experiments were therefore largely based on trial and error to optimise the size and position of the lesions. Due to the fact that the flexible electrode was not permanently mounted into the stereotaxic frame and had to be re-adjusted for each use, a further element of variation was introduced into the experimental set-up.

Lesion and fibre tract could clearly be seen under low magnification in unstained sections and a preliminary selection of suitable samples was made at this stage.

In animals that had received pure lesions without grafting of cell suspensions, biotin dextran (BD)-labelled axons were halted and sprouted at the point were they came into contact with the lesion site (Figure 26). They displayed typical growth cone-like structures at their tips and the axons thickened in the vicinity of the lesion. In incomplete lesions intact fibres that closely passed the injury site responded by thickening but did not sprout towards the lesion. The

injury site itself was characterized by significant and extensive tissue damage. A rim of fragmented pieces of tissue surrounded a homogenous necrotic core in the centre of the lesion. The periphery of the lesion counterstained stronger for neutral red than the surrounding intact tissue.

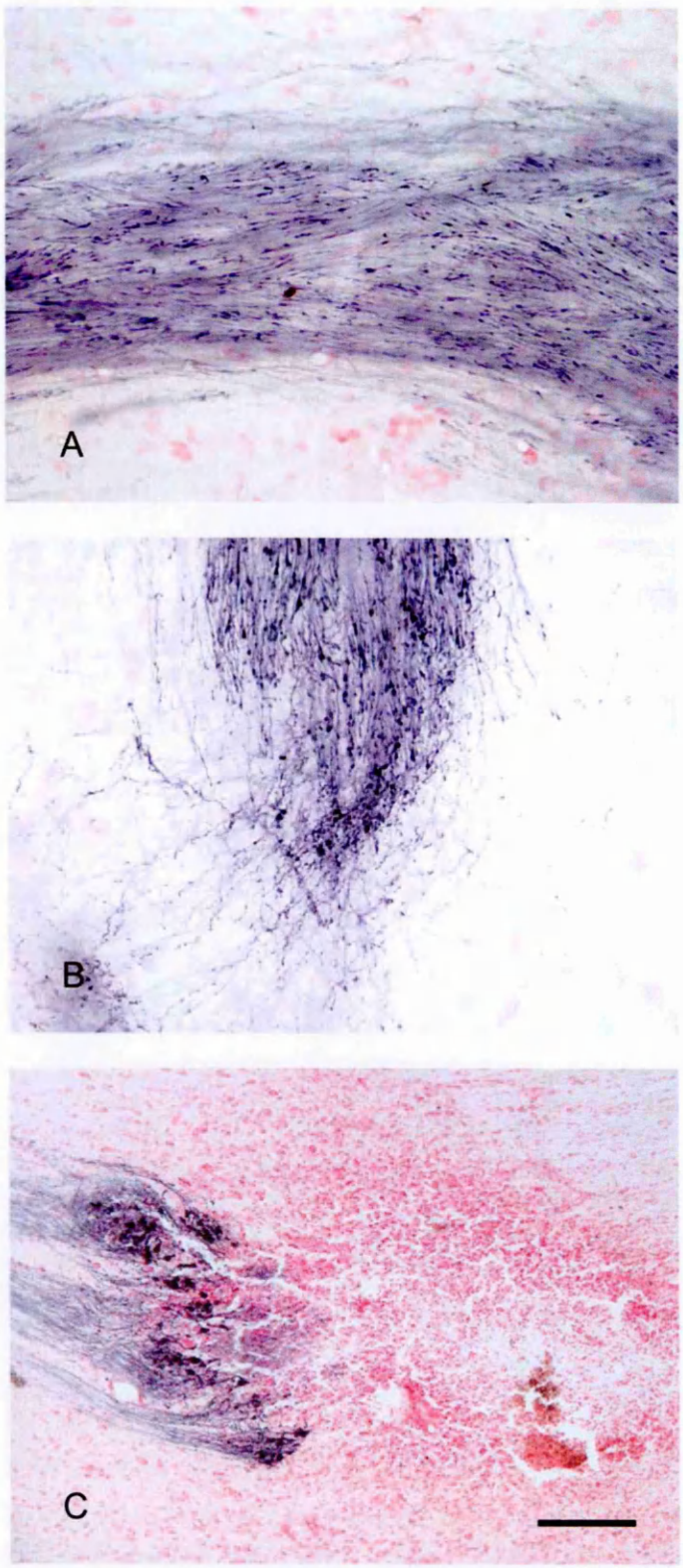

Figure 26 Histological appearance of the intact and lesioned fornix.

The fornix (black stain) is a well-defined white-matter tract that projects from the subiculum via its postcommissural pathway (**A**) to the mamillary body (**B**). The radiofrequency heat lesion (**C**) is characterised by a central necrosis surrounded by a diffuse demarcation zone. Tissue damage is extensive. Fornix fibres (black stain) cannot advance past the lesion site and form bulbous extensions. Reactive sprouting is also visible.

The scale bar represents (A,B) 100 μm (C) 200 μm.

General appearance of fornix grafts

A total of 23 samples were further examined following processing and immunostaining. The samples were judged for general appearance, lesion quality, fibre ingrowth, cell organization and migration of cells. Of these, 8 lesions were apparently complete, another 8 were incomplete and in the remaining 7 samples the tract appeared intact but staining was too weak to evaluate the fibre tract unambiguously. The naked lesion (Figure 26) was characterised by a central necrosis surrounded by a diffuse demarcation zone. Extensive tissue damage was noted. Fornix fibres were incapable of advancing past the lesion site and formed bulbous extensions. Reactive sprouting was also visible.

The appearance of the cell transplants bore a clear resemblance to the thalamic grafts. Although not primarily intended, typically a small column had formed at the dorsal site of the lesion, which ended in a cell globus filling the lesion cavity. Just as in the thalamic columns, cells ran in parallel strands aligning with the column. The bolus contained numerous cells orientated in whorls and circular structures. The cells in the bolus did not align with the course of the postcommissural fornix.

BD-labelling proved to be a reliable way of tracing the fornix to the lesion site. None of the cell transplants were associated with fibre

regeneration, neither into the graft nor beyond the lesion site. Although axons were unable to advance into the lesion site, cells were seen to migrate from the graft into the intact proximal and distal postcommissural fornix. These cells were properly aligned with the tract and intermingled with BD-labelled axons.

Neonatal Schwann cells

Neonatal Schwann cells (NSCs) (Figure 27) strongly expressed p75 and survived well in the grafted areas. They often formed a short column with well-aligned cells extending into the bolus at the ventral end. Cells in the bolus were poorly organised and had a scattered appearance. In a number of cases NSCs were circularly oriented around the central necrosis. The centre of the bolus was devoid of cells and filled with an amorphous substance indicating a necrotic process. The cells attracted NF-positive axons into the column where they were aligned with the NSCs, as in the thalamus grafts. NF-positive axons of short length were even detected in the bolus. But NSCs failed to guide BD-labelled postcommissural axons into and past the lesion site. The fibres stopped abruptly at the point where they came into contact with the lesioned area, which had become occupied by the grafted cells. Axons in close proximity to the lesion became thickened, exhibited many varicosities and often ended in growth cone-like expansions. NSCs migrated towards the proximal fornix. They extended only for a very short distance into the proximal fornix and ran in parallel with the tract direction. The cell

density was notably lower than in the bolus and p75 was less strongly expressed. A similar phenomenon was observed in the distal part of the fornix just past the lesion site. At the proximal end BD-labelled axons and NSCs came into contact with each other, forming an overlapping zone (Figure 27). In those grafts where the lesion maker had failed to disrupt the fornix completely NSCs were observed to become integrated into the fornix. It was impossible to decide whether these fibres were surviving fibres, which were merely surrounded by transplanted cells or newly regenerated fibres that had been attracted into the lesion area.

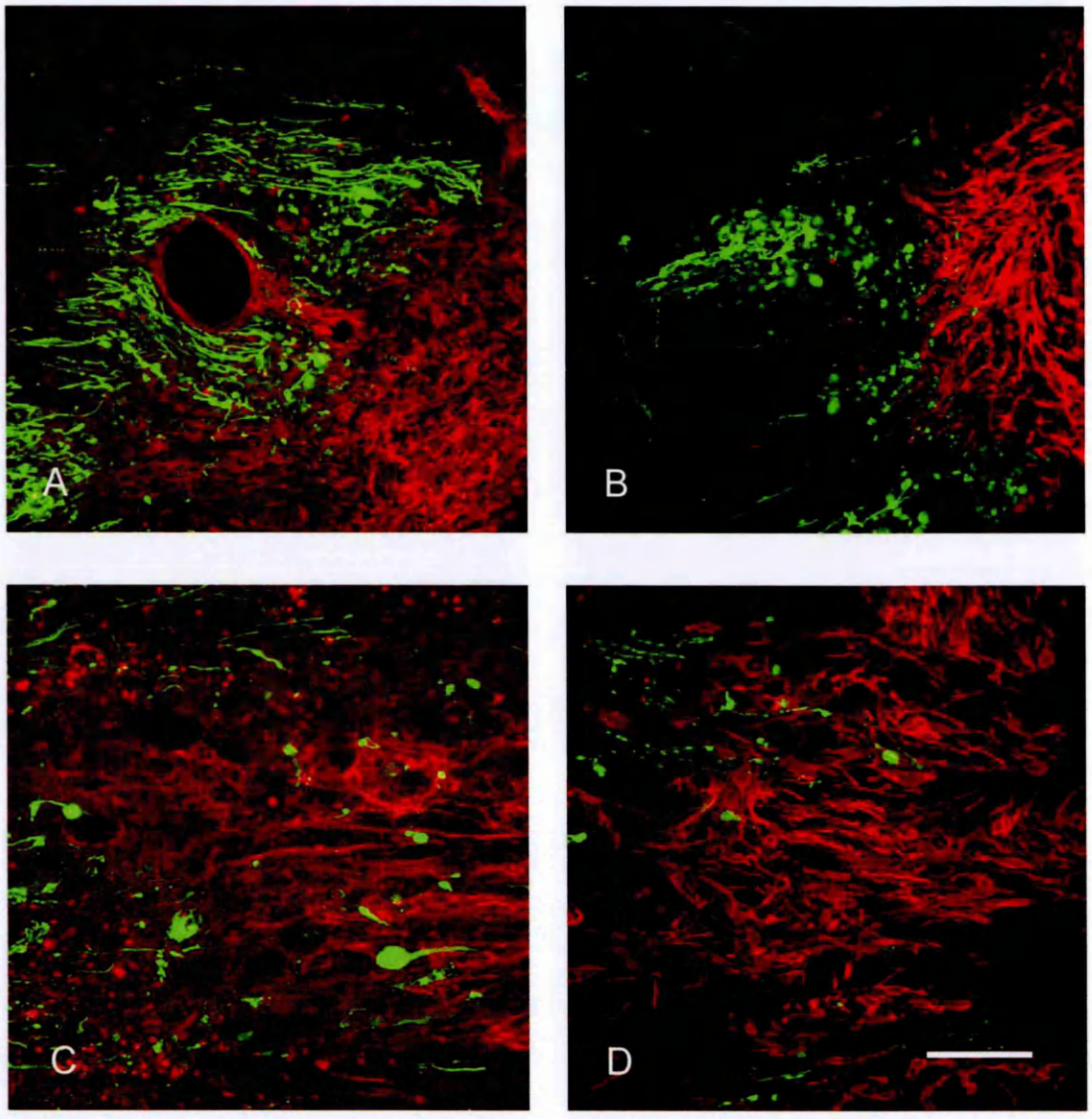

Figure 27 NSCs grafted into the lesioned postcommissural fornix.

Confocal images of neonatal Schwann cells (NSCs) from 4 different samples grafted into the lesioned post-commissural fornix 2 weeks after the procedure. Animals were labelled with biotin dextran (BD) immediately after lesioning and microinjection of cells. Scale bar: Top row: 100 μm. Bottom row: 50 μm.

Green fluorescent BD-labelled axons (**A**) fail to advance past the lesion/ transplant site. The grafted red fluorescent p75-positive NSCs (**B**) are typically arranged in a circular pattern around a central necrotic area.

NSCs migrate from the graft into both the proximal (**C**) and distal fornix where they line up and overlap with fornix fibres. Failure of disrupting the fornix (**D**) results in NSCs lining up with the tract direction and limited regeneration of fibres into the graft.

Olfactory ensheathing cells

BD-labelled axons responded to OECs (Figure 28) just as they did to NSCs. The lesion site was completely impenetrable to fibres and postcommissural fornix fibres were never seen entering the bolus. However, NF-immunoreactive axons of unknown origin were seen in both column and bolus (Figure 28D). They ran in parallel bundles in the column-like part of the graft, whereas in the bolus they followed a more circular course. OECs migrated into the proximal and distal ends of the severed fornix and intermingled with the axons.

Delayed transplantation

Delayed transplantation did not confer any benefit in terms of regeneration. OECs transplanted 4 weeks after the original lesion failed to attract any fornix fibres into the lesion site.

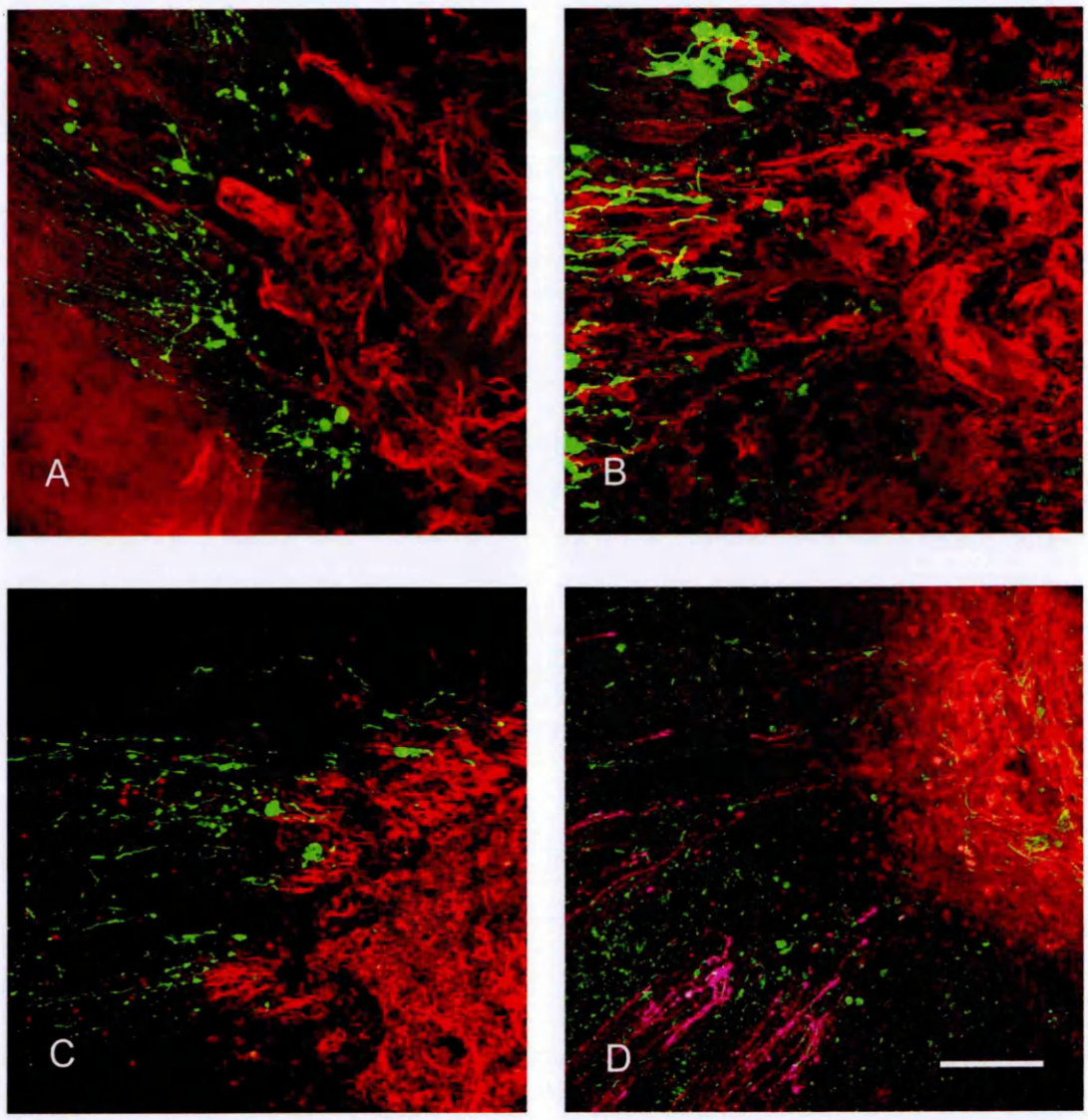

Figure 28 OECs transplanted into the lesioned fornix.

Olfactory ensheathing cells (OECs) grafted into the post-commissural fornix 14 days after surgery (**A,B**): Green-fluorescent biotin dextran (BD)-labelled fibres fail to enter the grafted cell bolus at the lesion site. OECs expressing p75 (red fluorescence) migrate into the proximal end of the fornix (more obvious in **B**).

The situation is unchanged (**C**) even 3 weeks post-operatively. Although BD-labelled purple-stained fornix fibres fail to regenerate (**D**) the p75-positive red-fluorescent graft manages to attract green-fluorescent NF-positive fibres of unknown origin.

Scale bar represents 100 μm except for B (50 μm).

Foetal brain cells

Embryonic rat brain cells comprising neurones and glia (Figure 29) harvested 14 days after conception, failed to enable regeneration past the lesion site just like in the other cell types. They did neither express p75 nor GFAP in the centre of the lesion. DAPI-stained nuclei of different shapes and sizes could be detected. The cells had a heterogeneous distribution and differentiated into various cell types. They sometimes appeared to be organised in subpopulations. Interestingly, cells in close contact with the fornix expressed p75. This was most obvious in an incomplete lesion, where BD-labelled uninterrupted fibres ran alongside the bolus. Cells adjacent to the fornix expressed p75 weakly and diffusely.

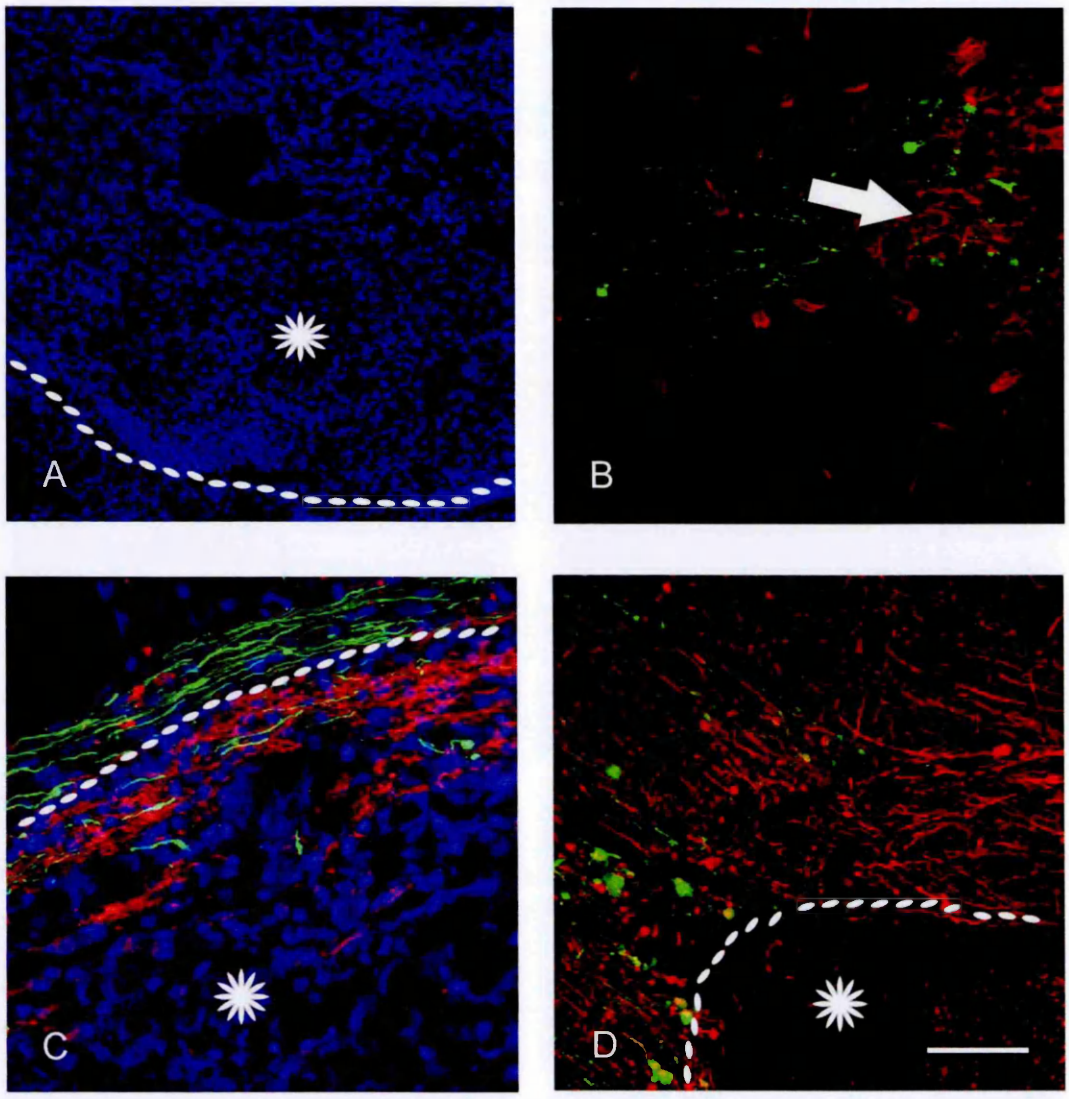

Figure 29 14 day old embryonic brain cells transplanted into the lesioned fornix.

DAPI staining of 2 weeks old embryonic (E14) brain cells (**A**) 2 weeks after microinjection into the fornix reveals heterogeneous cell populations. The approximate graft border (**A,B** and **D**) is marked by the white dashed line. The asterix lies within the graft. The scale bar represents 100 μm except for C (50 μm).

Red-fluorescent E14 cells (**B**) express p75 (arrow) when they migrate into the fornix. E14 cells only express p75 (**C,** red fluorescence) when they come in close contact with the fornix fibres (green fluorescence).

The transplant in the centre (**D**) expresses neither GFAP nor p75. NF-positive fibres (red fluorescence) are likewise not seen within the graft. The graft centre is devoid of any NF-positive fibres but fibres can be seen elsewhere corresponding to the normal anatomical appearance of the host.

Statistical results

The following self-explanatory ***Table 1*** provides a summarised view of all measurements obtained for the different transplant groups. The specific data were discussed in the previous sections in relation to each candidate repair cell type. The table is split into 2 subtables; an upper section relating to the mean axon density and a lower section relating to the mean axon length. The columns represent the time axis for life spans of 7,14 and 21 days and the rows represent the various cells types further subdivided into sample size, mean and standard error of mean.

Cell type	Days post OP	Axon density in mm^{-1} 7 days	14 days	21 days
ASC	sample size	15	13	6
	mean	53.833	68.742	63.095
	sem	13.621	9.028	13.454
OEC	sample size	21	9	9
	mean	29.327	31.019	91.429
	sem	2.625	4.593	18.039
NSC	sample size	6	10	3
	mean	76.944	91.681	126.667
	sem	5.618	10.853	27.437
OEC rat mucosa	sample size		5	8
	mean		101.857	79.048
	sem		16.143	11.359
OEC human mucosa	sample size	5	2	
	mean	48.890	90.000	
	sem	22.390	10.000	
Sham group	sample size		5	
	mean		35.000	
	sem		11.300	

Cell type		Axon length in mm 7 days	14 days	21 days
ASC	sample size	10	12	6
	mean	0.130	0.139	0.127
	sem	0.024	0.022	0.020
OEC	sample size	21	9	9
	mean	0.082	0.138	0.108
	sem	0.007	0.027	0.018
NSC	sample size	6	10	3
	mean	0.185	0.217	0.210
	sem	0.030	0.027	0.047
OEC rat mucosa	sample size		5	8
	mean		0.156	0.159
	sem		0.028	0.029
OEC human mucosa	sample size	3	2	
	mean	0.070	0.060	
	sem	0.010	0.010	
Sham group	sample size		5	
	mean		0.050	
	sem		0.010	

Table 1 Overview of measurements

Kruskal-Wallis Test

One of the most widely used tests in the biological sciences is Student's t-test which allows a pair-wise comparison of sample sets. One may be tempted to use this test for comparison of multiple samples but the t-test is not suitable for higher degrees of freedom (ie. more than 2 samples to compare) and also assumes a normal distribution (data should not be skewed either) of the data sets. Analysis of variance (ANOVA) should be used to compare the means of groups of measurement data.

The sample sizes for my data were of unequal size and, by drawing simple histograms, some of them did not appear to correspond to the classical Gaussian Bell curve distribution. This ruled out a simple analysis of variance (ANOVA) test since it relies on normally distributed data and equal sample sizes and relatively homogenous variances.

To overcome this problem I applied the Kruskal-Wallis test (Rohlf and R.R.Sokal, 1995) which does not make prior assumptions about the distribution of the data set. It is mathematically identical to the Mann-Whitney U test but enables comparison of more than 2 groups. The underlying principle of the Kruskal-Wallis test (named after William Kruskal and W. Allen Wallis) is the transformation of all data into simple rank numbers (integer numbers from 1 to the last sample

count) which are then redistributed to their respective sample group. Tied samples get average ranks i.e. if we had 4 samples with equal measurements occupying rank position 7,8,9 and 10 then 8.5 would be substituted for each measurement value (with ranks 7,8,9 and 10 absent from the table). However, it is recommended that the test has not too many tied values. The effect of this rank transformation is that widely disparate numbers are hence more equally distributed and closer to each other. The variances of the rank means for the groups are then compared. The test statistic H is calculated and then compared with the critical value of the chi-square table for (k – 1; where k is the sample size) degrees of freedom for a given significance level.

The formula to calculate the test statistic is:

$$H = 12/(N(N + 1))^* \text{SUM}(T^2_i/n_i) - 3(N + 1)$$

where H: test statistic

N: Highest rank

T_i: Total of rank numbers for each sample group i

n_i: Number of observations/ data for each sample group i

The null hypothesis H_0 states that there are no expected differences between the mean ranks.

The null hypothesis H_0 is rejected if H is larger then the critical value found in the chi-square table for the given significance level. A

rejection of the null hypothesis H_0 does not necessarily mean that there are statistically significant differences between all sample groups, it would be sufficient for one group to differ from the others. For this reason a pair-wise comparison may still be necessary.

The original table for the measured axon length in mm at 14 days post- operation was as follows:

ASC	OEC	NSC	sham	OEC mucosa	human OEC
0.05	0.3	0.3	0	0.2	0.07
0.15	0.06	0.2	0.07	0.1	0.05
0.15	0.14	0.28	0.03	0.08	
0.1	0.2	0.15	0.03	0.18	
0.1	0.06	0.15	0.05	0.22	
0.15	0.2	0.15			
0.07	0.1	0.2			
0.35	0.12	0.15			
0.15	0.06	0.35			
0.15		0.35			
0.15					
0.1					

The rank-transformed table is as follows:

ASC	OEC	NSC	sham	OEC mucosa	human OEC
5	39.5	39.5	1	34	11
25.5	8	34	11	16	5
25.5	20	38	2.5	13	
16	34	25.5	2.5	31	
16	8	25.5	5	37	
25.5	34	25.5			
11	16	34			
42	19	25.5			
25.5	8	42			
25.5		42			
25.5					
16					

Using the Kruskal-Wallis test:

T_i	259	186.5	331.5	22	131	17
T_i^2	67081	34782	109892	484	17161	289
n_i	12	9	10	5	5	2
T_i^2/n_i	5590	3865	10989	97	3432	145

Using the above values in the formula yields: 12/1806*24118-129=31.25

The null hypothesis is hence rejected as this value exceeds the critical value from the chi-square table which is 20.52 for 5 degrees of freedom and a significance level of P = 0.001. This means the differences seen between the samples are highly significant.

The calculation for the different cell groups without the sham group is similar. However, I have used a special Excel spreadsheet (http://udel.edu/~mcdonald/statkruskalwallis.html) for the calculation (rather than the by hand approach used for the example) which gave slightly different results because the tied samples were adjusted in a different way.

I first compared all groups including the sham group for the 14 day period. The differences observed were highly significant. I then omitted the sham group for the comparison and found that the differences were still significant but to a lesser degree. This would support the view that the observed differences were not just statistically significant when compared to the sham group but that there were also statistically significant differences between the various cell types.

The spreadsheet calculation for axon length at 14 days gave an adjusted H of 41.65 for all groups (highly significant) and an adjusted H of 32.53 for cell types only (still highly significant). There was also a statistically significant difference between OECs and NSC (H=7.1)

but this was not highly significant (p=0.008) and a comparison of OEC from bulb and mucosa yielded a test statistic of H=0.45 with p=0.5 which means that there was no significant difference between OECs derived from the bulb or the mucosa.

The spreadsheet calculation for axon density at 14 days gave an adjusted H of 31.04 for all groups which was highly significant and an adjusted H of 27.5 (still highly significant) for all cell groups. Inter-group comparison of OECs and NSCs resulted in an adjusted H of 13.6 and this was statistically highly significant. Likewise differences between OEC from bulb and mucosa were highly significant (H=9.1; p=0.002).

Discussion

The thalamus as a model

General considerations

The thalamus proved to be a useful model for the study of cell survival, host response and axon recruitment. A large number of candidate repair cells could be investigated. The results varied to some degree as anticipated in a biological system but still allowed meaningful interpretation of the findings. Descriptive statistics of the cells clearly showed differences in axon recruitment but otherwise there were striking similarities between the cells with regard to staining pattern and astrocytic response. Interestingly, the shape of the nuclei and the appearance of axons were a better guide to cell identity than p75, nestin or fibronectin staining. The staining pattern was largely indistinguishable between the various candidate repair cells but the shape and organisation of nuclei provided some clues as to the origin of the cells. Fasciculating axons with varicosities were most commonly seen in neonatal Schwann cells (NSCs). Olfactory ensheathing cells (OECs) from the mucosa had the thinnest and longest cell nuclei. But even for the same cell type there was a considerable degree of variability in the shape of the nuclei.

All the candidate repair cells were able to survive in the thalamus. Survival of candidate repair cells was, as expected, only a problem in xenografts. An interesting finding was that nestin and p75 stained Schwann cells and OECs in a similar pattern and this was clearly recognisable when adjacent sections from the same animal were examined. Nestin, commonly thought of as a marker of immature neuroepithelial cells, yielded a clearer and less diffuse staining pattern of the cells when compared to p75.

All cells were lining up in parallel with the column but cell nuclei were more organised and more elongated in NSCs and mucosal OECs than in bulbar OECs. All candidate repair cells but human OECs displayed migratory behaviour. The adjacent astrocytic scar response was only mild and did not differ significantly between the cells examined as would be expected from a lesion technique aimed at minimal disturbance of the host environment. Also, astrocytes (Wei et al., 2002;Lin et al., 1995) did not exhibit any signs of nestin-immunoreactivity in keeping with a low degree of activation.

The experiments have also shown that all candidate repair cells are able to recruit cells. NSCs stood out since they recruited both the largest number of axons and the longest axons. OECs from the mucosa came next in order with slightly less and shorter axons. But surprisingly, OECs from the bulb recruited only small numbers of

axons of short length. In fact, measurements of the axon density at 1 and 2 weeks were similar to the sham group.

Most likely, it is the exposure to neurotrophic factors that directly influences the length and number of axons. Younger cells like NSCs are more rich in neurotrophic factors and therefore provide better support for axons. The mucosal OEC may represent a younger version of the OEC (Au and Roskams, 2003) if one assumes that OECs of placodal origin arise from the mucosa in the adult animal and travel from there to the bulb while they undergo maturation. Alternatively, the mucosa may be the site of a putative OEC stem cell or OEC precursor cell (Chuah and Au, 1991) that may have given rise to less mature OECs in culture.

The method employed here to quantify the recruitment of axons is relatively simple and quick. The densest appearing group of axons within the graft is selected for counting. An imaginary line representing the width of the column is intersected by fibres which are then counted. It was my impression that axons are generally fairly evenly spaced but they do not always occupy the whole length of the transplant. The transplants are three-dimensional structures and the counting method used here is essentially one-dimensional in nature. This may introduce certain errors since the method heavily relies on the observer's perception of the area of highest axon density. Three-dimensional reconstruction of the slices would

theoretically have given more precise measurements since axon density may vary from layer to layer and it would have also taken into consideration the segmental distribution of axons favouring the ventral end of the column. In other words the method employed here is biased towards the best area of axon regeneration within the graft. Small localised areas of fibre recruitment are commonly seen in OEC grafts. In support of this method it can be said, that using a large enough sample size should have overcome the difficulty of selecting the most representative layer. The method was able to show a difference in axon density between OECs and NSCs in spite of a bias towards a higher density in OECs, where samples with a dense appearing area of axons that did not cover the whole of the column led to a potentially higher count. In other words, one might have expected an even greater difference between OECs and NSCs in reconstructed samples where the localised fibre recruitment observed in OECs related to the whole volume of the column would have potentially yielded very low counts.

Reconstruction would also have enabled a more accurate determination of actual axon length. Slices through tissue samples can be oblique in relation to the position of the column to varying degrees. Reconstruction would have helped to determine the direction of the fibres and measure their length more precisely. Again, one has to say that this error would lead to a shorter

measurement of axon length on average but be overcome by the fact that all cell grafts are equally affected by this effect.

The poor performance of OECs for the first 2 weeks is evident not just from descriptive axon statistics but also from the histological appearance of the graft. There were a number of failed grafts and even where the grafts had been successfully taken, macrophages and scattered cells with large and plump nuclei indicated problems with cell survival and cell integration. This is an interesting observation because OECs are better than Schwann cells in facilitating axon regeneration is the spinal cord. The thalamic column assay measures different properties of the OECs and is not directly predictive of repair in the spinal cord. The thalamus assay reflects the recruitment potential of OECs whereas a successful outcome in the spinal cord model depends on nerve fibres re-entering the CNS. Different culture conditions may have also affected the regenerative potential of OECs. In fact, it is through the process of culturing (Raisman, 2001) that OECs gain their regenerative potential in the first place and it may therefore not be surprising if even slight differences in culture conditions yield cells with different properties.

Axon recruitment goes hand in hand with the ingrowth of astrocytic processes Astrocytic processes are mingling with axons and directing them into the graft where they become aligned with other structures (Brook et al., 2001). The important relationship between

astrocytes and axons was apparent from all candidate cells examined. Failure of regeneration is also a failure of astrocytic processes entering the graft and providing support for axons. However, I was unable to establish a clear relationship between the extent of astrocytic scarring and the ingrowth of fibres. There appeared to be little difference in the amount of scarring between the different cell types observed. Since astrocytes are commonly viewed as responsible for the formation of an inhibitory glial scar impeding regeneration, this raises questions regarding their precise role in regeneration and points to a more complex picture.

The thalamus model does not lend itself to the study of axon re-entry. There is no clearly defined fibre tract that is suitable for labelling. Likewise, the origin of recruited axons is unclear although some evidence points at the reticular nucleus (RTN) (Vaudano et al., 1998a) as the source of recruited axons. In all grafting experiments, axons were mainly seen at the ventral end of the column as one might expect from axons originating from the RTN. It would therefore appear that candidate repair cells selectively recruit axons from this area of the thalamus. This is in line with other observations suggestive of differential recruitment depending on the type of candidate repair cell employed. Schwann cells can regenerate specific fibre tracts in the CNS (Wunderlich et al., 1994) (Montero-Menei et al., 1992) but fail to restore the corticospinal tract (Li and Raisman, 1994).

In the corticospinal tract OECs are the only cells that have been unambiguously shown to mediate regeneration of severed fibre tracts (Li et al., 1997;Ramon-Cueto and Nieto-Sampedro, 1994). Regeneration in the corticospinal tract results in axons re-entering the host and forming new synaptic connections with denervated target areas. There are a number of experimental models where OECs had no measurable effect on axon regeneration (Gomez et al., 2003) (Nieto-Sampedro, 2003). Interestingly, OECs from the bulb also appear to perform worse than other cell types in the thalamus model. This could possibly be related to varying culture conditions, the environment at the transplantation site or a differential response of thalamic axons to these cells. The disorganised appearance of OECs, however, strongly points at adverse environmental conditions at the lesion site or a higher sensitivity of OECs to environmental factors. The age at which OECs were transplanted varied slightly and cultures took at times longer to arrive at the desired stage owing to differences in serum. Young OEC cultures were noted for their higher mitotic activity in culture and it is possible that less mature OECs secret higher levels of neurotrophic factors than older OECs. This view is partly supported by studies comparing neurite outgrowth in the presence of immortalised pure neonatal and adult OECs cultures (Goodman et al., 1993). In these studies neonatal OECs stimulated the growth of marginally longer neurites. Nevertheless, the differences found were only small and the cells were obtained by simian virus 40 (SV40) large T antigen transduction. Older cultures

of OECs had a higher proportion of fibroblasts but also were more likely to contain dying OECs. It is hard to believe that culture conditions alone should account for the differences observed between OECs and NSCs since culture conditions were also varying to some degree in the other cell lines. The actual transplantation procedure and the host site must also play an important role. On the other hand, the possibility that culture conditions might be more crucial for OECs than other repair cell lines cannot be completely ruled out. It is possible that OECs from the bulb produce neurotrophic factors at lower concentrations than other candidate repair cells. It is their ability to enable severed nerve fibres to re-enter the uninjured host tissue that sets them apart from other candidate repair cells and forms the prerequisite for functional recovery. Many studies support the view that OECs exert their effects through direct cell-to-cell interactions (Lakatos et al., 2000) (Lakatos et al., 2003a) rather than through neurotrophic support. But in all likelihood the chief property measured by the thalamic assay is the neurotrophic support on nerve regeneration by the transplanted cells.

When given additionally to Schwann cell grafts, neurotrophic factors mostly failed to coerce axons into leaving the transplant but neurotrophic factors elicited stronger axon recruitment (Tuszynski et al., 1998) (Weidner et al., 1999a) into the grafts than Schwann cells alone did. These observations support the view that axon

recruitment into the graft depends critically on the level of neurotrophic factors but exposure of axons to neurotrophic factors does not necessarily facilitate host re-entry.

Schwann cell-filled seed channels in a thoracic spinal cord hemisection model were claimed to achieve regeneration of some axons into the distal spinal cord (Xu et al., 1999). This model was further refined by direct infusion of BDNF and NT-3 into the spinal cord distally to the seed channels and enabled the re-entry of fibres into the distal host parenchyma (Bamber et al., 2001).

It remains to be seen whether OECs from the mucosa are even more effective in spinal cord repair since they recruit larger numbers of axons in the thalamus than bulbar OECs but are also expected to share common properties with OECs from the bulb. Theoretically, cells that enable host re-entry as well as provide strong neurotrophic support should be particularly effective in white matter tract repair.

Histologically, OECs, NSCs, ASCs, mucosal OECs and even NCSCs were indistinguishable by their staining pattern. All of them stained for p75 and nestin. If one excludes the NCSCs, which were not examined for fibronectin, then all of them (as none of them were pure cultures) contain cells that express fibronectin. The similarities between OECs and Schwann cells are striking and extensively supported by the literature (Wewetzer et al., 2002). Both cell types

express Dhh (Smith et al., 2001), a molecule that regulates the formation of the epi- and perineurium and enables co-operation between Schwann cells and fibroblasts.

Evidence for differences between OECs and Schwann cells has come mainly from observations of axonal and astrocytic responses in culture and *in vivo* (Lakatos et al., 2003a). OECs naturally co-exist with astrocytes in the bulb. In culture, OECs freely intermingle with astrocytes (Van Den Pol and Santarelli, 2003) whereas Schwann cells induce astrogliosis and hypertrophy of astrocytes. Furthermore, Schwann cells and astrocytes are separated by basal laminae into distinct territories. OECs appear to act through a combination of direct cell-to-cell interactions and neurotrophic support (Li et al., 2004) and it is assumed that it is the former mechanism that facilitates re-entry of host fibres.

OECs do not only promote fibre regeneration through direct cell-to-cell interaction and neurotrophic support they also appear to be involved in myelination of regenerating fibres. However, it has been suggested that the myelination seen after OEC transplantation is due to Schwann cell contamination. Several studies appear to support this claim. The investigators of one *in vitro* study (Plant et al., 2002) observed that OECs co-cultured with dorsal root ganglion neurons did not exhibit a Schwann cell-like relationship to axons and did not form myelin. In contrast, previous in-vitro studies studies have

shown that OECs can myelinate dorsal root ganglion neurones (Devon and Doucette, 1995).

In vivo experiments have also yielded equivocal results. In one experiment, foetal rat OECs (Boyd et al., 2004) were labelled with a replication-deficient BAG retrovirus carrying the gene LacZ that encodes for the β-galactosidase enzyme. These LacZ expressing OECs were not found to make direct contact with axons but instead engulfed units of host-derived Schwann cells associated with axons. Another study (Akiyama et al., 2004), on the other hand, was able to show that Schwann cells and OECs in alkaline phosphatase-expressing transgenic rats were both associated with myelin formation in rats depleted of myelin by X-irradation and ethidium bromide. They could show that only the grafted alkaline phoshatase-expressing OECs or Schwann cells were responsible for myelination and not endogenous Schwann cells. Both the grafted Schwann cells and the OECs induced extensive remyelination. It was felt this it was unlikely the migration of endogenous Schwann cells could account for this extent of myelination in the presence of numerous identified transplant cells. The investigators of this study also thought exogenous contamination of the OEC suspension with Schwann cells from the transgenic donor animal was unlikely, given the high purity (> 95%) of their cultures.

There are other observations that shed new light on the interactions between endogenous Schwann cells and grafted OECs. Mucosal OECs labelled with green fluorescent protein (Ramer et al., 2004) transplanted into acute mouse and rat spinal cord lesions survived for less than 60 days and simultaneously promoted the migration of host Schwann cells into the lesion site. Although, migration of host Schwann cells has previously been observed in the lesioned spinal cord (Li et al., 1999), it has generally been difficult to distinguish grafted OECs from host Schwann cells due to their great similarity in appearance (they look alike and both stain for the same markers). It is therefore quite possible that some of the effects attributed to OECs might have been mediated by endogenous Schwann cells. On the other hand, it cannot be ruled out that there may be important differences between mucosal and bulbar OECs and studies with GFP-labelled bulbar OECs would have been useful. Unfortunately, the vector carrying GFP used in out laboratory turned out to be neurotoxic. The aforementioned study by Ramer highlighted two other interesting aspects. Firstly, OECs reorganised astrocytic processes and chondroitin sulphate proteoglycan (CSPG) deposition into longitudinal and radial streams which were re-aligned with astrocytic processes, akin to the arrangement seen in my own studies (Fig 10), whereas astrocytes formed a dense barrier in the control group. Secondly, these studies also reported a differential axonal response to mucosal OECs. The mucosal OECs recruited

only serotonin- and 5 hydroxytrytophan (5HT)-positive axons but did not facilitate the ingrowth of rubrospinal axons.

Neural crest stem cells

NCSCs demonstrated their ability to adopt either a neural or a glial fate. Those cells that had adopted a glial fate expressed nestin and p75 just like OECs and Schwann cells did. This is not surprising, after all, Schwann cells are derived from the neural crest. Some of the cells became NF- and peripherin-positive neurones. These newly formed neurones were mainly situated in the bolus part at the ventral end of the graft. There was a clear segregation into glial and neuronal populations. The glial cells were mostly seen in the column whereas neurones were encountered in the bolus at the ventral end of the graft. This would indicate that the cells are responding to specific local cues (Stemple and Anderson, 1993) (Mori et al., 1990) that determine their differentiation fate. This mechanism is well-known from the development of the neural crest and has also been observed in culture.

The grafts recruited axons which were distinctively different from axons normally observed in OEC and Schwann cell grafts. They were very fine and delicate. Their precise origin could not be established but it appears unlikely that the newly formed neurones gave rise to them. These neurones gave only rise to thicker and much shorter NF- and peripherin-positive axons than those seen in

the column part of the graft. Equally, it cannot be ruled out that peripherin might lack the sensitivity of NF in staining fine axons and hence the jury is still out on whether or not those axons observed are of host or donor origin. Another interesting observation was the fact that the newly formed neurones did not express any nestin. In culture all NCSCs express nestin, a marker of immature neuroepithelial tissue. Newly formed Schwann cells, on the other hand, retain their capacity to express nestin just like normal Schwann cells and OECs do.

Culturing of NCSCs proved to be extraordinarily difficult due to the high sensitivity of these cells and several cultures failed. For this reason only a small number of samples from only one animal could be investigated.

Human olfactory ensheathing cells

The main purpose of this investigation lay in demonstrating that human and rat OECs are similar cell types in terms of their regenerative potential and hence human OECs could reasonably be expected to work in human CNS injuries. My experiments have clearly shown that human OECs can survive in the thalamus and attract axons. The recruitment process of axons, however, is impeded by the host immune response. Anti-human mitochondria (MIT)-staining in rats that had received only oral cyclosporine revealed a honeycomb-like morphology and areas of cell necrosis

interspersed with surviving areas. Very few axons were ever seen in these samples. Blood vessels adjacent to the graft displayed the tale-tell sign of perivascular cuffing and there was also an intense infiltration of the graft by T-lymphocytes. Oral administration of cyclosporine may not lead to sufficient levels of the drug at the site of the graft(Mehl et al., 2003) (Noble and Markham, 1995). Erratic absorption from the gut is a common problem in many drugs and cyclosporine is no exception to this rule. Furthermore, the cyclosporine preparation administered in the rat's drinking water is only meant to be used for systemic intravenous infusion in humans.

Systemic immunosuppression with cyclosporine failed to abolish rejection completely but improved cell survival and axon recruitment. Perivascular cuffing was not seen and although T-cell infiltration was evident by 7 days it was only weakly detectable by 14 days. MHC II-complex expression was fairly pronounced and indicated that rejection still occurred. MHC-I complex was only mildly and diffusely expressed by the graft. Many of the cells expressing MHC II-complex had a microglia-like appearance and lay in the brain parenchyma at the border to the graft. This finding would imply that antigen presentation by microglia is an important mechanism of rejection, even in the presence of systemic immunosuppression with cyclosporine. Observations in rats and mice receiving embryonic ventral mesencephalic tissue from the pig have identified CD8-

positive cells and microglia (Larsson et al., 2001) as the main effector cells in the late, cyclosporin A-resistant rejection stage.

The axon measurements show that it is mainly axon elongation rather than the actual number of axons that is affected by the immune response. In keeping with falling levels of infiltrating T-lymphocytes the number of axons increased by 14 days. The measured length of axons was very short and comparable to the sham group. Clearly, the conditions for axon growth were suboptimal in these xenografts. One might speculate that neurotrophic factors attracted axons in the graft but that local inhibitory factors like complement, antibodies and reactive oxygen species from immune cells and macrophages stunted the growth of axons. Another more likely possibility would be that the immune response interfered with normal donor cell function, hence leading to attenuated levels of neurotrophic support.

Unfortunately, attempts at using liposomal tacrolimus failed. Perhaps tacrolimus had a neurotoxic effect on the cell suspensions. Tacrolimus is known to be neurotoxic and liposomes can be difficult to prepare (Alemdar,A.Y, personal communication). Thus, differences in preparation may play a possible role.

The fornix as a model

Failure of axon regeneration

Partial lesions were discarded from further examination. It was often difficult to tell whether a lesion was entirely complete and this required the careful study of stained adjacent sections. Samples where intact fornix fibres were seen at the periphery of the lesion or without an apparent lesion were considered as incomplete. Surviving fibres were seen in samples with lesions off the centre of the tract or where the lesion had become smaller than the width of the fornix.

It is hard to tell why the experiments on the fornix did not lead to any axon regeneration. None of the cells tested (OECs, NSCs and embryonic brain cells (E14) cells) had any impact on regeneration. Previous experiments (Stichel et al., 1996) on the postcommissural fornix apparently demonstrated a high ability of this fibre tract to regenerate in the presence of Schwann cells. Those lesions were made by simply severing the tract with a wire knife and only caused minimal mechanical damage. Stichel's work has a number of methodological shortcomings. The fornix is a very flexible structure and lowering a knife down to sever it may lead to some displacement of the fornix. Hence, the lesion may not be complete and what appears to be a regenerated tract might actually be nothing more than surviving axons. The lesions were also not reconstructed in 3

dimensions to prove their completeness. The results have yet to be reproduced by other groups.

Radiofrequency heat lesions under conditions of high electrical resistance due to the deep position of the electrode can be expected to cause fairly extensive tissue damage. The histological sections of pure lesions clearly show that this is indeed the case. Most lesions, including those with cell transplants, harbour a necrotic core in the centre. Cells and astrocytic processes are organised in a concentric fashion around the central necrosis. It may be that candidate repair cells are encountering such adverse conditions that regeneration is simply not possible.

Stichel's group believes that there is only a very short time-window of less than 24 hours (Stichel et al., 1999a) for axon regeneration when NSCs are used to repair the severed postcommissural fornix. However, it is not clear whether this is related to intrinsic properties of the NSCs. Experiments have yet to establish the capacity of OECs in immediate and delayed transplantation of the severed fornix and compare them to Schwann cells. Interestingly, axons derived from other parts of the CNS were observed in the delayed grafts which were not of subicular origin. The same authors had claimed in previous studies (Stichel et al., 1999b) that reduction of the basal membrane formation allowed fornix regeneration up to 3 days after the original injury.

It is therefore at present unclear whether it is the damage caused by the lesion itself or certain intrinsic properties of the fornix that are responsible for regenerative failure. Although the former possibility is partly supported by the extensive tissue damage seen at the lesion site, the detection of axons in the lesion raises questions regarding intrinsic properties of various fibre tracts.

Another reason for investigating E14 cells was to find out if immature cells with a high developmental potential would confer any advantage over normal more mature glial cells. The experiments clearly show that this is not the case. Axons failed to penetrate the graft. The graft had a heterogenous appearance and lacked specific expression of markers like p75, GFAP and NF. Nestin expression was not investigated. Interestingly, diffuse p75 expression was only seen where the graft was in close proximity to the fornix. Hence, some of the E14 cells were able to differentiate into glial cells provided they had contact with the fornix. This is in keeping with the ability of immature and stem cells to differentiate according to local cues . The lack of specific markers for the remaining cells indicates that they retained a high degree of immaturity.

Improved experimental design for future studies

Donor cell purification

Future studies will ensure that defined protocols are strictly followed for each donor cell type, using comparable passage stages and with careful monitoring of culture quality. This should reduce the amount of variability between cultures and ultimately improve the consistency of the cell transplantation experiments.

The donor cells to be studied include Schwann cells derived from adult (ASCs) and neonatal (NSCs) rats and olfactory ensheathing cells (OECs) derived from both the rat and human olfactory bulb and the olfactory mucosa. It may be worthwhile comparing neonatal and adult olfactory ensheathing cells from the bulb and comparing cells from cultures at different passage stages.

Schwann cells derived from neonatal tissue

Schwann cells will be derived from neonatal rat pups (postnatal day 1-2) using cytosine arabinoside to reduce the number of rapidly dividing cells, followed by a complement kill using guinea pig or rabbit complement and Thy 1 IgM antibody (Brockes et al., 1979;Raisman et al., 1993;Lakatos et al., 2000). These purification steps result in a concentration of approximately 95-98% neonatal Schwann cells. A further purification can be achieved because of the

differential adhesion properties of fibroblasts and Schwann cells (Wrathall et al., 1984).

Schwann cells derived from adult tissue

The explant technique previously described by Morrissey et al., 1991 to obtain Schwann cells from adult sciatic nerves yielded Schwann cells of up to 98 % purity when combined with glial derived growth factor and forskolin to expand Schwann cell numbers. In practice, without the use of these chemicals the usual purity obtained was closer to 80 – 90 % (Brook et al., 1994). However, purification of the cell suspension can be further improved using differential adhesion (Wrathall et al., 1984). The complement kill method does not work well on more mature fibroblasts. The distinct morphology of Schwann cells (spindle-shaped) and fibroblasts (large, flattened) *in vitro* permits assessment of culture purity using phase contrast microscopy. Using this method it will be possible to assess donor cell purity prior to transplantation.

In order to determine the effect of contaminating fibroblasts, defined mixtures of purified cells may also be transplanted since there is evidence to show that mixed cultures compared to purified cultures have no apparent negative effect on axon regeneration (Keyvan-Fouladi et al., 2005) and also anecdotal evidence that mixed cultures may have superior regeneration potential (Prof G. Raisman, personal communication). Therefore, prior to transplantation purified cultures

of Schwann cells could be mixed in defined concentration (5 % and 10 %) with fibroblasts left over from the Schwann cell preparation.

Olfactory ensheathing cells

Adult olfactory ensheathing cells (OECs), of both human and rat origin from either the olfactory bulb or the olfactory mucosa, will be cultured as previously described (see page 50 and 52) and further purified either 1) by fluorescence-activated cell sorting exploiting the fact that these cells express O4 but not Gal-C (Barnett et al., 1993) or 2) by magnetic beads loaded with anti-p75 antibody. Since OECs express the p75 low affinity nerve growth factor receptor they bind to the beads and the beads can be collected by a magnet (Barnett et al., 2000).

Donor cell purity could be assayed by immunofluorescence using p75 antibody to detect OECs and Schwann cells and fibronectin to detect fibroblasts in the sample.

Labelling of donor cells

It is important to clearly identify transplanted donor cells to exclude the possibility of endogenous cells from the meninges, the subventricular zone or the olfactory bulb migrating to the site of the graft. Labelling the donor cells would permit their unambiguous identification. There are a number of methods available.

i) Cultured cells can be labelled with bromodeoyxuridine (BrdU), a synthetic nucleoside that is incorporated in place of thymidine in the replicating DNA of dividing cells. BrdU can be identified with antibodies following denaturation of the DNA by incubation in an acid or a base or by simple heat treatment. The intensity of the signal depends on the number of cell divisions after incubation since each division dilutes the concentration of BrdU. Cell cultures can be incubated overnight with 10 µl BrdU added to each ml of tissue culture solution at a concentration of 1 mM working solution of BrdU (BD Biosciences Pharmingen). After a further 24 -48 hours in normal culture medium the cells are ready to be transplanted. After transplantation the cells can be detected by a specific antibody against BrdU (Pollock et al., 1999).

ii) Another method of cell identification involves the transplantation of male donor cells into female recipients. The Y-chromosome in the cell nucleus is detected by fluorescence in-situ hybridization (FISH). It is possible to unequivocally identify donor cells using immunofluorescence for a specific antibody combined with FISH for the Y chromosome (Trotman et al., 2004).

iii) LacZ is the gene coding for ß-galactosidase, an enzyme found in E. coli bacteria but not expressed by eukaryotic cells. Hence it can be used as a reporter and marker gene. Potential donor cells can be infected by a replication-deficient retrovirus carrying the LacZ gene in vitro and LacZ expression by grafted cells can be identified with a specific antibody against ß–galactosidase (Boyd et al., 2004).

iv) Green fluorescent protein (GFP) derived from the jellyfish *Aequorea victoria* is widely used as a method for identifying donor cells. Donor cells can be derived from commercially available transgenic animals expressing GFP. Alternatively donor cells can be transfected with GFP in culture. Transfection is usually achieved by using appropriate vectors. Lentiviruses are particularly suitable as they are capable of infecting both dividing and non-dividing cells. A direct transfer of DNA through electrical or chemical permeabilization of the target cell membrane is also possible but less effective.

Olfactory ensheathing cells have previously been successfully transfected by means of the stable viral producer line PA317 with the retroviral vector plasmid DNA pLXSN-GFP using the ecotropic packaging cell line psi-2 (Tuszynski et al., 1996). The donor cells in culture at an early passage stage are then infected with replication-deficient virus collected from the packaging cell line's medium. GFP-expressing donor cells can then be enriched by a fluorescent-activated cell sorting procedure.

Labelling with GFP has a number of advantages, since the cells can be identified directly under the confocal microscope, without the need for antibodies and the whole cell is displaying green fluorescence (unlike the techniques which label the nucleus alone).

Transplantation sites and improved lesioning techniques

The thalamus (see page 36) remains the transplantation area of choice. The model is well-established and no specific modification to the method of injecting cell suspensions into the thalamus is required.

The fornix (see page 47) was selected as another transplant site since it had the potential to show axon re-entry into the host and reconnection of axons to the target area. Unfortunately, the radiothermic lesions were probably too destructive to allow regeneration of the post-commissural formix tract (see page 176). In the original experiment axon fibres were severed with a wire-knife (Stichel et al., 1996). The potential risk with this approach is that fibre tracts may be displaced rather then severed. I would like to use this lesioning technique with transplantation but combine it with a three-dimensional reconstruction in order to distinguish regenerating axons from surviving or displaced host axon fibres. Three-dimensional reconstruction of fibres labelled with biotin dextran (BD) or other tracers (since BD has been reported to cause unreliable labeling, (Tsai et al., 2001)would distinguish remaining undamaged axons from regenerating axons which could be identified with antibodies to neurofilament protein or GAP 43. The 3D reconstructions could be made using confocal microscopy of thick sections of the tissue sample. Confocal microscopy allows each thick section to be

scanned in micron intervals. However, it would be necessary to scan several adjacent sections to build up a 3D image. Alternatively sections may be assessed using a conventional microscope with an image analysis package.

It might be worthwhile to label the subiculum with an anterograde tracer and the mammillary body with a retrograde label (although the latter method is technically very challenging) to assay the degree of regeneration through the fornix after lesioning and transplantation.

Control of host immune response

The transplantation of human cells into a rat host poses a particular challenge since xenografts are forcefully rejected by the host immune system. It is only possible to reliably assess the intrinsic survival capacity and the ability of grafted human OECs to influence axon recruitment under conditions that are not adversely affected by the influx of immune cells directed against the human xenografts. Various methods exist to suppress the host immune response. Cyclosporine or tacrolimus only suppress T-cell mediated immunity but do not protect from preformed antibodies acting via complement lysis or via antibody-dependent cellular cytotoxicity. Another draw-back of these drugs is their high nephrotoxicity leaving only a small therapeutic time window. Various other strategies can be employed to improve survival in neural xenotransplantation. These range from the administration of anti-CD4 monoclonal antibody (Wood et al.,

1996) or blocking of the IL-2 receptor (Honey CR et al., 1990) to more complex multi-antibody therapies (Larsson et al., 2003) aimed at blocking multiple activation receptors of the immune response. Much interest has also focused on finding ways of protecting the grafted cells from the effects of apoptosis (Hansson et al., 2000). More recent experiments have also raised the possibility of inducing immune tolerance (Fandrich et al., 2002) by grafting embryonic stem cells prior to grafting of a specific organ. The holy grail of transplant medicine is to achieve true immunotolerance to a given antigen but this technology is in its infancy and therefore not a practical alternative.

However, proof of principle can be achieved using athymic rats which are commercially available. They must be reared under germ-free and specific pathogen-free conditions and care must be taken during surgery to reduce the risk of infection. They are incapable of producing sufficient numbers of T-cells and hence mounting a T-cell mediated immune response since T-cell development and maturation depend on the thymus (Pearse, 2006). Only a few T-lymphocyte marker-positive cells are found in the athymic nude rat but they do have normal levels of B-lymphocytes (Hougen, 1991). However, they have been successfully employed as recipients of canine OECs (Smith et al., 2002) and also of human OECs when transplanted into the spinal cord (Deng et al., 2006).

Immunohistochemistry

Light microscopy

Sections will be fixed in either acetic alcohol or 4 % paraformaldehyde depending on the sensitivity of the antibodies used. Slides will then be washed in PBS followed by quenching of endogenous peroxidase activity by incubation in 0.3 % of H_2O_2 in water, further rinsing and then be blocked in 5 % defatted milk in PBS followed by incubation overnight at 4°C with the primary antibody. Triton or Tween may be used to improve antibody penetration. Primary antibodies will be diluted in a solution of 0.05 % azide (NaN_3) and 1 % BSA in PBS. After another wash cycle a secondary biotinylated antibody directed against the primary antibody will be used. The final steps involve the incubation with avidin-biotin complex conjugated with horseradish peroxidase (Vectastain ABC Kit, Vector Laboratories Ltd.) and processing as previously described (see page 73).

In any staining protocol some sections will be left in blocking solution without primary antibodies as negative controls. Any staining observed after application of the secondary antibody would hence be non-specific and indicate cross-reactivity with the sample tissue itself. Similarly, secondary antibodies may be omitted to see if there is non-specific tissue staining.

Confocal microscopy

Sections will be fixed in either acetic alcohol or 4 % paraformaldehyde depending on the antibodies used. Alternatively animals may be perfusion-fixed with paraformaldehyde. This is essential for animals where donor cells have been labelled with GFP since my previous studies have shown a tendency for GFP to leak out from the cells if they are not fixed immediately after the death of the animal.

Sections will then be washed and incubated overnight in the primary antibodies (mouse and rabbit in conjunction) diluted in 1 % bovine serum albumin and 0.05 % azide in PBS plus 0.2% Triton). After washing, sections will be incubated in two different fluorochrome-conjugated secondary antibodies which recognise the animal in which the primary antibodies were raised.

For the negative controls the primary or secondary antibodies may be omitted. This will permit the identification of autofluorescent macrophages.

Antibodies

The standard panel of antibodies will be used as described before (see page 71) supplemented by a number of specific antibodies, outlined below. OECs and Schwann cells display a similar immunostaining pattern for nestin and p75. Co-localisation studies will be required to verify these observations. Nestin gives a clearer

and more reliable staining pattern than p75 and would be the ideal replacement for p75 in many instances.

Markers of immunorejection or inflammation: A number of antibodies are available to detect lymphocytes, the MHC complexes and macrophages and microglia. OX-18 recognises rat MHC class I antigen and OX-6 recognises MHC class II antigen. Anti-rat CD4 (W3/25) recognises the CD4 receptor expressed by helper T-cells and to a lesser degree by microglia and macrophages and anti-rat CD8 (OX-8) recognises mainly the CD8 receptor expressed by suppressor T-cells. Microglia and macrophages can be detected by OX42 and CD68. Other markers that might be useful are the pan B-cell marker CD19 and the pan-leukocyte antibody CD18). The different cell types assayed may provoke differing degrees of microglial response or immune response which will be of importance for translational studies.

Detection of regenerating axons: GAP 43 (growth-associated protein 43 with a molecular weight of 43 and above) is expressed by both developing and regenerating axons. Other markers associated with regeneration or response to injury of axons are CAP-23, SCG10, c-jun, L1 and CHL1 (Chaisuksunt et al., 2000). These proteins are upregulated when peripheral nerves are grafted into the cerebellum. Rabbit polyclonal antibodies to GAP43 and c-jun are commercially available. These two proteins have been shown to correlate with

those axons from the thalamus, in particular those arising from the thalamic reticular nucleus that are attracted into peripheral nerve grafts (Vaudano et al., 1998b). Therefore, both the axons seen in the thalamus model and the ones seen in the fornix model should be examined for the presence of these two markers.

Markers of scar formation and non-specific inflammation: Injury to the CNS in its mildest form (eg. insertion of micropipette) only leads to very mild non-specific inflammation (Davies SJ et al., 1996). Where injury is more extensive there is an intense reactive gliosis (Silver and Miller, 2004) resulting in the formation of a 'glial scar'. This scar is heterogeneous in its composition and consists of reactive astrocytes, macrophages, fibroblasts, oligodendrocytes, endothelial cells, leukocytes and various non-cellular extracellular matrix components such as proteoglycans (Asher et al., 2001). Chondroitin sulfate proteoglycan (CSPG) is one of the components of the extracellular matrix that contributes to the inhibition of axon regeneration. It can be identified using various antibodies directed against different epitopes of CSPG (Yick et al., 2003). Reactive astrocytes can be detected by the presence of GFAP as previously described and macrophages/ microglia and oligodendrocytes (also inhibitory to axon regrowth) can be detected by antibodies raised against OX42 and myelin basic protein respectively.

An absolute pre-requisite for successful graft taking is the rapid formation of a good blood supply. More samples should therefore be investigated for the expression of von Willebrand factor (vWF), a marker expressed by endothelial cells. My preliminary findings seem to suggest that the amount of p75-immunoreactivity corresponds roughly to the extent of vascularisation or in other words that surviving p75 positive donor cells are positively correlated to the ingrowth of blood vessels. This relationship is by no means certain and a sufficient number of samples would be required to support it. Antibodies directed against vWF can be used to elucidate the vascular response to injury (intense scar formation will lead to the formation of new blood vessels) but is also useful to show the desired neovascularisation of the graft itself.

Data collection and analysis

Slides should be analysed blind. This can be achieved by a co-worker assigning random codes to the slides prior to axon counting by another co-worker (who is unaware of the various treatments).
Axons should be counted on several slides per individual sample and the two-dimensional count should be compared with the three-dimensional reconstruction count. With the appropriate software it should also be possible to obtain automatic counts which would not be affected by human bias.

It will be useful to have equal numbers of animals for each donor cell type and each survival time. This will make the statistical analysis easier and a parametric test like ANOVA (analysis of variance, a test that depends on normally distributed data and equal group sizes) can then be employed. The sample size needs to be large enough to estimate whether the sample distribution corresponds to the expected Gaussian distribution. If these criteria are not fulfilled a rank-transformed test like the Kruskal-Wallis one-way analysis of variance can be used.
Application of these improvements should yield more clearly interpretable data in relation to axon regrowth and host tissue responses which, in turn, may contribute to the use of these cells in translational studies for the clinic.

Conclusions

My experiments have shown that the thalamus is a suitable assay system for assessing cell survival, host/graft interactions and axon recruitment. Cell suspensions can be grafted in to the thalamus in a short space of time and the appearance of the grafts is relatively consistent. The experiments have shown that all candidate repair cells in the absence of a strong immune attack can survive in the thalamus. All the candidate repair cells were able to recruit axons. There appeared to be a relationship between the degree of cell organisation and the mean length and density of axons attracted into the graft. The more immature neonatal Schwann cells (NSCs) fared best in this respect, closely followed by olfactory ensheathing cells (OECs) from the mucosa. Both cell types were highly organised with long and slender nuclei nicely arranged in parallel tiers. OECs from the bulb had large and plump nuclei and appeared overall more scattered. They were associated with fibres of shorter mean length and density. It was unexpected that OECs from different locations would behave so differently. It seems that cell cultures from these two primary tissues are actually quite different. OECs from the mucosa might consist of more immature cells, possibly closer to the NSC. The fact that the olfactory mucosa harbours putative stem cells which may give rise to OECs would lend support to this theory.

Neural crest stem cells (NCSSs) transplanted into the thalamus differentiated into separated populations of glial and neural cells

corresponding to their behaviour *in vitro* and in development. The axons recruited into the NCSS columns were thinner than axons observed in the other cell grafts. This may represent the fact that this is a different class of axons from those recruited into the other cell columns, or the thinner diameter reflects an axonal response to differing local conditions in the graft.

The thalamus is particularly useful in performing studies where graft rejection poses a problem. Survival of human OECs from the mucosa was impaired by a vigorous immune response in rats that had only received oral cyclosporine but was better controlled by systemic administration of cyclosporine. Nevertheless, the immune response was not completely abolished by systemic administration of cyclosporine. Migratory behaviour of cells was not observed in human OECs. Axon recruitment was poor and practically indistinguishable from the sham group, although the mean axon density was higher after 14 days than in the sham group. The immune response impairs the growth of fibres in the graft. Nevertheless, these studies raise hopes that human OECs share common properties with rat OECs from the mucosa and could be useful for clinical applications in axon regeneration. Treating both the animal and the cells suspension with cyclosporine might improve survival and it would be worth repeating the experiments under those conditions and perhaps in immuno-incompetent nude rats as recipients.

The fornix was chosen for its accessibility and structural simplicity, representing predominantly a unilateral projection from the subiculum to the mammillary body. It was hoped that this model would allow evaluation of the impact of the candidate repair cells on axon re-entry into the host. The fornix tract was severed not with a knife but through the creation of a radiofrequency heat lesion. This was followed by grafting of cells and labelling of the tract. Unfortunately, none of the NSC and OEC grafts led to axon recruitment into the graft even if NSCs were transplanted after a 14 day delay. Surprisingly, the cell grafts recruited axons of unknown origin from outside the fornix. Grafted cells did respond to the fornix and migrated away from the bolus into the remaining fibre tract, both proximal and distal to the lesion.

Foetal brain cells survived in the lesions but likewise had no influence on fornix regeneration. They did not display any of the typical glial or neuronal markers except when they came in direct contact with the uninjured fornix and expressed p75.

The failure of fornix fibres to regenerate into the graft could either be related to the extensive tissue damage associated with the radiofrequency lesions or might reflect certain intrinsic properties of the fornix. It remains to be seen whether the fornix is a suitable assay system from which one can draw conclusions relevant to other parts of the CNS, like the spinal cord. Future studies need to address this and focus on scar tissue formation at the lesion site as

well as compare OECs and NSCs in animals having the fornix tract severed by mechanical means only.

Acknowledgements

I would like to express my gratitude to my supervisors; Dr Geoffrey Raisman who conceived the idea for an assay system and Dr Daqing Li who guided me through its realisation. My special thanks go to Mrs Harsha Jani whose extensive knowledge of stem cells and culture techniques helped to further this project and who was always eager to discuss ideas and suggestions and also provided some of the cultures. I would also like to thank Mr Lucas Raimondi and Mr Grant Roalfe for providing some of the cultures and their technical expertise on culture techniques. Finally, I would also like to acknowledge Mr Ben Blackburne who was a valuable help in choosing the right statistical tools.

Reference List

1. Akiyama, Y., Lankford, K. L., Radtke, C., Greer, C. A., and Kocsis, J. D. Remyelination of spinal cord axons by olfactory ensheathing cells and Schwann cells derived from a transgenic rat expressing alkaline phosphatase marker gene. Neuron Glia Biology [1], 47-55. 2004.

2. Alemdar AY, Baker KA, Sadi D, McAlister VC, Mendez I (2001) Liposomal tacrolimus administered systemically and within the donor cell suspension improves xenograft survival in hemiparkinsonian rats. Exp Neurol 172: 416-424.

3. Asher RA, Morgenstern DA, Moon LD, Fawcett JW (2001) Chondroitin sulphate proteoglycans: inhibitory components of the glial scar. Prog Brain Res 132: 611-619.

4. Au E, Roskams AJ (2003) Olfactory ensheathing cells of the lamina propria in vivo and in vitro. Glia 41: 224-236.

5. Baehr M, Bunge RP (1990) Growth of adult rat retinal ganglion cell neurites on astrocytes. Glia 3: 293-300.

6. Bamber NI, Li H, Lu X, Oudega M, Aebischer P, Xu XM (2001) Neurotrophins BDNF and NT-3 promote axonal re-entry into the distal host spinal cord through Schwann cell-seeded mini-channels. Eur J Neurosci 13: 257-268.

7. Barnett SC, Alexander CL, Iwashita Y, Gilson JM, Crowther J, Clark L, Dunn LT, Papanastassiou V, Kennedy PG, Franklin RJ (2000) Identification of a human olfactory ensheathing cell that can effect transplant-mediated remyelination of demyelinated CNS axons. Brain 123 (Pt 8): 1581-1588.

8. Barnett SC, Hutchins AM, Noble M (1993) Purification of olfactory nerve ensheathing cells from the olfactory bulb. Dev Biol 155: 337-350.

9. Blau HM, Brazelton TR, Weimann JM (2001) The evolving concept of a stem cell: entity or function? Cell 105: 829-841.

10. Bonetti B, Valdo P, Ossi G, De Toni L, Masotto B, Marconi S, Rizzuto N, Nardelli E, Moretto G (2003) T-cell cytotoxicity of human Schwann cells: TNFalpha promotes fasL-mediated apoptosis and IFN gamma perforin-mediated lysis. Glia 43: 141-148.

11. Boruch AV, Conners JJ, Pipitone M, Deadwyler G, Storer PD, Devries GH, Jones KJ (2001) Neurotrophic and migratory properties of an olfactory ensheathing cell line. Glia 33: 225-229.

12. Boyd JG, Lee J, Skihar V, Doucette R, Kawaja MD (2004) LacZ-expressing olfactory ensheathing cells do not associate with myelinated axons after implantation into the compressed spinal cord. Proc Natl Acad Sci U S A 101: 2162-2166.

13. Bradbury EJ, Moon LD, Popat RJ, King VR, Bennett GS, Patel PN, Fawcett JW, McMahon SB (2002) Chondroitinase ABC promotes functional recovery after spinal cord injury. nat 416: 636-640.

14. Bradbury MW, Westrop RJ (1983) Factors influencing exit of substances from cerebrospinal fluid into deep cervical lymph of the rabbit. J Physiol 339: 519-534.

15. Bregman BS, Kunkel-Bagden E, Schnell L, Dai HN, Gao D, Schwab ME (1995) Recovery from spinal cord injury mediated by antibodies to neurite growth inhibitors. nat 378: 498-501.

16. Brevig T, Meyer M, Kristensen T, Zimmer J, Holgersson J (2001) Xenotransplantation for brain repair: reduction of porcine donor tissue immunogenicity by treatment with anti-Gal antibodies and complement. Transplantation 72: 190-196.

17. Brockes JP, Fields KL, Raff MC (1979) Studies on cultured rat Schwann cells. I. Establishment of purified populations from cultures of peripheral nerve. Brain Res 165: 105-118.

18. Brook GA, Lawrence JM, Raisman G (2001) Columns of Schwann cells extruded into the CNS induce in-growth of astrocytes to form organized new glial pathways. Glia 33: 118-130.

19. Brook GA, Lawrence JM, Shah B, Raisman G (1994) Extrusion transplantation of Schwann cells into the adult rat thalamus induces directional host axon growth. Exp Neurol 126: 31-43.

20. Brundin P, Nilsson OG, Gage FH, Bjorklund A (1985) Cyclosporin A increases survival of cross-species intrastriatal grafts of embryonic dopamine-containing neurons. Exp Brain Res 60: 204-208.

21. Bush TG, Puvanachandra N, Horner CH, Polito A, Ostenfeld T, Svendsen CN, Mucke L, Johnson MH, Sofroniew MV (1999) Leukocyte infiltration, neuronal degeneration, and neurite outgrowth after ablation of scar-forming, reactive astrocytes in adult transgenic mice. Neuron 23: 297-308.

22. Cai J, Limke TL, Ginis I, Rao MS (2003) Identifying and tracking neural stem cells. Blood Cells Mol Dis 31: 18-27.

23. Cai JL, Wu YY, Mirua T, Pierce JL, Lucero MT, Albertine KH, Spangrude GJ, Rao MS (2002) Properties of a fetal multipotent neural stem cell (NEP cell). Dev Biol 251: 221-240.

24. Cajal, S. Degeneration and Regeneration of the Nervous System. 1928. New York, Hafner.

25. Carbonell AL, Boya J (1988) Ultrastructural study on meningeal regeneration and meningo-glial relationships after cerebral stab wound in the adult rat. Brain Res 439: 337-344.

26. Caroni P, Schwab ME (1988) Two membrane protein fractions from rat central myelin with inhibitory properties for neurite growth and fibroblast spreading. J Cell Biol 106: 1281-1288.

27. Castilho RF, Hansson O, Brundin P (2000) FK506 and cyclosporin A enhance the survival of cultured and grafted rat embryonic dopamine neurons. Exp Neurol 164: 94-101.

28. Chaisuksunt V, Zhang Y, Anderson PN, Campbell G, Vaudano E, Schachner M, Lieberman AR (2000) Axonal regeneration from CNS neurons in the cerebellum and brainstem of adult rats: correlation with the patterns of expression and distribution of messenger RNAs for L1, CHL1, c-jun and growth-associated protein-43. Neuroscience 100: 87-108.

29. Chen MS, Huber AB, van der Haar ME, Frank M, Schnell L, Spillmann AA, Christ F, Schwab ME (2000) Nogo-A is a myelin-associated neurite outgrowth inhibitor and an antigen for monoclonal antibody IN-1. nat 403: 434-439.

30. Chitilian HV, Laufer TM, Stenger K, Shea S, Auchincloss H, Jr. (1998) The strength of cell-mediated xenograft rejection in the mouse is due to the CD4+ indirect response. Xenotransplantation 5: 93-98.

31. Choi D, Raisman G (2003) Immune rejection of a facial nerve xenograft does not prevent regeneration and the return of function: An experimental study. Neuroscience 121: 501-507.

32. Chuah MI, Au C (1991) Olfactory Schwann cells are derived from precursor cells in the olfactory epithelium. J Neurosci Res 29: 172-180.

33. Chuah MI, Tennent R, Jacobs I (1995) Response of olfactory Schwann cells to intranasal zinc sulfate irrigation. J Neurosci Res 42: 470-478.

34. Colomar A, Marty V, Combe C, Medina C, Parnet P, Amedee T (2003) [The immune status of Schwann cells: what is the role of the P2X7 receptor?]. J Soc Biol 197: 113-122.

35. Cserr HF, Knopf PM (1992) Cervical lymphatics, the blood-brain barrier and the immunoreactivity of the brain: a new view. Immunol Today 13: 507-512.

36. Dahlstrand J, Lardelli M, Lendahl U (1995) Nestin mRNA expression correlates with the central nervous system progenitor cell state in many, but not all, regions of developing central nervous system. Brain Res Dev Brain Res 84: 109-129.

37. Davies SJ, Field PM, Raisman G (1996) Regeneration of cut adult axons fails even in the presence of continuous aligned glial pathways. Exp Neurol 142: 203-216.

38. Davies SJ, Goucher DR, Doller C, Silver J (1999) Robust regeneration of adult sensory axons in degenerating white matter of the adult rat spinal cord. J Neurosci 19: 5810-5822.

39. De Winter F, Holtmaat AJ, Verhaagen J (2002) Neuropilin and class 3 semaphorins in nervous system regeneration. Adv Exp Med Biol 515: 115-139.

40. Delaney CL., Brenner M, Messing A (1996) Conditional ablation of cerebellar astrocytes in postnatal transgenic mice. J Neurosci 16: 6908-6918.

41. Deng C, Gorrie C, Hayward I, Elston B, Venn M, Mackay-Sim A, Waite P (2006) Survival and migration of human and rat olfactory ensheathing cells in intact and injured spinal cord. J Neurosci Res 83: 1201-1212.

42. Devon R, Doucette R (1995) Olfactory ensheathing cells do not require L-ascorbic acid in vitro to assemble a basal lamina or to myelinate dorsal root ganglion neurites. Brain Res 688: 223-229.

43. Dong Y, Benveniste EN (2001) Immune function of astrocytes. Glia 36: 180-190.

44. Duan WM, Westerman MA, Wong G, Low WC (2002) Rat nigral xenografts survive in the brain of MHC class II-, but not class I-deficient mice. Neuroscience 115: 495-504.

45. Duan WM, Widner H, Brundin P (1995) Temporal pattern of host responses against intrastriatal grafts of syngeneic, allogeneic or xenogeneic embryonic neuronal tissue in rats. Exp Brain Res 104: 227-242.

46. Dupin E, Real C, Glavieux-Pardanaud C, Vaigot P, Le Douarin NM (2003) Reversal of developmental restrictions in neural crest lineages: transition from Schwann cells to glial-melanocytic precursors in vitro. Proc Natl Acad Sci U S A 100: 5229-5233.

47. Fandrich F, Lin X, Chai GX, Schulze M, Ganten D, Bader M, Holle J, Huang DS, Parwaresch R, Zavazava N, Binas B (2002) Preimplantation-stage stem cells induce long-term allogeneic graft acceptance without supplementary host conditioning. Nat Med 8: 171-178.

48. Feron F, Perry C, McGrath JJ, Mackay-Sim A (1998) New techniques for biopsy and culture of human olfactory epithelial neurons. Arch Otolaryngol Head Neck Surg 124: 861-866.

49. Field P, Li Y, Raisman G (2003) Ensheathment of the olfactory nerves in the adult rat. J Neurocytol 32: 317-324.

50. Filbin MT (2003) Myelin-associated inhibitors of axonal regeneration in the adult mammalian CNS. Nat Rev Neurosci 4: 703-713.

51. Fouad K, Klusman I, Schwab ME (2004) Regenerating corticospinal fibers in the Marmoset (Callitrix jacchus) after spinal cord lesion and treatment with the anti-Nogo-A antibody IN-1. Eur J Neurosci 20: 2479-2482.

52. Friedman HC, Aguayo AJ, Bray GM (1999) Trophic factors in neuron-Schwann cell interactions. Ann N Y Acad Sci 883: 427-438.

53. George Paxinos. The Rat Brain in Stereotaxic Coordinates. 1997. Academic Press, Ltd.

54. Gloor SM, Wachtel M, Bolliger MF, Ishihara H, Landmann R, Frei K (2001) Molecular and cellular permeability control at the blood-brain barrier. Brain Res Brain Res Rev 36: 258-264.

55. Goldstein BJ, Schwob JE (1996) Analysis of the globose basal cell compartment in rat olfactory epithelium using GBC-1, a new monoclonal antibody against globose basal cells. J Neurosci 16: 4005-4016.

56. Gomez VM, Averill S, King V, Yang Q, Perez ED, Chacon SC, Ward R, Nieto-Sampedro M, Priestley J, Taylor J (2003) Transplantation of olfactory ensheathing cells fails to promote significant axonal regeneration from dorsal roots into the rat cervical cord. J Neurocytol 32: 53-70.

57. Goodman MN, Silver J, Jacobberger JW (1993) Establishment and neurite outgrowth properties of neonatal and adult rat olfactory bulb glial cell lines. Brain Res 619: 199-213.

58. Gottlieb DI (2002) Large-scale sources of neural stem cells. Annu Rev Neurosci 25: 381-407.

59. Graziadei PP, Graziadei GA (1979) Neurogenesis and neuron regeneration in the olfactory system of mammals. I. Morphological aspects of differentiation and structural organization of the olfactory sensory neurons. J Neurocytol 8: 1-18.

60. Hansson O, Castilho RF, Kaminski Schierle GS, Karlsson J, Nicotera P, Leist M, Brundin P (2000) Additive effects of caspase inhibitor and lazaroid on the survival of transplanted rat and human embryonic dopamine neurons. Exp Neurol 164: 102-111.

61. Hermanns S, Wunderlich G, Rosenbaum C, Hanemann CO, Muller HW, Stichel CC (1997) Lack of immune responses to immediate or delayed implanted allogeneic and xenogeneic Schwann cell suspensions. Glia 21: 299-314.

62. Honey CR, Clarke DJ., Dallman MJ., Charlton HM (1990) Human neural graft function in rats treated with anti-interleukin II receptor antibody. NeuroReport 1: 247-249.

63. Hougen HP (1991) The athymic nude rat. Immunobiological characteristics with special reference to establishment of non-antigen-specific T-cell reactivity and induction of antigen-specific immunity. APMIS Suppl 21: 1-39.

64. Huang DW, McKerracher L, Braun PE, David S (1999) A therapeutic vaccine approach to stimulate axon regeneration in the adult mammalian spinal cord. Neuron 24: 639-647.

65. Huard JM, Youngentob SL, Goldstein BJ, Luskin MB, Schwob JE (1998) Adult olfactory epithelium contains multipotent progenitors that give rise to neurons and non-neural cells. J Comp Neurol 400: 469-486.

66. Imaizumi T, Lankford KL, Waxman SG, Greer CA, Kocsis JD (1998) Transplanted olfactory ensheathing cells remyelinate and enhance axonal conduction in the demyelinated dorsal columns of the rat spinal cord. J Neurosci 18: 6176-6185.

67. Imitola J, Raddassi K, Park KI, Mueller FJ, Nieto M, Teng YD, Frenkel D, Li J, Sidman RL, Walsh CA, Snyder EY, Khoury SJ (2004) Directed migration of neural stem cells to sites of CNS injury by the stromal cell-derived factor 1{alpha}/CXC chemokine receptor 4 pathway. Proc Natl Acad Sci U S A 101: 18117-18122.

68. Kawano H, Li HP, Sango K, Kawamura K, Raisman G (2005) Inhibition of collagen synthesis overrides the age-related failure of regeneration of nigrostriatal dopaminergic axons. J Neurosci Res 80: 191-202.

69. Keyvan-Fouladi N, Raisman G, Li Y (2003) Functional repair of the corticospinal tract by delayed transplantation of olfactory ensheathing cells in adult rats. J Neurosci 23: 9428-9434.

70. Keyvan-Fouladi N, Raisman G, Li Y (2005) Delayed repair of corticospinal tract lesions as an assay for the effectiveness of transplantation of Schwann cells. Glia 51: 306-311.

71. Ko S, Nakajima Y, Kanehiro H, Yoshimura A, Nakano H (1994) The pharmacokinetic benefits of newly developed liposome-incorporated FK506. Transplantation 58: 1142-1144.

72. Koshizuka S, Okada S, Okawa A, Koda M, Murasawa M, Hashimoto M, Kamada T, Yoshinaga K, Murakami M, Moriya H, Yamazaki M (2004) Transplanted hematopoietic stem cells from bone marrow differentiate into neural lineage cells and promote functional recovery after spinal cord injury in mice. J Neuropathol Exp Neurol 63: 64-72.

73. Kruger GM, Mosher JT, Bixby S, Joseph N, Iwashita T, Morrison SJ (2002) Neural crest stem cells persist in the adult gut but undergo changes in self-renewal, neuronal subtype potential, and factor responsiveness. Neuron 35: 657-669.

74. Lakatos A, Barnett SC, Franklin RJ (2003a) Olfactory ensheathing cells induce less host astrocyte response and chondroitin sulphate proteoglycan expression than schwann cells following transplantation into adult cns white matter. Exp Neurol 184: 237-246.

75. Lakatos A, Franklin RJ, Barnett SC (2000) Olfactory ensheathing cells and Schwann cells differ in their in vitro interactions with astrocytes. Glia 32: 214-225.

76. Lakatos A, Smith PM, Barnett SC, Franklin RJ (2003b) Meningeal cells enhance limited CNS remyelination by transplanted olfactory ensheathing cells. Brain 126: 598-609.

77. Larsson LC, Corbascio M, Pearson TC, Larsen CP, Ekberg H, Widner H (2003) Induction of operational tolerance to discordant dopaminergic porcine xenografts. Transplantation 75: 1448-1454.

78. Larsson LC, Czech KA, Widner H, Korsgren O (1999) Discordant neural tissue xenografts survive longer in immunoglobulin deficient mice. Transplantation 68: 1153-1160.

79. Larsson LC, Frielingsdorf H, Mirza B, Hansson SJ, Anderson P, Czech KA, Strandberg M, Widner H (2001) Porcine neural xenografts in rats and mice: donor tissue development and characteristics of rejection. Exp Neurol 172: 100-114.

80. Lawrence JM, Morris RJ, Raisman G (1994) Anatomical evidence that microglia are involved in both the immune presenting and immune attack phases of intracerebral allograft rejection. Neuropathol Appl Neurobiol 20: 203-205.

81. Lawrence JM, Morris RJ, Wilson DJ, Raisman G (1990) Mechanisms of allograft rejection in the rat brain. Neuroscience 37: 431-462.

82. Leavitt BR, Hernit-Grant CS, Macklis JD (1999) Mature astrocytes transform into transitional radial glia within adult mouse neocortex that supports directed migration of transplanted immature neurons. Exp Neurol 157: 43-57.

83. Lee MJ, Straubinger RM, Jusko WJ (1995) Physicochemical, pharmacokinetic and pharmacodynamic evaluation of liposomal tacrolimus (FK 506) in rats. Pharm Res 12: 1055-1059.

84. Levison SW, Druckman SK, Young GM, Basu A (2003) Neural stem cells in the subventricular zone are a source of astrocytes and oligodendrocytes, but not microglia. Dev Neurosci 25: 184-196.

85. Li Y, Carlstedt T, Berthold CH, Raisman G (2004) Interaction of transplanted olfactory-ensheathing cells and host astrocytic processes provides a bridge for axons to regenerate across the dorsal root entry zone. Exp Neurol 188: 300-308.

86. Li Y, Decherchi P, Raisman G (2003) Transplantation of olfactory ensheathing cells into spinal cord lesions restores breathing and climbing. J Neurosci 23: 727-731.

87. Li Y, Field PM, Raisman G (1997) Repair of adult rat corticospinal tract by transplants of olfactory ensheathing cells. Sci 277: 2000-2002.

88. Li Y, Field PM, Raisman G (1998) Regeneration of adult rat corticospinal axons induced by transplanted olfactory ensheathing cells. J Neurosci 18: 10514-10524.

89. Li Y, Field PM, Raisman G (1999) Death of oligodendrocytes and microglial phagocytosis of myelin precede immigration of Schwann cells into the spinal cord. J Neurocytol 28: 417-427.

90. Li Y, Field PM, Raisman G (2005) Olfactory ensheathing cells and olfactory nerve fibroblasts maintain continuous open channels for regrowth of olfactory nerve fibres. Glia 52: 245-251.

91. Li Y, Raisman G (1994) Schwann cells induce sprouting in motor and sensory axons in the adult rat spinal cord. J Neurosci 14: 4050-4063.

92. Li Y, Raisman G (1995) Sprouts from cut corticospinal axons persist in the presence of astrocytic scarring in long-term lesions of the adult rat spinal cord. Exp Neurol 134: 102-111.

93. Lin RC, Matesic DF, Marvin M, McKay RD, Brustle O (1995) Re-expression of the intermediate filament nestin in reactive astrocytes. Neurobiol Dis 2: 79-85.

94. Lipson AC, Widenfalk J, Lindqvist E, Ebendal T, Olson L (2003) Neurotrophic properties of olfactory ensheathing glia. Exp Neurol 180: 167-171.

95. Liu Z, Martin LJ (2003) Olfactory bulb core is a rich source of neural progenitor and stem cells in adult rodent and human. J Comp Neurol 459: 368-391.

96. Lu J, Feron F, Ho SM, Mackay-Sim A, Waite PM (2001) Transplantation of nasal olfactory tissue promotes partial recovery in paraplegic adult rats. Brain Res 889: 344-357.

97. Lu J, Feron F, Mackay-Sim A, Waite PM (2002) Olfactory ensheathing cells promote locomotor recovery after delayed transplantation into transected spinal cord. Brain 125: 14-21.

98. Lu P, Jones LL, Snyder EY, Tuszynski MH (2003) Neural stem cells constitutively secrete neurotrophic factors and promote extensive host axonal growth after spinal cord injury. Exp Neurol 181: 115-129.

99. Mackay-Sim A, Kittel P (1991) Cell dynamics in the adult mouse olfactory epithelium: a quantitative autoradiographic study. J Neurosci 11: 979-984.

100. Maslov AY, Barone TA, Plunkett RJ, Pruitt SC (2004) Neural stem cell detection, characterization, and age-related changes in the subventricular zone of mice. J Neurosci 24: 1726-1733.

101. Mason DW, Charlton HM, Jones AJ, Lavy CB, Puklavec M, Simmonds SJ (1986) The fate of allogeneic and xenogeneic neuronal tissue transplanted into the third ventricle of rodents. Neuroscience 19: 685-694.

102. Masri MA (2003) The mosaic of immunosuppressive drugs. Mol Immunol 39: 1073-1077.

103. Mehl ML, Kyles AE, Craigmill AL, Epstein S, Gregory CR (2003) Disposition of cyclosporine after intravenous and multi-dose oral administration in cats. J Vet Pharmacol Ther 26: 349-354.

104. Menei P, Montero-Menei C, Whittemore SR, Bunge RP, Bunge MB (1998) Schwann cells genetically modified to secrete human BDNF promote enhanced axonal regrowth across transected adult rat spinal cord. Eur J Neurosci 10: 607-621.

105. Mirsky R, Jessen KR, Brennan A, Parkinson D, Dong Z, Meier C, Parmantier E, Lawson D (2002) Schwann cells as regulators of nerve development. J Physiol Paris 96: 17-24.

106. Mirsky R, Parmantier E, McMahon AP, Jessen KR (1999) Schwann cell-derived desert hedgehog signals nerve sheath formation. Ann N Y Acad Sci 883: 196-202.

107. Montero-Menei CN, Pouplard-Barthelaix A, Gumpel M, Baron-Van Evercooren A (1992) Pure Schwann cell suspension grafts promote regeneration of the lesioned septo-hippocampal cholinergic pathway. Brain Res 570: 198-208.

108. Moon LD, Brecknell JE, Franklin RJ, Dunnett SB, Fawcett JW (2000) Robust regeneration of CNS axons through a track depleted of CNS glia. Exp Neurol 161: 49-66.

109. Mori N, Birren SJ, Stein R, Stemple D, Vandenbergh DJ, Wuenschell CW, Anderson DJ (1990) Contributions of cell-extrinsic and cell-intrinsic factors to the differentiation of a neural-crest-derived neuroendocrine progenitor cell. Cold Spring Harb Symp Quant Biol 55: 255-264.

110. Morrissey TK, Kleitman N, Bunge RP (1991) Isolation and functional characterization of Schwann cells derived from adult peripheral nerve. J Neurosci 11: 2433-2442.

111. Mujtaba T, Mayer-Proschel M, Rao MS (1998) A common neural progenitor for the CNS and PNS. Dev Biol 200: 1-15.

112. Murrell W, Bushell GR, Livesey J, McGrath J, MacDonald KP, Bates PR, Mackay-Sim A (1996) Neurogenesis in adult human. NeuroReport 7: 1189-1194.

113. Nieto-Sampedro M (2003) Central nervous system lesions that can and those that cannot be repaired with the help of olfactory bulb ensheathing cell transplants. Neurochem Res 28: 1659-1676.

114. Noble S, Markham A (1995) Cyclosporin. A review of the pharmacokinetic properties, clinical efficacy and tolerability of a microemulsion-based formulation (Neoral). Drugs 50: 924-941.

115. Norenberg MD (1994) Astrocyte responses to CNS injury. J Neuropathol Exp Neurol 53: 213-220.

116. Oehmichen M, Gruninger H, Wietholter H, Gencic M (1979) Lymphatic efflux of intracerebrally injected cells. Acta Neuropathol (Berl) 45: 61-65.

117. Pachter JS, de Vries HE, Fabry Z (2003) The blood-brain barrier and its role in immune privilege in the central nervous system. J Neuropathol Exp Neurol 62: 593-604.

118. Pearse G (2006) Normal structure, function and histology of the thymus. Toxicol Pathol 34: 504-514.

119. Plant GW, Bates ML, Bunge MB (2001) Inhibitory proteoglycan immunoreactivity is higher at the caudal than the rostral Schwann cell graft-transected spinal cord interface. Mol Cell Neurosci 17: 471-487.

120. Plant GW, Currier PF, Cuervo EP, Bates ML, Pressman Y, Bunge MB, Wood PM (2002) Purified adult ensheathing glia fail to myelinate axons under culture conditions that enable Schwann cells to form myelin. J Neurosci 22: 6083-6091.

121. Pollock GS, Franceschini IA, Graham G, Marchionni MA, Barnett SC (1999) Neuregulin is a mitogen and survival factor for olfactory bulb ensheathing cells and an isoform is produced by astrocytes. Eur J Neurosci 11: 769-780.

122. Raineteau O, Fouad K, Noth P, Thallmair M, Schwab ME (2001) Functional switch between motor tracts in the presence of the mAb IN-1 in the adult rat. Proc Natl Acad Sci U S A 98: 6929-6934.

123. Raisman G (2001) Olfactory ensheathing cells - another miracle cure for spinal cord injury? Nat Rev Neurosci 2: 369-375.

124. Raisman G, Lawrence JM, Brook GA (1993) Schwann cells transplanted into the CNS. Int J Dev Neurosci 11: 651-669.

125. Ramer LM, Au E, Richter MW, Liu J, Tetzlaff W, Roskams AJ (2004) Peripheral olfactory ensheathing cells reduce scar and cavity formation and promote regeneration after spinal cord injury. J Comp Neurol 473: 1-15.

126. Ramon-Cueto A, Nieto-Sampedro M (1992) Glial cells from adult rat olfactory bulb: immunocytochemical properties of pure cultures of ensheathing cells. Neuroscience 47: 213-220.

127. Ramon-Cueto A, Nieto-Sampedro M (1994) Regeneration into the spinal cord of transected dorsal root axons is promoted by ensheathing glia transplants. Exp Neurol 127: 232-244.

128. Ramon-Cueto A, Plant GW, Avila J, Bunge MB (1998) Long-distance axonal regeneration in the transected adult rat spinal cord is promoted by olfactory ensheathing glia transplants. J Neurosci 18: 3803-3815.

129. Reier PJ, Houle JD (1988) The glial scar: its bearing on axonal elongation and transplantation approaches to CNS repair. Adv Neurol 47: 87-138.

130. Reynolds BA, Weiss S (1992) Generation of neurons and astrocytes from isolated cells of the adult mammalian central nervous system. Sci 255: 1707-1710.

131. Richardson PM, McGuinness UM, Aguayo AJ (1980) Axons from CNS neurons regenerate into PNS grafts. nat 284: 264-265.

132. Richardson PM, McGuinness UM, Aguayo AJ (1982) Peripheral nerve autografts to the rat spinal cord: studies with axonal tracing methods. Brain Res 237: 147-162.

133. Rohlf, F. J. and R.R.Sokal. Statistical tables. 3rd edition. 1995. W. H. Freeman and Co.: New York.

134. Roitbak T, Sykova E (1999) Diffusion barriers evoked in the rat cortex by reactive astrogliosis. Glia 28: 40-48.

135. Schwab ME (2004) Nogo and axon regeneration. Curr Opin Neurobiol 14: 118-124.

136. Schwab ME, Caroni P (1988) Oligodendrocytes and CNS myelin are nonpermissive substrates for neurite growth and fibroblast spreading in vitro. J Neurosci 8: 2381-2393.

137. Schwab ME, Thoenen H (1985) Dissociated neurons regenerate into sciatic but not optic nerve explants in culture irrespective of neurotrophic factors. J Neurosci 5: 2415-2423.

138. Scott BS (1977) Adult mouse dorsal root ganglia neurons in cell culture. J Neurobiol 8: 417-427.

139. Sicard G, Feron F, Andrieu JL, Holley A, Mackay-Sim A (1998) Generation of neurons from a nonneuronal precursor in adult olfactory epithelium in vitro. Ann N Y Acad Sci 855: 223-225.

140. Silver J, Miller JH (2004) Regeneration beyond the glial scar. Nat Rev Neurosci 5: 146-156.

141. Smith PM, Lakatos A, Barnett SC, Jeffery ND, Franklin RJM (2002) Cryopreserved cells isolated from the adult canine olfactory bulb are capable of extensive remyelination following transplantation into the adult rat CNS. Exp Neurol 176: 402-406.

142. Smith PM, Sim FJ, Barnett SC, Franklin RJ (2001) SCIP/Oct-6, Krox-20, and desert hedgehog mRNA expression during CNS remyelination by transplanted olfactory ensheathing cells. Glia 36: 342-353.

143. Stanfield BB, Nahin BR, O'Leary DD (1987) A transient postmamillary component of the rat fornix during development: implications for interspecific differences in mature axonal projections. J Neurosci 7: 3350-3361.

144. Stemple DL, Anderson DJ (1992) Isolation of a stem cell for neurons and glia from the mammalian neural crest. Cell 71: 973-985.

145. Stemple DL, Anderson DJ (1993) Lineage diversification of the neural crest: in vitro investigations. Dev Biol 159: 12-23.

146. Stichel CC, Hermanns S, Lausberg F, Muller HW (1999a) Effects of schwann cell suspension grafts on axon regeneration in subacute and chronic CNS traumatic injuries. Glia 28: 156-165.

147. Stichel CC, Lausberg F, Hermanns S, Muller HW (1999b) Scar modulation in subacute and chronic CNS lesions: Effects on axonal regeneration. Restor Neurol Neurosci 15: 1-15.

148. Stichel CC, Lips K, Wunderlich G, Muller HW (1996) Reconstruction of transected postcommissural fornix in adult rat by Schwann cell suspension grafts. Exp Neurol 140: 21-36.

149. Stichel CC, Niermann H, D'Urso D, Lausberg F, Hermanns S, Muller HW (1999c) Basal membrane-depleted scar in lesioned CNS: characteristics and relationships with regenerating axons. Neuroscience 93: 321-333.

150. Taylor JS, Bampton ET (2004) Factors secreted by Schwann cells stimulate the regeneration of neonatal retinal ganglion cells. J Anat 204: 25-31.

151. Timpl R, Brown JC (1996) Supramolecular assembly of basement membranes. Bioessays 18: 123-132.

152. Trotman W, Beckett T, Goncz KK, Beatty BG, Weiss DJ (2004) Dual Y chromosome painting and in situ cell-specific immunofluorescence staining in lung tissue: an improved method of identifying donor marrow cells in lung following bone marrow transplantation. Histochem Cell Biol 121: 73-79.

153. Tsai EC, van Bendegem RL, Hwang SW, Tator CH (2001) A novel method for simultaneous anterograde and retrograde labeling of spinal cord motor tracts in the same animal. J Histochem Cytochem 49: 1111-1122.

154. Tuszynski MH, Gabriel K, Gage FH, Suhr S, Meyer S, Rosetti A (1996) Nerve growth factor delivery by gene transfer induces differential outgrowth of sensory, motor, and noradrenergic neurites after adult spinal cord injury. Exp Neurol 137: 157-173.

155. Tuszynski MH, Weidner N, McCormack M, Miller I, Powell H, Conner J (1998) Grafts of genetically modified Schwann cells to the spinal cord: survival, axon growth, and myelination. Cell Transplant 7: 187-196.

156. Van Den Pol AN, Santarelli JG (2003) Olfactory ensheathing cells: Time lapse imaging of cellular interactions, axonal support, rapid morphologic shifts, and mitosis. J Comp Neurol 458: 175-194.

157. Vaudano E, Campbell G, Hunt SP, Lieberman AR (1998a) Axonal injury and peripheral nerve grafting in the thalamus and cerebellum of the adult rat: upregulation of c-jun and correlation with regenerative potential. Eur J Neurosci 10: 2644-2656.

158. Vaudano E, Campbell G, Hunt SP, Lieberman AR (1998b) Axonal injury and peripheral nerve grafting in the thalamus and cerebellum of the adult rat: upregulation of c-jun and correlation with regenerative potential. Eur J Neurosci 10: 2644-2656.

159. Verdu E, Garcia-Alias G, Fores J, Gudino-Cabrera G, Muneton VC, Nieto-Sampedro M, Navarro X (2001) Effects of ensheathing cells transplanted into photochemically damaged spinal cord. NeuroReport 12: 2303-2309.

160. Verdu E, Rodriguez FJ, Gudino-Cabrera G, Nieto-Sampedro M, Navarro X (2000) Expansion of adult Schwann cells from mouse predegenerated peripheral nerves. J Neurosci Methods 99: 111-117.

161. Wei LC, Shi M, Chen LW, Cao R, Zhang P, Chan YS (2002) Nestin-containing cells express glial fibrillary acidic protein in the proliferative regions of central nervous system of postnatal developing and adult mice. Dev Brain Res 139: 9-17.

162. Weidner N, Blesch A, Grill RJ, Tuszynski MH (1999a) Nerve growth factor-hypersecreting Schwann cell grafts augment and guide spinal cord axonal growth and remyelinate central nervous system axons in a phenotypically appropriate manner that correlates with expression of L1. J Comp Neurol 413: 495-506.

163. Weidner N, Grill RJ, Tuszynski MH (1999b) Elimination of basal lamina and the collagen "scar" after spinal cord injury fails to augment corticospinal tract regeneration. Exp Neurol 160: 40-50.

164. Wekerle, H (1986) Cellular immune reactivity within the CNS. Trends Neurosci [6], 271-277.

165. Wewetzer K, Verdú E, Angelov DN, Navarro X (2002) Olfactory ensheathing glia and Schwann cells: two of a kind? Cell Tissue Res 309: 337-345.

166. Wiessner C, Bareyre FM, Allegrini PR, Mir AK, Frentzel S, Zurini M, Schnell L, Oertle T, Schwab ME (2003) Anti-nogo-a antibody infusion 24 hours after experimental stroke improved behavioral outcome and corticospinal plasticity in normotensive and spontaneously hypertensive rats. J Cereb Blood Flow Metab 23: 154-165.

167. Wood MJ, Sloan DJ, Wood KJ, Charlton HM (1996) Indefinite survival of neural xenografts induced with anti-CD4 monoclonal antibodies. Neuroscience 70: 775-789.

168. Wrathall JR, Kapoor V, Kao CC (1984) Observation of cultured peripheral non-neuronal cells implanted into the transected spinal cord. Acta Neuropathol (Berl) 64: 203-212.

169. Wunderlich G, Stichel CC, Schroeder WO, Muller HW (1994) Transplants of immature astrocytes promote axonal regeneration in the adult rat brain. Glia 10: 49-58.

170. Xu XM, Zhang SX, Li H, Aebischer P, Bunge MB (1999) Regrowth of axons into the distal spinal cord through a Schwann-cell-seeded mini-channel implanted into hemisected adult rat spinal cord. Eur J Neurosci 11: 1723-1740.

171. Yick LW, Cheung PT, So KF, Wu W (2003) Axonal regeneration of Clarke's neurons beyond the spinal cord injury scar after treatment with chondroitinase ABC. Exp Neurol 182: 160-168.

172. Zhang Y, Campbell G, Anderson PN, Martini R, Schachner M, Lieberman AR (1995) Molecular basis of interactions between regenerating adult rat thalamic axons and Schwann cells in peripheral nerve grafts I. Neural cell adhesion molecules. J Comp Neurol 361: 193-209.